



**Patrícia Monte Lira
Rodrigues da Costa**

**Silenciamento da LAP1 utilizando a estratégia de
*shRNA***

**Knocking-down LAP1 using the short hairpin RNA
strategy**



Patrícia Monte Lira
Rodrigues da Costa

Silenciamento da LAP1 utilizando a estratégia de *shRNA*

Knocking-down LAP1 using the short hairpin RNA strategy

Dissertação apresentada à Universidade de Aveiro para cumprimento dos requisitos necessários à obtenção do grau de Mestre em Biomedicina Molecular, realizada sob a orientação científica da Professora Doutora Sandra Maria Tavares da Costa Rebelo, Professora Auxiliar Convidada da Secção Autónoma de Ciências da Saúde da Universidade de Aveiro.

Este trabalho contou com o apoio do Centro de Biologia Celular (CBC) da Universidade de Aveiro, e é financiado por fundos FEDER através do Programa Operacional Factores de Competitividade – COMPETE e por Fundos nacionais da FCT – Fundação para a Ciência e Tecnologia, no âmbito dos projectos REEQ/1023/BIO/2005, PTDC/QUI-BIQ/101317/2008 e PEst OE/SAU/UI0482/2011.



Dedico este trabalho a todos aqueles que sempre acreditaram em mim e no meu valor. Aos meus pais e ao meu irmão. A todos os amigos do Centro de Biologia Celular. A todos vocês pelo apoio incondicional e por terem caminhado ao meu lado sempre.

o júri

presidente

Professora Doutora Odete Cruz e Silva
Professora auxiliar com agregação da Universidade de Aveiro

Professora Doutora Sandra Maria Tavares da Costa Rebelo
Professora auxiliar convidada da Universidade de Aveiro

Doutora María Gómez Lázaro
Técnica de investigação do Instituto Nacional de Engenharia Biomédica da Universidade do Porto

agradecimentos

À Professora Sandra Rebelo, pela orientação da tese, entusiasmo e pelos conhecimentos partilhados. Por de, certa forma, ter acompanhado o meu percurso académico, começando como minha primeira tutora que me recebeu na UA, em 2008, e terminando como minha orientadora de tese de Mestrado, cinco anos depois. Obrigada.

À Professora Odete da Cruz e Silva agradeço por me ter proporcionado a experiência enriquecedora de trabalhar no laboratório de Neurociências. Muito obrigada.

À Mariana, por tudo aquilo que não consigo expressar por palavras... O quanto eu te agradeço por teres estado sempre ao meu lado, mesmo quando eu não pedi. Por todo o apoio incondicional, força, tranquilidade, amizade e pelos laços que criámos. Admiro-te muito pelo teu profissionalismo mas, fundamentalmente pelo ser humano excepcional que és. Por todos os gestos e por todas as atitudes que me ficaram no coração. Obrigada por teres feito de mim o que sou hoje, por todos os ensinamentos e palavras certas nos momentos certos. Não me esqueço nunca de quem me faz bem e, por isso, sei que nunca me vou esquecer de ti. Foi um privilégio trabalhar contigo e tenho imenso orgulho em ti, em nós. Mais do que um agradecimento, é dizer que te valorizo imenso e que gosto muito de ti.

À Filipa Martins, por teres estado sempre pronta a ajudar nos momentos em que mais precisei, apesar das "minhas asneiras"! Pelo teu profissionalismo e pelo apoio desmedido que me deste quando me viste quase a ser vencida pelo cansaço.

À Pati, por me teres feito rir sempre nos momentos piores, pelo grande apoio e por teres estado ao meu lado sempre. Pelos conselhos, pela compreensão, pelo teu coração e pela tua força enorme. Guardo em mim cada gesto teu.

À Lili, pela tua sensibilidade, pelo apoio, pelo teu abraço e carinho. Pelos teus gestos que eu não esqueço. Ao Roberto e à Regina por terem sido sempre impecáveis comigo. À Rochinha pelo ânimo e à Oli pela tranquilidade.

A todos os meus colegas de Mestrado que embarcaram comigo nesta aventura. Por estarmos sempre uns para os outros. Que assim seja sempre, porque somos o futuro e mesmo não conseguindo mudar tudo, podemos sempre tentar mudar o nosso bocadinho. A ti Ju, pelo teu carácter, apoio e compreensão. Pela tua força, pelo impacto das tuas palavras. À Ana Maria, pelo companheirismo e apoio, pelas sugestões, força e carinho. Por estares sempre disposta a ajudar e pelas gargalhadas que demos juntas. À Catarina e à Luísa, por estarem sempre comigo, pela preocupação, pelos conselhos, pelos risos, pela alegria, pela ajuda e por nunca me terem falhado quando eu precisei. À Marta pelo apoio e pela tranquilidade. À Sónia, João e ao Mega, pelo apoio, companheirismo e pelas brincadeiras malucas. A todos por estarem sempre lá para mim. Gosto muito de vocês!

À FCT pelo financiamento dos projetos, REEQ/1023/BIO/2005, PTDC/QUI-BIQ/101317/2008, Pest-OE/SAU/UI0482/2011

A todos os colegas e investigadores do Laboratório de Neurociências, Laboratório de Transdução de Sinais e Laboratório de Biogénese de Organelos. À Mónica por todo o apoio e simpatia.

Àqueles que eu admiro e que dizem muito em poucas palavras.

À minha Família, em especial aos meus Pais e irmão. Aos tios e primos.

Aos meus Amigos de sempre.

Muito obrigada a todos, sem vocês nada disto teria sido possível, sem a força de cada um de vocês nada se teria concretizado. Este trabalho não é só meu, é nosso.

palavras-chave

Proteína 1B associada com a lâmina (LAP1B); membrana interna nuclear (INM); lamina nuclear; invólucro nuclear (NE); microtúbulos; mitose; RNA de interferência pela variante de *short hairpin* (shRNA).

resumo

A proteína 1B associada com a lâmina é uma proteína intrínseca da membrana interna nuclear que está abundantemente expressa nos tecidos neuronais, nomeadamente no estriado, tronco cerebral e cerebelo. A LAP1 está associada com a lâmina nuclear e pensa-se que estabiliza a arquitetura do invólucro nuclear (NE). A função da LAP1B ainda não é compreendida, mas pensa-se que serve de local de ligação entre a lâmina e a membrana interna nuclear. Além disso, a LAP1 pode estar também envolvida na organização dos microtúbulos do fuso mitótico durante a mitose. Uma vez que a função da LAP1 não é conhecida, induziu-se o *knockdown* em células de neuroblastoma humanas através da estratégia de RNA de interferência pela variante *short hairpin*, para mimetizar o comportamento da célula na ausência da LAP1. Através de *immunoblotting* e de microscopia de fluorescência, confirmou-se a diminuição dos níveis da LAP1B, assim como da LAP1C, uma isoforma ainda não sequenciada até ao momento. Novamente, por *immunoblotting*, os níveis intracelulares da lâminaB1, α -tubulina acetilada e da Polimerase poli ADP-Ribose (PARP) foram avaliados por uma análise global da integridade celular. Por microscopia confocal, a morfologia dos núcleos celulares e a distribuição da α -tubulina acetilada foram observados para analisar a integridade do invólucro nuclear. Os nossos dados sugerem que a LAP1B parece ser essencial para a distribuição da α -tubulina acetilada e, conseqüentemente, para a estabilidade dos microtúbulos durante a mitose. Existem evidências que a outra isoforma parece desempenhar um papel mais importante na morfologia e integridade do invólucro nuclear. Ambas as isoformas parecem desempenhar um papel essencial na regulação da mitose. Contudo, são necessários estudos adicionais para confirmar estes resultados e desvendar a função específica das isoformas da LAP1 durante a mitose.

keywords

Lamina-associated polypeptide 1B (LAP1B); inner nuclear membrane (INM); nuclear lamina; nuclear envelope (NE); microtubules; mitosis; short hairpin RNA interference (shRNA).

abstract

Lamina-Associated Polypeptide 1 (LAP1) is a type two integral inner nuclear membrane (INM) protein that is abundantly expressed in neural tissues, namely striatum, mid-brain and cerebellum. LAP1 protein is associated with nuclear lamina, which is thought to stabilize the nuclear envelope (NE) architecture. The function of LAP1 protein is not already understood but it is thought to function as a lamina attachment site into the inner nuclear membrane (INM). Additionally, LAP1 may also be involved in assembly of mitotic microtubule spindle during mitosis. Since the function of LAP1 remains unknown, we induced the knockdown of LAP1, in human neuroblastoma cells, through the short hairpin RNA interference strategy, in order to mimic the cellular behavior in the absence of LAP1. Through immunoblotting and fluorescence microscopy, we confirmed the decrease of intracellular levels of LAP1B as well as in another isoform not sequenced so far. Once more, through immunoblotting, the levels of laminB1, acetylated α -tubulin and cleaved poly ADP-Ribose Polymerase (PARP) were evaluated for an overall analysis of cellular integrity. By confocal microscopy, cell nuclei morphology and acetylated α -tubulin distribution were observed to analyze the nuclear envelope integrity. Our data suggest LAP1B seems to be essential for acetylated α -tubulin distribution and, therefore, for microtubule stability during mitosis. There is evidence that the other isoform seems to play a more pronounced role in nuclear envelope integrity and morphology. Together, both isoforms seem to play an essential role in mitosis regulation. However, further studies are required to confirm these results and unravel the specific function of LAP1 isoforms during mitosis.

ABBREVIATIONS

AA	Antibiotic Antimycotic
AAA ⁺	ATPases - ATPases Associated to several cellular Activities
Ago	Argonaute protein
APS	Ammonium Persulfate
BCA	Bicinchoninic Acid
BSA	Bovine Serum Albumin
Bp	Base pairs
cDNA	Complementar Deoxyribonucleic Acid
C1	huLAP1 construct 1
C2	huLAP1 construct 2
CK1	Casein Kinase 1
CK2	Casein Kinase 2
CNS	Central Nervous System
DAPI	4'6-diamidino-2-phenylindole
DNA	Deoxyribonucleic Acid
DGCR8	DiGeorge syndrome Critical Region gene 8
dsRNA	Double-stranded Ribonucleic Acid
ECL	Enhanced Chemiluminescence
EOTD	Early Onset Torsion Dystonia
ER	Endoplasmic Reticulum
<i>E. coli</i>	<i>Escherichia coli</i>
FBS	Fetal Bovine Serum
FDA	Food and Drug Administration
HBV	Hepatitis B virus
HCV	Hepatitis C virus

HIV	Human Immunodeficiency Virus
Hypb	Hydrophobic region
Ig	Immunoglobulin
GC	Guanine-cytosine content
GSK3	Glycogen Synthase 3
huLAP1	Human Lamin-Associated Polypeptide 1
INM	Inner Nuclear Membrane
LAP	Lamin-Associated Polypeptides
LB	Loading Buffer
LB medium	Luria-Bertani medium
LBR	Lamin B Receptor
LD	Luminal Domain
LGB	Lower Gel Buffer
LEMD3	LEM domain-containing protein 3
LINC	Linker of Nucleoskeleton and Cytoskeleton Complex
MEM	Minimal Essential Medium
miRNA	Micro Ribonucleic Acid
mRNA	Messenger Ribonucleic Acid
NE	Nuclear Envelope
NLS	Nuclear-Localization Signal
NPC	Nuclear Pore Complex
NRBOX	Nuclear Receptor Box Motif
ONM	Outer Nuclear Membrane
PARP	Poly (ADP-Ribose) Polymerase
PACT	PKR activating protein
PBS	Phosphate Buffered Saline
PCR	Polymerase Chain Reaction

PLK	Polo-Like-Kinase
Pol II/III	RNA Polymerase II/III
PP1	Protein Phosphatase 1
pri-shRNA	Primary shRNA Transcript
PTD	Primary Torsion Dystonia
Ran	Ras related GTPase
RE	Restriction Enzyme
RISC	RNA-induced Silencing Complex
RLC	RISC Loading Complex
RNAi	Ribonucleic Acid interference
rpm	Rotations per minute
rRNA	Ribosomal Ribonucleic Acid
RT-PCR	Reverse Transcription Polymerase Chain Reaction
SDS	Sodium Dodecyl Sulphate
SDS-PAGE	Sodium Dodecyl Sulphate - Polyacrylamide Gel Electrophoresis
SEC	shRNA Expression Cassette
siRNA	Small interfering Ribonucleic Acid
shRNA	Short hairpin Ribonucleic Acid
SS	Signal Sequence
TAE buffer	Tris-Acetate-EDTA buffer
TBS	Tris-Buffered Saline solution
TBST	Tris-Buffered Saline solution with Tween detergent
TE	Tris-EDTA buffer
TEMED	N, N, N', N'-Tetramethylethylenediamine
TM	Transmembrane Domain
TorA	TorsinA
Tor1AIP1	TorsinA Interacting Protein 1

TRBP	Tat-RNA-binding protein
UGB	Upper Gel Buffer
UTR	Untranslated Region
WR	Working Reagent

INDEX

INTRODUCTION	15
1. EUKARYOTIC CELL NUCLEUS	17
2. INNER NUCLEAR MEMBRANE PROTEINS	20
2.1. LAMINA-ASSOCIATED POLYPEPTIDES	20
2.1.1. LAMINA-ASSOCIATED POLYPEPTIDES 1 (LAP1)	21
2.1.1.1. LAP1 TOPOLOGY AND TISSUE DISTRIBUTION	21
2.1.1.2. LAP1 ISOFORMS	23
2.1.1.3. HUMAN LAP1B ISOFORM	24
2.1.1.4. LAP1 PUTATIVE FUNCTIONS	25
2.1.1.5. LAP1 INTERACTION WITH LAMINS DURING MITOSIS	25
2.1.1.6. LAP1 INTERACTION WITH TORSINA	27
3. IMPACT OF THE INNER NUCLEAR MEMBRANE PROTEINS IN HUMAN DISORDERS	29
4. RNA INTERFERENCE STRATEGY	32
4.1. SHORT HAIRPIN INTERFERING RNA STRATEGY	34
4.2. shRNA MECHANISM	36
4.3. APPLICATIONS OF RNAi AND shRNA BENEFITS	38
AIMS	41
MATERIALS AND METHODS	45
5. shRNA SEQUENCE DESIGN	47
5.1. SELECTION OF TARGET SEQUENCES	47
5.2. OLIGONUCLEOTIDES DESIGN	48
6. CLONING INTO RNAi-READY pSIREN-RETROQ VECTOR	49

6.1. shRNA OLIGONUCLEOTIDES ANNEALING	49
6.2. LIGATION OF OLIGONUCLEOTIDES INTO pSIREN VECTOR	50
6.3. BACTERIAL TRANSFORMATION AND DNA ISOLATION.....	51
6.3.1. TRANSFORMATION OF <i>E.coli</i> XL1-BLUE	51
6.3.2. EXTRACTION OF PLASMID DNA - ALKALINE LYSIS METHOD	51
6.3.3. DNA RESTRICTION AND ELECTROPHORETIC ANALYSIS	52
6.4. DNA SEQUENCING	53
6.4.1. DNA PURIFICATION WITH COLUMN QIAQUICK	53
6.4.2. PCR SEQUENCING	53
6.4.3. PRECIPITATION OF AMPLIFIED DNA.....	54
6.5. DNA ISOLATION AND PURIFICATION	54
6.5.1. MAXIPREP DNA PURIFICATION SYSTEM	54
6.5.2. DNA PRECIPITATION AND CONCENTRATION MEASUREMENT	55
7. CELL CULTURE	55
7.1. RESAZURIN CELL VIABILITY ASSAY	56
7.2. TRANSIENT TRANSFECTION WITH shRNA CONSTRUCTS	56
7.2.1. TRANSIENT TRANSFECTION USING LIPOFECTAMINE 2000™	56
7.2.2. TRANSIENT TRANSFECTION OF SH-SY5Y USING TURBOFECT™	57
8. BCA PROTEIN CONCENTRATION ASSAY	58
9. SDS-POLYACRILAMIDE GEL ELECTROPHORESIS (SDS-PAGE)	59
10. IMMUNOBLOTTING.....	58
10.1. MEMBRANES INCUBATION	58
10.2. IMMUNODETECTION.....	60
11. IMMUNOCYTOCHEMISTRY	61
12. CONFOCAL MICROSCOPY	62

RESULTS	63
13. GENERATION OF HUMAN LAP1 shRNA CONSTRUCTS	65
13.1. SELECTION OF TARGET SEQUENCES	65
13.2. OLIGONUCLEOTIDES DESIGN	67
13.2.1. shRNA OLIGONUCLEOTIDES ANNEALING	69
13.2.2. RESTRICTION ANALYSIS	70
13.2.3. DNA SEQUENCING	70
14. ESTABLISHMENT OF SH-SY5Y CELLS TRANSFECTION CONDITIONS FOR huLAP1 shRNA CONSTRUCTS	71
14.1. OPTIMIZATION OF CELL TRANSFECTION CONDITIONS	72
14.1.1. 24 HOURS POST-TRANSFECTION	73
14.1.2. 48 HOURS POST-TRANSFECTION	74
15. To DETERMINE THE EFFECTS OF huLAP1 KNOCKDOWN USING BIOCHEMICAL ASSAYS	77
16. To EVALUATE THE EFFECTS OF huLAP1B/C KNOCKDOWN IN CELLULAR INTEGRITY BY MICROSCOPY	81
DISCUSSION	83
CONCLUDING REMARKS	91
FUTURE PERSPECTIVES	95
REFERENCES	99
APPENDIX	107

INTRODUCTION

1. EUKARYOTIC CELL NUCLEUS

The eukaryotic cells are essentially constituted by the plasma membrane, the cytoplasm (containing the cytosol, cytoskeleton and cell organelles) and the nucleus. The latter is a highly specialized and spherical-shaped organelle that is enclosed within the nuclear envelope (NE), which delimits the nuclear content from the cytoplasm components, separating the activity of both cellular compartments (**Figure 1A**). The nucleus is the most prominent cell organelle which contains the genetic information packaged into chromatin, which is composed of DNA and chromosomal proteins (histones). Additionally, the nucleolus is also a nuclear component, where the rRNA is synthesized, as well as nucleoplasmic fibrils that are involved in processing and transport of mRNA to cytoplasm. Therefore, the nucleus is considered a quite essential organelle for genome integrity and stability, DNA replication and gene expression (1–3).

The nuclear envelope connects the nucleus and the cytoplasm through the linker of the nucleoskeleton and cytoskeleton complex (LINC), which is formed by integral SUN proteins of the inner nuclear membrane (INM) and nesprin proteins of the outer nuclear membrane (ONM). The NE is essentially composed of nuclear pore complexes (NPCs), the nuclear lamina and the double-membrane system that comprises the INM and the ONM (**Figure 1B**) (3–5). The NPCs are protein structures with different polypeptides subunits, which join both nuclear membranes, allowing the exchange of some substances between cytoplasm and nucleoplasm. Between the dual membrane there is also a perinuclear lumen separating the INM and ONM (3,4,6).

The nuclear lamina is a fibrous network of protein fibrils that can be interpreted as a cytoskeletal structure, since it is composed by intermediate filaments and membrane associated proteins (5,7). Accordingly, lamina is quite important for cell structure and mechanic stability. The nuclear lamina is composed of several proteins known as lamins, which were also found in nucleoplasm beyond their concentration in nuclear periphery (8). Such findings suggested that lamins may be required for cell cycle regulation, chromatin organization, DNA replication, differentiation as well as apoptosis (2,9). Furthermore, lamins also bind chromatin and function as anchoring site, for instance, for interphase chromosomes

and membrane associated proteins. It has been suggested that lamina controls the assembly and reformation of NE, its size and shape (5,7,10).

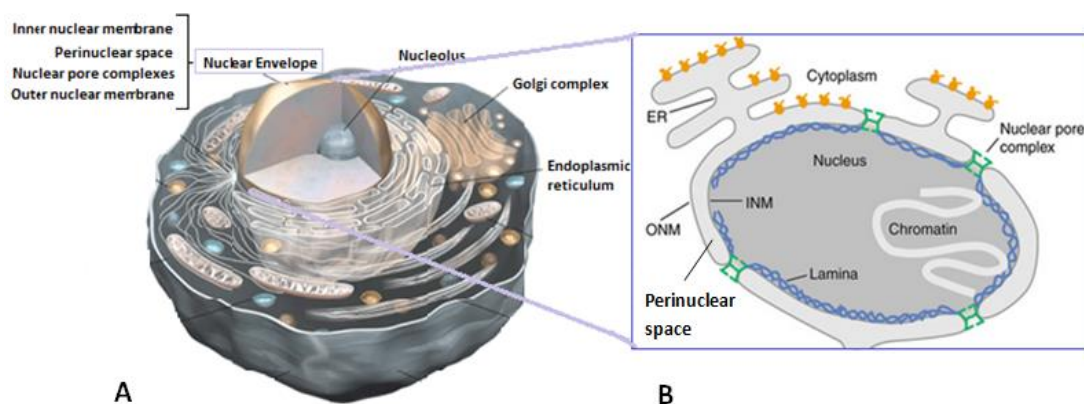


Figure 1 - Schematic representation of the nuclear envelope and nuclear membranes. A) The NE is a double-membrane system, continuous with the ER, which encloses the nuclear compounds, essentially the nucleolus, nuclear lamina and chromatin. Among nuclear membranes there is a lumen termed perinuclear space. **B)** The NE is comprised of a dual membrane divided into the ONM and INM. This double membrane system separates nuclear contents from the cytoplasm. Both membranes are joined by NPCs, which also appear to regulate the transport between nucleus and cytoplasm. The ONM is biochemically similar to peripheral ER and the INM contains a set of integral membrane proteins, many of which bind to lamins and/or to chromatin. In higher eukaryotes, the NE is lined by a protein network, the nuclear lamina, which is an attachment site for NPCs and chromatin. *ER*, inner nuclear membrane; *INM*, inner nuclear membrane; *NE*, nuclear envelope; *NPC*, nuclear pore complex; *ONM*, outer nuclear membrane. Adapted from (11,12).

In mammalian eukaryotic cells, the nuclear lamina mainly contains one to four nuclear lamins that are type V intermediate filament proteins. They are classified as lamins A, B1, B2 and C and are similar to intermediate filaments in their structure and biochemical properties. Additionally, lamins can be categorized according to their primary sequence and expression pattern as A-type and B-type lamins. The A-type lamins comprises the lamin A and lamin C, which are alternatively spliced products of the same gene, the *LMNA* gene, being only expressed in differentiated cells and tissues (13). The B-type lamins are expressed in every embryonic and somatic tissues studied. In vertebrates, lamins B1 and B2 are specialized for meiosis and early embryogenesis and have a similar sequence but they arise from different genes, the *LMNB1* and *LMNB2* genes, respectively. The lamins share a common globular N- and C-terminal domains and a nuclear-localization signal (NLS) close to four α -helical segments (coil 1a, coil 1b, coil 2a and coil 2b) that are separated by a non- α -helical linker sequence. The lamin structure is represented in **Figure 2** (2,3,5).

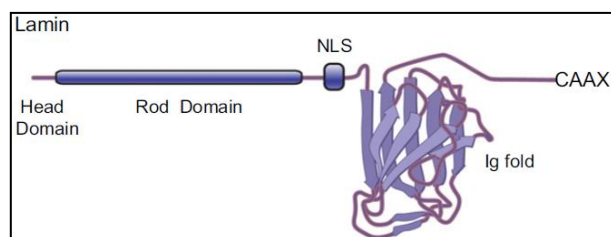


Figure 2 - Generic lamin structure with several characteristic domains. Lamins comprise a helical rod domain highly conserved among all intermediate filament proteins, the head and tail domains. Within the tail domain, there is a NLS and an Ig fold. Most lamins contain at their C-terminal a CAAX motif that allows chemical reactions, leading to protein modification. *Ig*, immunoglobulin; *NLS*, nuclear-localization signal. Taken from (14).

The outer nuclear membrane is continuous with the rough endoplasmic reticulum (ER), containing few proteins, like nesprins, and is covered by ribosomes. In turn, the INM is continuous with the nuclear lamina and includes a particular group of integral membrane proteins (**Figure 3**), which interact with nuclear lamins, remaining closely associated with the nuclear lamina (2,3,15). As shown below, the INM proteins include, for example, the firstly identified Lamin B Receptor (LBR), SUN proteins, MAN1/LEMD3 (LEM domain-containing protein 3), Emerin and the Lamina-Associated Polypeptides (LAPs). The latter will be extensively discussed during this work.

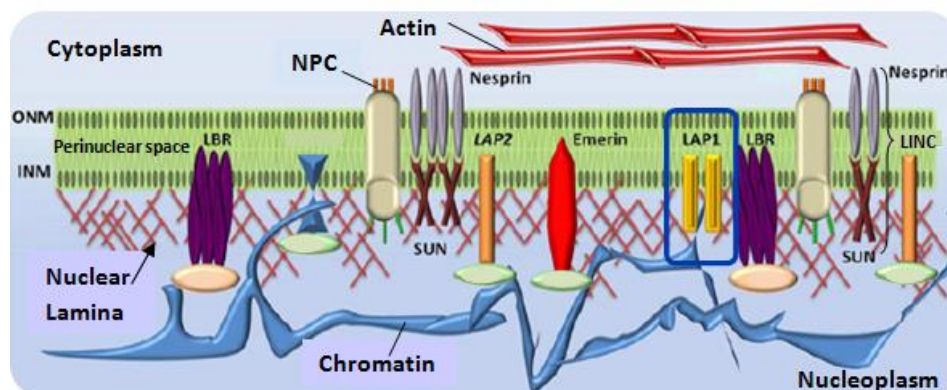


Figure 3 - Inner nuclear membrane proteins and their associations with lamina and nuclear contents. The INM is associated with the nuclear lamina and chromatin. The integral INM proteins like LBR, SUN, emerin, LAP1 and transmembrane isoforms of LAP2 bind to lamina components and chromatin. SUN proteins of the INM bind to nesprins in the ONM, composing the LINC complex. SUN proteins bind to lamins and some nesprin isoforms bind to cytoskeletal proteins, like actin. *INM*, inner nuclear membrane; *LAP*, lamin-associated polypeptides; *LBR*, lamin B receptor; *LINC*, linker of nucleoskeleton and cytoskeleton complex; *NPC*, nuclear pore complex; *ONM*, outer nuclear membrane. Adapted from (16).

2. INNER NUCLEAR MEMBRANE PROTEINS

Integral proteins of the inner nuclear membrane are synthesized on the rough ER and reach the INM through lateral diffusion where they are retained by nuclear ligands (17). The INM is composed of approximately 70 transmembrane proteins, many of which interact with the nuclear lamina and/or chromatin proteins, being related with chromatin organization and postmitotic reassembly of the nucleus (18). As mentioned before, among the INM proteins are lamin B receptor (LBR), MAN1, Emerin, SUNs and LAPs. Loss-of-function studies in biologic models suggested that proper expression of several integral INM proteins is essential for normal development (11,14). For example, the loss of expression of the LBR leads to the aggregation of heterochromatin in the nuclei of neutrophils, showing to be essential for their morphological maturation (19). Additionally, it is known that loss of emerin in humans causes significant cardiac and skeletal muscle disease and the deletion of genes encoding SUN proteins mainly results in cell migration and nuclear positioning defects (14,20).

2.1. Lamina-Associated Polypeptides

Lamina-associated polypeptides (LAPs) are integral membrane proteins, since they are permanently attached to the inner nuclear membrane. Thus, LAPs are biochemical markers for INM integrity and are very useful models for nuclear membrane biogenesis studies (5).

Most of NE membrane proteins are localized in the INM, including LAPs that were primarily identified in NE fractions extracted from rat livers. These results were achieved by immunogold labeling of the RL13 and RL29 antibodies that recognizes LAPs. Therefore, the latter were specifically localized in INM (4,5). Three rat LAP1 isoforms were identified: LAP1A, LAP1B, LAP1C through RL13 antibody and another distinct protein, LAP2, was detected by the RL29 antibody (4,5,15).

Fluorescence microscopy analysis of both LAP1 and 2 revealed that they are localized in the nuclear periphery. Therefore, is reasonable to deduce that both variants may be involved in attaching lamins to the NE, since the co-localization of LAPs and lamins is quite similar (**Figure 4**). The association between LAPs and nuclear lamina was also supported by the results of chemical extraction of NE, which showed the presence of almost the entire LAP1A, B and LAP2 in the pellet along with insoluble lamins. Regarding LAP1, the localization

of RL13 epitope on nucleoplasm, where lamina is found, also contributed to this conclusion (4).

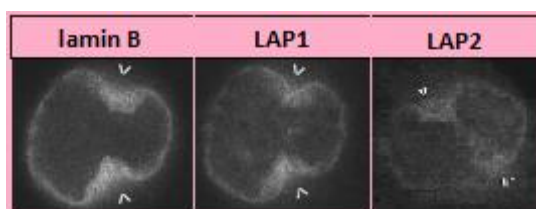


Figure 4 - Immunolocalization of B-type lamins and LAPs (LAP1 and LAP2). Immunofluorescence microscopy images of the lamin, LAP1 and LAP2 during the prophase. LAP1, LAP2 and lamin B are well localized in perinuclear region during prophase. *LAP*, Lamin-Associated Polypeptides. Adapted from (21).

LAP2 proteins are type two integral membrane proteins that are also divided into isoforms, α , β , γ , δ , ε and ξ , which are products of alternative splicing of a single individual gene, *TMPO*. Some findings show that LAP2 associates only with lamin B1 and directly with chromosomes, when the protein is phosphorylated. It is likely that LAP2 may play a role in initial reassembly of NE and also in the association between membrane and chromosomes (2,4).

2.1.1. Lamina-Associated Polypeptides 1 (LAP1)

2.1.1.1. LAP1 topology and tissue distribution

Integral membrane proteins can be synthesized differently and they assume different types, depending on its organizational structure. LAP1s are type two integral membrane proteins, since their amino-terminal domains face the nucleoplasm, being potential binding partners of nuclear proteins (17,22). LAP1 includes a long hydrophilic N-terminal nucleoplasmic portion, a single hydrophobic transmembrane domain and a shorter luminal C-terminal domain (**Figure 5**). The conserved C-terminal and transmembrane domains are encoded by a single exon in both in rat, mouse and human, suggesting that LAP1 isoforms differ only in their nucleoplasmic domain (2,23).

Kyte/Doolittle hydrophobicity analysis revealed that rat LAP1C has a single transmembrane domain located between residues 311-333. Based on that, residues 1-311 could be located on the nucleoplasm and residues 334-506 in the perinuclear space or *vice*

versa. The topology of rat LAP1s was established using the anti-LAP1 RL13 antibody (6). The RL13 epitope was shown to localize in the nucleoplasm (5). Several deletion constructs of rat LAP1C were prepared to determine whether they are immunoadsorbed by anti-LAP1 RL13. Full-length LAP1C and the deletion construct comprising amino acids 1-325 was immunoadsorbed by RL13 antibody. A construct where the residues 129-303 were deleted was unreactive with RL13 antibody. Therefore, a nucleoplasmic localization of the amino-terminal sequence of LAP1C was established and, consequently, the C-terminal is confined to luminal domain, located within membranes as represented in **Figure 5** (6).

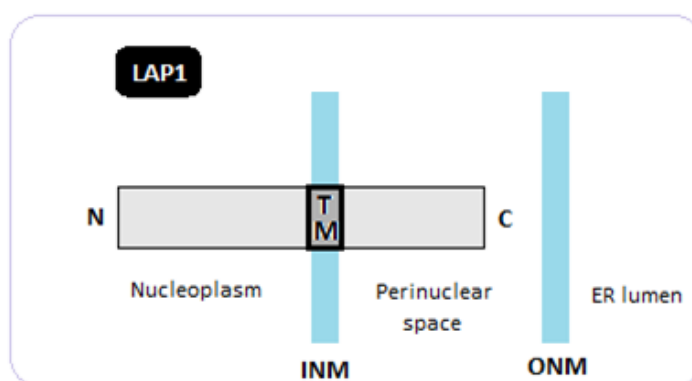


Figure 5 - Schematic representation of LAP1 protein structure. LAP1 protein is an inner nuclear membrane protein, which is composed by a N-terminal domain localized in the nucleoplasm, a TM domain and a shorter C-terminal domain localized in the luminal space. The later domains are encoded by only a single exon (common to all isoforms) while the longer N-terminal of LAP1 sequence is the site where the alternative splicing occurs, yielding the three isoforms of the protein: LAP1A, LAP1B and LAP1C. *ER*, endoplasmic reticulum; *INM*, inner nuclear membrane; *LAP1*, lamin-associated polypeptide 1; *ONM*, outer nuclear membrane; *TM*, transmembrane. Adapted from (23).

LAP1s are closely related INM proteins present in most cell types, being expressed in both neural and non-neural tissues (**Figure 6**). LAP1 protein is essentially present in striatum, mid-brain and cerebellum, concerning to neural tissues. Additionally, LAP1 is abundantly expressed in non-neural tissues, namely the kidney, liver and heart (23,24).

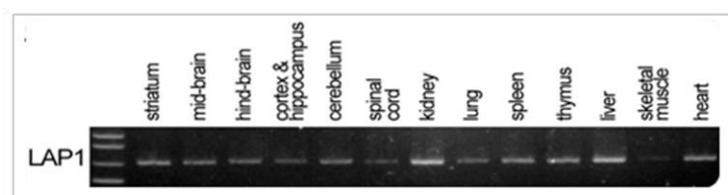


Figure 6 - Tissue distribution of mouse LAP1. RT-PCR of mouse LAP1 from whole extracted tissue RNA. *LAP*, Lamin-Associated Polypeptides; *RT-PCR*, Reverse Transcription Polymerase Chain Reaction. Taken from (23).

2.1.1.2. LAP1 isoforms

LAP1 protein is expressed in three isoforms in rat, LAP1A, LAP1B and LAP1C, resulting from alternative splicing of the same gene: *TOR1AIP1* (1,6,25). The isoforms are closely related based on their cross-reaction with RL13 antibody (6). However, they differ in the N-terminal region and their expression during development is supposed to be distinct. These alterations of expression may contribute for nuclear structure regulation (5,6,26). Such information was obtained from several rat studies, since the information about rat LAP1 sequences is known and available: rat LAP1C isoform was the only full-length cDNA sequenced (6). A class of rat LAP1 cDNAs was isolated, which contains two protein-coding nucleotide insertions in LAP1C sequence. These probably encode part of rat LAP1A/B, since the isolation of independent LAP1C-like cDNAs are likely to contain partial length clones derived from LAP1A/B. Thus, rat LAP1A and 1B sequences were partially characterized since they are believed to consist of rat LAP1C with 2 additional insertions (1,25).

Rat LAP1A is the 75 kDa LAP1 isoform, which seems to have the strongest association with lamins A, B1 and C. As LAP1A, rat LAP1B (68 kDa) strongly interacts with these same lamins (2,4,6). Both isoforms interact indirectly with mitotic chromosomes (4–6). The rat LAP1C (55 kDa) is the only rat LAP1 isoform with a complete determined 506 aminoacid sequence (6) and the most abundant in cultured cells (4,6,21). LAP1C was not shown to interact with any lamin *in vitro*, but there are evidence of association with lamin A and C *in vivo* (4). The nuclear localization of LAP1C is likely to change, depending on lamin A presence and seems to be the only integral protein capable of moving between nucleus and cytoplasm. It was reported the LAP1C translocation between INM and ONM in undifferentiated murine embryonal carcinoma P19 cells. However, when the cells were transfected with lamin A, LAP1C accumulated at the INM, what suggests lamin A as a potential LAP1C binding protein. (10). Other research reports that LAP1C might be part of a multimeric complex including the LAP1A isoform and B-type lamins, for example (2,10).

Regarding LAP1 isoforms in humans, less information is available. In fact, no evidence of a predicted human LAP1A was seen until now and human LAP1C (huLAP1C) is only partially known. Two additional insertions in one huLAP1C clone were reported when it was compared with human LAP1B (huLAP1B) (25), as previously described for rat LAP1C and LAP1B (6). Unpublished data from our laboratory indicated that at least two isoforms are present in

humans (**Figure 7**). The 68 kDa isoform corresponds to the well characterized huLAP1B and the other, for comparison with rat isoforms, it is believed to be huLAP1C. These results are now being confirmed by mass spectrometry (Santos, M., unpublished data). However, at this moment, this is only a putative huLAP1C but, for simplicity, for now long we will always call it huLAP1C, during this work.

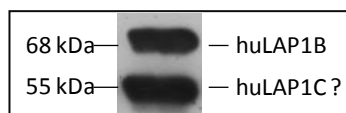


Figure 7 - Human LAP1B (68 kDa) and human LAP1C (55 kDa) isoforms in SH-SY5Y cells. *huLAP1B*, human LAP1B; *huLAP1C*, human LAP1C.

2.1.1.3. Human LAP1B isoform

The gene *TOR1AIP1* encodes 10 exons which are localized on chromosome 1 (1q24.2). The huLAP1B protein includes 584 aminoacids and has no significant homology with known two type INM proteins (23,25,27).

As previously mentioned in LAP1 structure, it includes a short luminal C-terminal, a single transmembrane domain and a longer nucleoplasmic N-terminal. The C-terminal luminal domain is highly conserved, in spite of its function is being unclear. However, there is a putative regulatory role for maintenance of nuclear structure and organization. The huLAP1B is retained within the nucleus through interactions of the nuclear components with the nucleoplasmic portion of the protein. The N-terminal nucleoplasmic domain is responsible for interaction with lamins as well as chromosomes and, together with the transmembrane (TM) span, it allows the proper localization of huLAP1B within the nucleus (25,28). Additionally, the N-terminal includes several phosphorylation sites. Nevertheless, the function of LAP1 phosphorylation is still poorly understood (27). A bioinformatic approach of huLAP1B also revealed the presence of a nuclear receptor box motif (NRBOX) in the luminal domains, which allows binding to a nuclear receptor (27).

In order to clarify the function of huLAP1B and its targeting mechanism to INM, it would be significant to recognize the binding proteins and explore them (25). It was shown that huLAP1B nucleoplasmic domain interacts directly with lamins A, C and B1 and possibly indirectly with chromosomes (4,5). Moreover, the luminal domain of LAP1 was found to

associate with torsinA (torA) (23), the protein involved in DYT1 dystonia (further described). In addition, LAP1 co-immunoprecipitated with all four members of the human torsin family: torsinA, torsinB, torsin2 and torsin3 (29). Recently, huLAP1B was found to interact with protein phosphatase 1 (PP1) in yeast two hybrid screens(27,30,31). Specifically, PP1 interacts with huLAP1B through a known PP1 binding motif located in the nucleoplasmic domain. Thus, huLAP1B may be dephosphorylated by PP1 (27). Indeed, LAP1 was found to be phosphorylated in several residues, but the kinases involved are not well described. However, rat LAP1B was found to be phosphorylated by cyclin-dependent kinase 1 on Ser142 (homologous to huLAP1B Ser143) (32).

2.1.1.4. LAP1 putative functions

The function of LAP1 remains unclear, although it has been hypothesized that LAP1 isoforms may have a role as lamina attachment sites and assembly in the INM (4–6). Additional putative functions have been related with the arrangement and structure of lamin filaments and reassembly of the NE at the end of mitosis (7). Since torsinA is an interacting protein of huLAP1, it is being hypothesized that LAP1 is a substrate or a cofactor of torA, though it is not totally clear yet. LAP1 may be responsible for catalytically activate torsinA AAA⁺ function (ATPase associated to several cellular activities), stimulating ATP hydrolysis. Thus, LAP1 may work as a positive regulator of torA ATPase activity (23,33). Additionally, a recent report suggests that LAP1 is associated with the mitotic microtubule spindle assembly (29). Such putative function arose from a LAP1 knockdown approach, in which the spindle formation was impaired in prometaphase. Thus, the centrosomes only formed weak mitotic asters and failed to align chromosomes, leading to cell death (34).

2.1.1.5. LAP1 interaction with lamins during mitosis

During mitosis, the nuclear membranes lose their identity as a subcompartment of the ER, supporting the notion that the sorting of specific membrane proteins to the NE is driven by binding interactions at chromosome surfaces, at the end of the mitotic process (7). Thus, LAP1 is dispersed throughout the ER membranes, however, depending on the mitotic phase (**Figure 8**), LAP1 localization may diverge slightly (7).

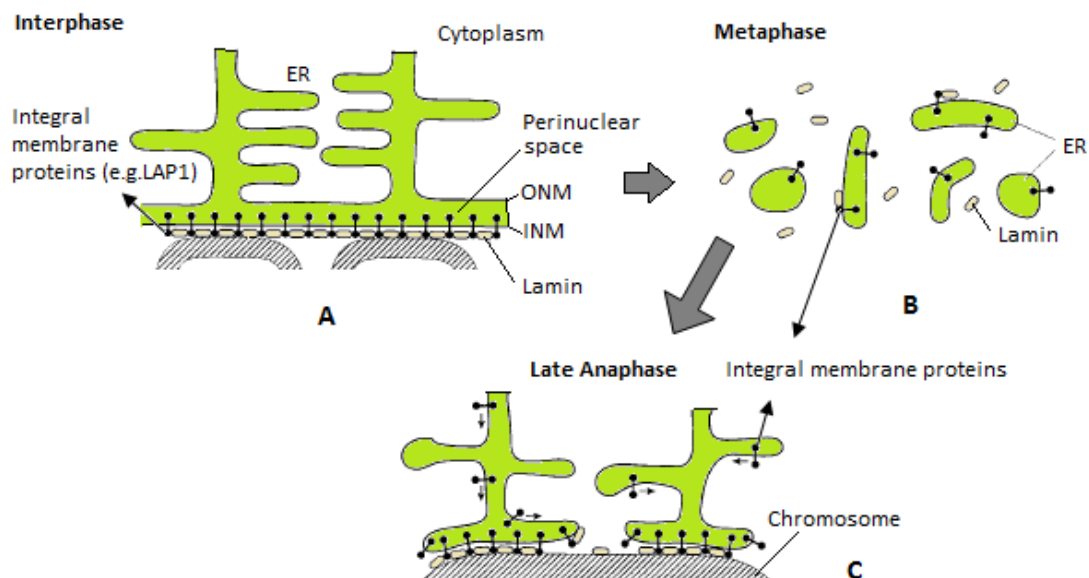


Figure 8 - Distribution of inner nuclear membrane proteins during mitosis. A) The interphase NE is morphologically continuous with the peripheral ER but is a specialized ER subcompartment that contains integral membrane proteins specific to the INM. For instance, the LAP1 forms multimeric assemblies which are associated with B-type lamins during interphase. **B)** The NE breaks down in prophase and it becomes difficult to distinguish it from other components of the peripheral ER. Here, inner nuclear proteins as LAP1 seemed to remain localized all over the ER, as well as in metaphase. **C)** It was proposed that proteins are resorted to the NE during late anaphase and subsequently associate with binding sites at the chromosomes. Reformation of the NE may involve cooperative assembly of lamins and integral proteins of the INM. *ER*, endoplasmic reticulum; *INM*, inner nuclear membrane; *LAP1*, lamin-associated polypeptides 1; *NE*, nuclear envelope; *ONM*, outer nuclear membrane. Adapted from (7).

During interphase, LAP1 forms multimeric assemblies which are associated with B-type lamins. LAP1 was visualized in a nuclear edge pattern in the ER, whose membranes were seen as a widespread vesicular network extending from the nuclear envelope to the cell periphery (7,21). Afterwards, in prophase, the NE breaks down and it becomes difficult to distinguish it from other components of the peripheral ER, where LAP1 is also present homogeneously. Then, the NE is disassembled in prometaphase, during which LAP1 seemed to remain localized all over the entire ER, as well as in metaphase, persisting until the mid-anaphase (7). Subsequently, in late anaphase, nuclear membranes reassemble through the association of membrane vesicles with chromosome surfaces and through the membrane fusion. Thus, there are evidence of LAP1 starting to be segregated from endoplasmic membranes at chromosomes periphery (4,7). In addition, in some late anaphase cells, LAP1 remaining in the peripheral ER were not uniformly localized, but appeared to be concentrated

in particular elements of ER. Finally, LAP1 was exclusively perinuclear during the telophase, in which it was more concentrated because of the increasing of the nuclear envelope surface area and the reduced synthesis of other proteins (7).

2.1.1.6. LAP1 interaction with torsinA

The torsinA (torA) protein is one of the LAP1 interacting proteins, which deserves particular emphasis. LAP1 is also termed torsinA interacting protein 1 (tor1AIP1) due to LAP1-torsinA interaction, which occurs via the conserved luminal domain of LAP1 that is common to all LAP1 isoforms (23,35). TorsinA is primarily located in the ER (36) but it was also found in the NE. The mutant form of torA, which causes DYT1 dystonia, is relocated to the NE (37). LAP1 luminal domain (LD) was shown to be implicated in controlling the subcellular localization of torA, since LAP1 seems to recruit torsinA to the NE. This conjecture derives from the observation that the ectopic expression of LAP1 constructs that include the LDs change the subcellular localization of TorA, but constructs that lack them do not. Afterwards, it was concluded that LAP1 associates with torA (**Figure 9**), preferentially in its ATP-bound form, through LD interaction (23,33).

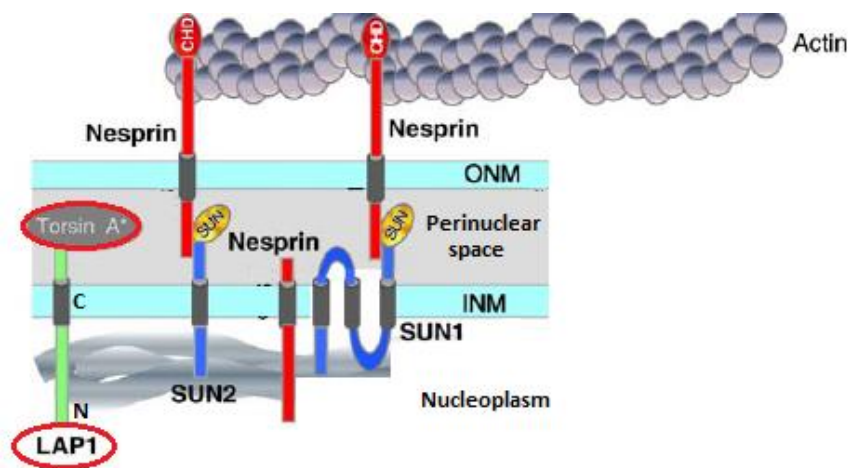


Figure 9 - Schematic representation of INM proteins and nucleoplasmic proteins, specifically LAP1 and torsinA interaction in perinuclear space. TorsinA interacts with luminal domain of LAP1. *INM*, inner nuclear membrane; *LAP1*, lamina-associated protein 1. Adapted from (13).

The torsinA protein is encoded by the *TOR1A/DYT1* gene that includes 5 exons and is located on chromosome 9q. The torA is a 332-aminoacid protein that belongs to torsin proteins family, which are members of the AAA⁺ ATPases superfamily. TorA is predominantly

localized in the continuous lumen of the ER and NE. This protein is broadly expressed in human tissues but it seems to play the most critical role in the central nervous system, since it is abundantly expressed during development. In adulthood, the expression of torsinA is higher in dopaminergic neurons in *substantia nigra pars compacta*, striatum, cortex, thalamus, hippocampus, cerebellum, brainstem and spinal cord. TorA has been implicated in several cellular central nervous system pathways including NE integrity, cytoskeleton organization, degradation of misfolded proteins, ER stress sensitivity, dynamics of secretory and synaptic vesicles and modulation of dopamine neurotransmission (38).

TorsinA assembles into the hexameric structure of an active AAA⁺ protein and contains an N-terminal ER signal sequence (SS), a hydrophobic region (Hypb) and the characteristic AAA⁺ domain. The latter domain contains the Walker A and Walker B motifs (responsible for ATP hydrolysis), the ATP sensing motifs (sensor I and II) and six conserved cysteine residues. The torsinA structure is represented in **Figure 10** (24,38).

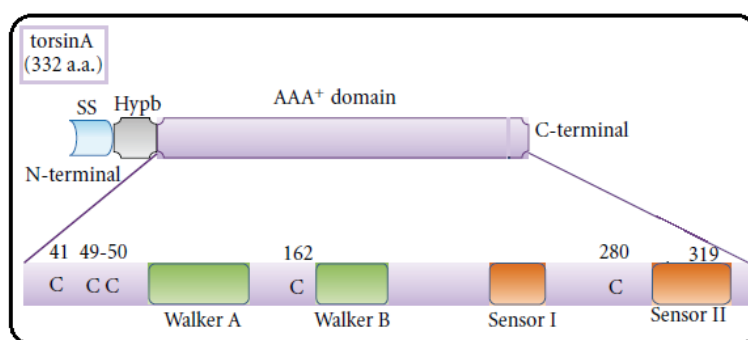


Figure 10 - Schematic representation of torsinA protein. The torsinA includes a signaling sequence, a hydrophobic domain and the AAA⁺ domain. The AAA⁺ domain consists of Walker A/B motifs (green), sensor I/II (orange) motifs, and six conserved cysteines. AAA⁺, *ATPases associated to several cellular activities*; Hypb, *hydrophobic*; SS, *signaling sequence*. Adapted from (38).

LAP1 has been associated with torsinA in the NE, since LAP1 null mice, homozygous lacking tor1A and mutated tor1A share the same abnormal membrane perinuclear inclusions that could not be morphologically distinguished from each other. In heterozygous *TOR1AIP1 knockout* mice there were no alterations from wild-types. On the other hand, the homozygous lacking LAP1 exhibited such membrane bound protuberances derived from the INM. It is often termed bleb formation, which abnormally happens in all brain regions and also in many different non-neural tissues, including the liver, kidney, striated muscle and skin.

Moreover, it was observed perinatal lethality in homozygous *TOR1AIP1* deleted mice which was indeed a very curious and important finding (29).

The ultrastructural changes were visualized in all investigated brain areas, namely striatum, thalamus, cortex and spinal cord, and it seems to impair the interaction torsinA-LAP1 in addition to other binding protein associations. Thus, these observations may mean that torsinA and LAP1 are involved in a widespread biological process to which neurons are more susceptible and, in this way, LAP1 may play a role in a torsinA pathway, which is central in DYT1 dystonia, discussed briefly later (29).

3. IMPACT OF THE INNER NUCLEAR MEMBRANE PROTEINS ON HUMAN DISORDERS

In spite of several diseases be attributable to defects in the NE, its molecular structure remains poorly understood. Alterations in the nuclear membrane may contribute to disease through increased fragility of the nucleus under mechanical stress, structural alterations in chromatin or misregulation of transcription factors, all of which culminate in changes in gene expression (39).

The INM and the lamina seem to have crucial roles in fundamental processes for human health, such as the function of striated muscle, osteogenesis, lipid and glucose metabolism and aging. Thus, an increasing number of diseases have been associated to genes encoding for lamins, integral proteins of the INM and associated proteins, some referred as laminopathies (3). Laminopathies comprise a heterozygous inherited group of disorders that include muscular dystrophies, lipodystrophies and premature aging syndromes, caused by nuclear lamina alterations (13,39). Mutations in the gene encoding for A-type lamins origin several inherited disorders whose injured tissue differs according to the type of mutation. These mutations can affect striated muscle, adipose tissue or multiple systems. For instance, the Emery-Dreifuss muscular dystrophy is one of the most prevalent muscular dystrophies in adulthood as well as the Hutchinson-Gilford progeria syndrome with a premature aging phenotype and the Dunnigan-type familial dystrophy affecting adipose tissue (2,3).

Interestingly, a movement disorder called DYT1 dystonia may also involve huLAP1 protein, since it interacts with torsinA (mutant protein in DYT1 dystonia) and shared similar phenotypes when they were deleted (29). The term “movement disorders” has been evolving

over the years and it represents a set of neurologic dysfunctions based on clinical patterns, in which there is either an excess of motility or a loss of voluntary and autonomous movements. The first group characterized by excessive motion includes the hyperkinesias (uncoordinated and exaggerated movements), dyskinesias (abnormal movements) and atypical involuntary actions. The hypokinesia (decreased amplitude of movement), bradykinesia (slowness of motility) and akinesia (movement loss) are integrated in the movement loss group (40). Here, we will focus on DYT1 dystonia since it is the third most prevalent movement disorder in humans, following the essential tremor and Parkinson's disease, where it is believed that huLAP1 could be involved (38,41).

The term "dystonia" was first used by Oppenheim in 1911 and its definition and classification have changed over time (40). This movement disorder may also be referred as a basal ganglia disorder, since patients with secondary dystonia have lesions in these limbic structures (38). Torsion dystonia has been recognized as a hyperkinetic movement disorder that involves involuntary and sustained muscle spasms that forces twisting and repetitive movements or irregular postures without presenting significant structural brain abnormalities (40,42). Occasionally, dystonic movements are exacerbated by a specific task, such as writing, which is called Writer's Cramp Dystonia (43).

It has been demonstrated that dystonia affects 15 to 30 per 100 000 people. Primary Torsion Dystonia (PTD) accounts for around 75% of dystonic patients and it mainly affects people over fifty years of age, which suggests that it is quite common among aging population. A higher prevalence in Ashkenazi Jews was also reported, which is the result of a mutation that arose about 350 years ago. Dystonia can be classified triply based on age of onset, etiology and its distribution throughout the body (43,44).

This neurologic disorder can occur at any age and it can be divided into early (<26 years) and late onset (>26 years) (43). The age of onset is important because it provides information about the prognosis of dystonia. Normally, the most severe is the DYT1 dystonia which, in turn, can be subdivided into *DYT1* early onset generalized dystonia and non-*DYT1* early onset dystonia (40,45). In what concerns to the symptoms distribution, torsion dystonia can manifest itself as localized in a particular region, segmental (continuous in two regions of body) or multifocal. On the other hand, dystonia can be generalized or only affect one side of

the body (hemidystonia) (43). The etiology approach involves two main dystonia types: the primary and secondary dystonia. The most frequent variant, primary torsion dystonia, occurs when the phenotype arises spontaneously without any existing cause, related disease or neurodegeneration. Focal cervical dystonia is the most recurrent type of focal PTD, which results in aberrant shoulder, neck and head positions. The secondary dystonia has an acquired cause as a result of an environmental factor or brain lesions, namely in basal ganglia, and it describes additional symptomatic features. The usual affected neurologic structures are the caudate, globus pallidus, putamen and thalamus. Furthermore, there are also evidence of cerebellar and brainstem impairment (38,40). Additionally, it is known the “primary-plus dystonia” and the heredodegenerative dystonia. The first is associated with other movement disorder, such as parkinsonism, in the absence of neuronal degeneration and the latter emerges in a context of a neurodegenerative disorder, such as Huntington’s disease (38,43).

The *TOR1A* gene, encoding the torsinA protein, is involved in the most common form of dystonia, the *DYT1* dystonia. Thus, the *DYT1* has been the most studied variant because it is one of the few forms of the disease with a consistent gene mutation found in a great number of patients (28,38,45). The most frequent cause of early onset PTD (around 70%) is a mutation in the coding region of the *TOR1A* gene resulting in a deletion of three base pairs (Δ GAG) in exon 5, that originates a loss of one glutamate residue (Δ E302/303) near the C-terminal of torsinA (**Figure 11**). This mutation is normally referred as mutant torsinA Δ E (26,38,42).

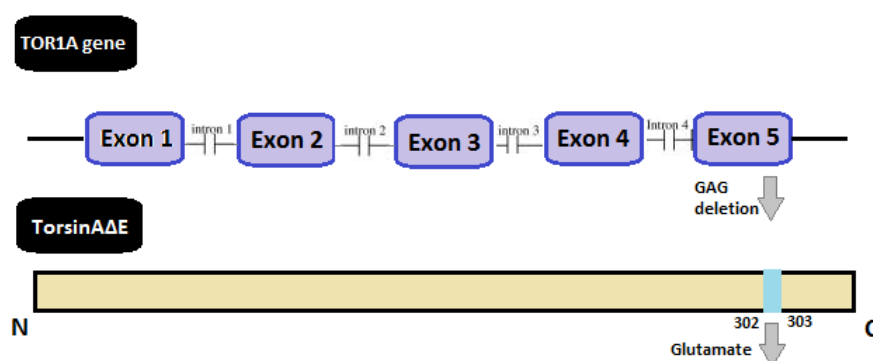


Figure 11 - Diagram of *TOR1A* gene and torsinA protein. The *TOR1A* gene is composed of five exons and the torsinA protein has 332 aminoacids. The mutated *TOR1A* gene comprises a GAG deletion in exon 5, which results in loss of one glutamate residue (Δ E302/303) near the C-terminus. This mutation is the most common cause of early onset dystonia.

In spite of the mutated torsinA Δ E be responsible for most cases of early onset torsion dystonia, as referred previously, it is believed huLAP1 is also involved in the torsinA pathway, in which a disruption of interaction among both may contribute to DYT1 dystonia pathogenesis (26,28,29,35).

4. RNA INTERFERENCE STRATEGY

The RNA interference (RNAi) approach is a natural specific and selective process, through which expression of a targeted gene is knocked down by a double-stranded RNA homologous to its own gene to mimic what happens at a cellular level, if it is absent or weakly expressed. Thus, RNAi is part of the loss-of-function methods such as gene silencing, which represent powerful strategies for unraveling the putative gene function in mammalian cells (46–48). Furthermore, this strategy has been recognized as an effective and resourceful tool in biomedical science which can also be performed in large-scale functional genomics experiments and it has been progressively expanded to clinical field and as a way of gene therapy (48). Despite post-translational gene silencing has been firstly observed in petunia plants, the underlying mechanism was not yet well defined and understood (46,47,49,50). In this case, a gene copy that encodes an enzyme responsible for the anthocyanin floral pigment, chalcone synthase, was inserted into the plants. Surprisingly, it was shown a suppression of the endogenous gene function caused by this additional copy (49,51). Later on 1998, the RNA interference process was described, by Andrew Fire and Craig (52) who tested it using a nematode worm biological model *Caenorhabditis elegans*, whose genome has been discovered through this same process. In these experiments, it was induced sequence-specific gene silencing through the introduction of exogenous dsRNA (46,47,50,51). Afterwards, the RNAi technique was also established in a large range of organisms, such as *Drosophila*, trypanosomes, planaria, hydra, zebrafish and mammals (47,50).

The current model of the RNAi mechanism involves two steps, the initiator and the effector (50,53,54). The first step involves the digestion of the exogenous double-stranded RNA (dsRNA) into small interfering RNAs (siRNAs) mediated by the Dicer enzyme (**Figure 12A**), which is member of the RNase III family of dsRNA-specific ribonucleases (55). The cleavage of the dsRNA is dependent of ATP, generating 19 to 21 basepairs siRNA duplexes with a 3' overhang of two nucleotides. The effector step is achieved when the duplexes bind to a

multicomponent nuclease complex and form the RNA-induced Silencing Complex (RISC) (**Figure 12A**). The latter is then activated by the ATP-dependent unwinding of the siRNA and, subsequently, the complex binds to the substrates through their homology to siRNA by base pairing. The mRNA is targeted for destruction through its cleavage at approximately 12 nucleotides from the 3' end of the siRNA, resulting in gene-specific knockdown (46,54,56).

Recently, the RNAi technology has been considered as one of the greatest accomplishments for the future decades and several variants of regulatory RNAs can be used (50). Among these methods are the small interfering RNAs (siRNAs) (**Figure 12A**), short hairpin RNAs (shRNAs), endogenous or artificial micro RNAs (miRNAs) and bi-functional shRNAs (**Figure 12B**). These interfering RNA variants allow the conserved cellular pathway of RNAi which leads to specific hybridization to the mRNA target and to following degradation or translational repression (47,48).

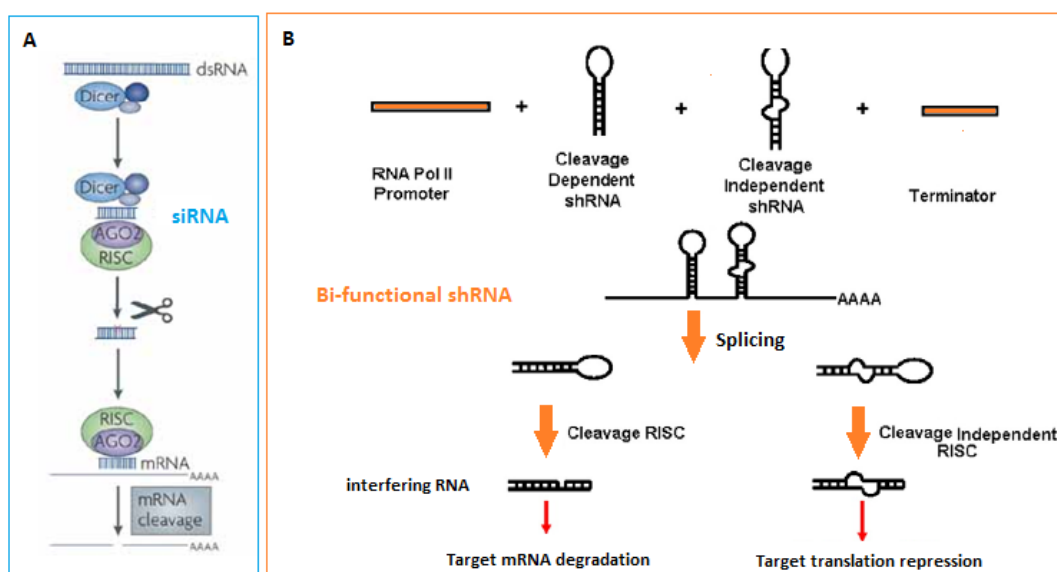


Figure 12 - Variants of RNA interference pathways of different interfering RNAs: siRNA and bi-functional shRNA. A) The siRNA strategy starts with cleavage of long dsRNA by the Dicer enzyme complex into siRNA. Such siRNAs are incorporated into a complex where is present the AGO2 and the RISC. Then, AGO2 cleaves the passenger strand so that active RISC containing the guide strand is produced. This mRNA strand recognizes target sites, resulting in mRNA cleavage. **B)** The bi-functional concept is to design two shRNAs for each targeted mRNA; one with perfect match and other with mismatches. The purpose of the bi-functional design is to promote loading of mature shRNAs onto both cleavage-dependent and cleavage-independent RISCs, for a more efficient knockdown of target mRNA, through mRNA degradation and also via translational repression. *AGO2, Argonaute 2; RISC, RNA-induced Silencing Complex; siRNA, small interfering RNA; shRNA, short hairpin RNA.* Adapted from (48,57).

Some years ago the RNAi technology was considered a remarkable tool in cultured mammalian cells, since siRNAs can selectively suppress gene expression without evidence of non-specific responses, like interferon (47). Nevertheless, owing to the transient nature of the synthetic siRNAs, the activation of the interference mechanism is limited because mammalian cells lose the amplification machinery, which triggers and keeps the gene silencing in *Caenorhabditis elegans* and *Drosophila*. Thus, using siRNAs the silencing of gene expression only lasts a short period no longer than one week (47). However, in 2002, short hairpin interfering RNAs (shRNAs) expressed from RNA polymerase III promoters were constructed by several researchers and the gene expression was suppressed for a longer period of time. Thus, this drawback was successfully crossed over (47).

4.1. Short hairpin interfering RNA strategy

After the breakthrough of siRNAs, vectors engineered to express shRNAs emerged to mediate a long-lasting gene silencing. The target gene silencing occurs after stable transfection of target cells by shRNA expression cassette (SEC) into the host genome, which can be reached by retroviral, lentiviral or adenoviral vectors (47). The producing short hairpin RNA vectors process shRNAs *in vivo* into siRNA-like molecules able to origin gene-specific down-regulation. For this purpose, potential target sites within the gene of interest must be identified, so that the corresponding oligonucleotides can be designed for shRNA generation (46,58). The shRNA oligonucleotide design starts with the selection of a region of 19 nucleotides into the target gene. The candidate sequence ought not to be within the first 75 bases, since the nearby start codon regions may have several regulatory protein binding sites. The untranslated regions (UTRs) and the consecutive run of three or more thymidine residues must also be avoided; the first because UTR-binding proteins and/or translation initiation complexes may interfere with binding of the RISC and the second due to a possible premature transcription termination. Furthermore, the guanine-cytosine content should be considered, ensuring that it is around 40%-60% and the secondary structure of oligonucleotides should be checked too, because it can interfere in the annealing. Finally, it is very important to align some candidate sequences against a suited genome database to verify if there is no homology to other genes (50,59,60).

An usual shRNA oligonucleotide has five bases for the restriction site at the 5' end and one for restriction at the 3' end, 19 bases of sense strand and other 19 of antisense strand. Accordingly, the shRNA contains a perfect double stranded with one of them identical to the target mRNA and another ensuring proper orientation for correct hairpin loop formation. The hairpin loop sequence is composed by 7 to 9 bases linking both strands, in which the most effective is 5'-TTCAAGAGA-3'. After that, there are 6 bases of terminator and, eventually, other 6 of a unique restriction site, which allows the restriction digestion analysis to confirm the presence of the cloned insert (**Figure 13**). Thereby, the result is an oligonucleotide of 63 three to 65 basepairs (46,47,61,62).

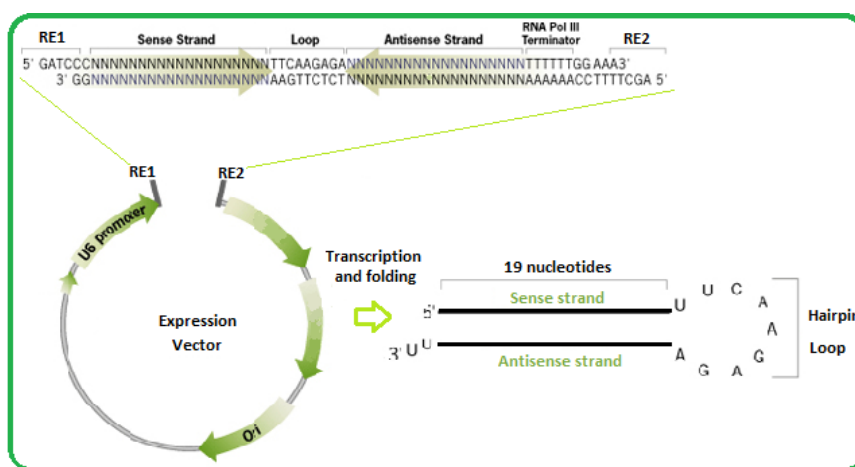


Figure 13 - Schematic representation of a shRNA oligonucleotide. Firstly, the DNA target sequence is chosen. Next, the designed oligonucleotide is inserted into the vector, which is delivered into the host cell. The shRNA is transcribed and folds into a loop structure. *RE1/2*, restriction enzyme 1 and 2; *shRNA*, short hairpin RNA. Adapted from (63).

Once complete the construction, the vectors contain a DNA sequence that encodes the shRNA cloned between a Polymerase III promoter, like the human U6 promoter, and the transcription termination site. These vectors represent a definite improvement in initiating RNAi, as they use the cell's RNA polymerase III enzyme to transcribe the previously designed shRNA. The human U6 promoter provides high levels of expression in numerous cell types, resulting in target gene knockdown (64).

The transcript is terminated at position 2 of the terminator and folds subsequently into a loop structure with 3' overhangs. The shRNA terminations are processed *in vivo*,

converting it into twenty one nucleotides siRNA-like molecules, which in turn trigger the RNA interference (65).

4.2. shRNA mechanism

To be successful, the shRNAs are designed to follow the rules defined by the details of the cellular machinery and are probably processed in the same way to the microRNA maturation pathways. Thus, studies on the synthesis and maturation of miRNAs have provided the background for shRNA synthesis (48,58,66). Once shRNA expression vector introduced into the cell cytoplasm (**Figure 14A**), it is transported to the nucleus for specific shRNA synthesis. Further, the shRNA is processed and transported to the cytoplasm and finally incorporated into the RISC for interference, as will be described below (48,64).

In the nucleus of transfected cells, the shRNA can be transcribed by either RNA polymerase II or III (Pol II or III), through RNA polymerase II or III promoters on the shRNA expression cassette (SEC), respectively (48,50). As a result, the generated primary transcript (pri-shRNA) includes a hairpin loop structure (**Figure 14B**), which is processed by a complex formed by RNase III endonuclease enzyme Drosha and double-stranded RNA-binding domain protein DGCR8 (DiGeorge syndrome critical region gene 8; Figure 13). Such complex measures the hairpin and accurately processes the long primary transcripts into pre-shRNAs (**Figure 14C**) which are individual shRNAs with two nucleotides 3' overhang (48,67). Subsequently, the pre-shRNA is transported to the cytoplasm by the carrier protein exportin 5 through a Ras related GTPase (Ran), followed by loading on the RNase III complex endonuclease Dicer, TRBP (Tat-RNA-binding protein) and PACT (PKR activating protein) (**Figure 14D**). Such complex removes the hairpin to origin the mature shRNA (**Figure 14E**), which is composed by a double-stranded siRNA with two nucleotides 3' overhangs (48).

Afterwards, the dicer containing complex coordinates the mature shRNA loading on the Argonaute 2 protein (Ago-2) containing RISC (**Figure 14F**), since the pre-shRNA has been found to be part of the RISC Loading Complex (RLC), composed of at least Ago-2, dicer and TRBP. Such data may mean that pre-shRNA may directly associate with RLC rather than through a process of two steps via a different Dicer/TRBP/PACT complex (48).

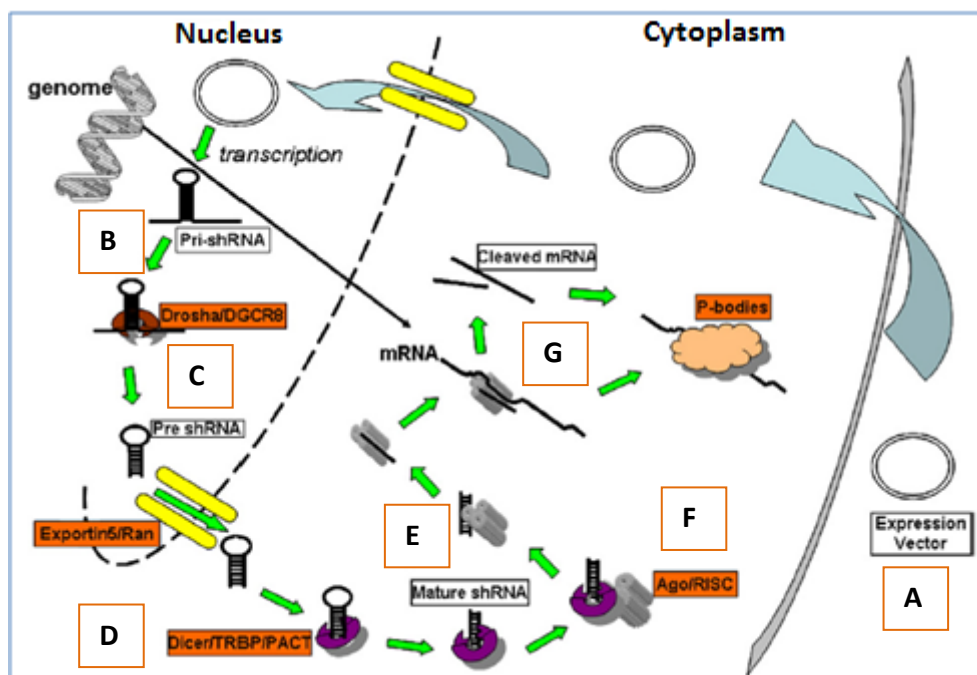


Figure 14 - Representation of the shRNA interference strategy and the involved proteins. The shRNA expression vector is delivered into the cytoplasm (A) and then to the nucleus for being transcribed. The pri-shRNA transcripts are processed (B) and form pre-shRNAs (C), which, in turn, are carried out to the cytoplasm, to be loaded onto the Dicer/TRBP/PACT complex (D), where they become mature (E). Next, they associate with Ago containing RISC (F), providing RNA interference either via mRNA cleavage and degradation, or through translational suppression via p-bodies (G). *Ago*, Argonaute protein; *DGCR8*, DiGeorge syndrome critical region gene 8; *Pri-shRNA*, primary shRNA; *PACT*, PKR activating protein; *RISC*, RNA-induced Silencing Complex; *TRBP*, Tat-RNA-binding protein (48).

After loading onto RLC and passenger strand departure, both shRNA and siRNA should behave equally in the RISC (68). The major component of this complex is the Argonaute family of proteins, of which only Ago-2 exhibits endonuclease activity to cleave the shRNA into a single-stranded stem. Other argonaute proteins also belong to RISC, despite lack of identifiable endonuclease activity. The Ago-2 protein cleaves mRNA to start its degradation, while other Argonaute proteins without endonucleolytic activity bind to partially complementary target sites located at the 3' UTR for translation repression, in processing bodies (p-bodies). Such mechanism in p-bodies is still not totally known, but it is thought to be processed through target mRNA sequestration and deadenylation, leading to its destabilization. Thus, the target mRNA is either cleaved or conformationally changed (**Figure 14G**) following which both types of structures are direct to p-bodies (48).

In conclusion, mature shRNA in the Dicer/TRBP/PACT complex are associated with Ago-2 containing RISC and provide RNAi either through mRNA cleavage and degradation, or through translational suppression via p-bodies (48).

4.3. Applications of RNAi and shRNA Benefits

RNAi has been evolving over the years as a powerful tool for identification of specific targets for several diseases therapy. In addition to research of novel ways for clinical treatments, this technique has also been used to analyze gene function, to recognize and eliminate invading parasites and to create model systems, through quick and simple generation of loss-of-function phenotypes (47,50). For instance, some studies have shown that it is possible to silence a neuron-specific gene in a model system for neuronal differentiation, which may point out to a possible application of RNAi in neurogenesis and differentiation studies in mammals (58).

Indeed, the shRNA producing vectors are the most suitable to human disorders treatment, specifically to reduce or even abolish the abnormal gene expression typical of some diseases, for example, the spinocerebellar ataxia type one, amyotrophic lateral sclerosis and Alzheimer disease (51). Such antisense shRNAs have the potential to selectively knockdown specific cancer targets, allowing an effective personalized treatment, improving the conventional therapies (48). Additionally, this therapeutics useful to attenuate viral and parasite infections, at least *in vitro*, for example hepatitis B and C viruses (HBV and HCV) and human immunodeficiency virus (HIV). Moreover, shRNA strategy was already approved for clinical trial by Food and Drug Administration (FDA) in treating human hepatitis and, more recently, anti-HIV therapies based on RNAi have also been used (50). The effectiveness of this therapeutic method is determined in part by intracellular availability of interfering RNAs, so the current goals are mostly related to development of systems and vectors, for transporting great amounts of dsRNA to the target tissue or organ (51). Normally, the most used vectors are viral because of their high transfection rate and effective integration of exogenous DNA. It is actually important the optimization of shRNA constructs for obtaining powerful and long-lasting effects using few copies of shRNA, since it can be continuously produced by the host cell. It is believed that less than five copies of shRNA integrated in host genome are enough to achieve an effective gene knockdown, whereas additional copies are required in siRNA

approach. Thus, such difference in copy numbers may result in less off-target effects in shRNA strategy, which can also be explained by the endogenous processing and nuclear regulation, after the transcription of shRNAs. Therefore, the siRNA method is more susceptible to degradation in cytoplasm, which provides a higher probability of off-target silencing (48,69).

RNAi therapy has been shown to be well tolerated in several animal models, allowing the transition into the medical field. So, further investigation of the features and limitations of such techniques is crucial before large-scale applications become routine (48,50). For example, *in vitro* data have shown that the introduction of both synthetic siRNA and shRNA oligomers can trigger a partial interferon response, because the insertion of dsRNA more than about thirty basepairs into mammalian cells may result in activation of a similar pathway to the mechanism against viral infection, which can result in overall degradation of mRNA and thus broad inhibition of translation (48,70,71).

Even so, the ability of this valuable tool of reducing gene expression marks a major biomedical advance in the development of human disease therapies, mostly for dominantly inherited disorders (50), such as the early onset torsion dystonia already addressed in this work.

AIMS

RNA interference approaches represent powerful strategies for unraveling putative gene functions in mammalian cells. Since the function of LAP1 remains poorly understood, we induced the knockdown of huLAP1 through the short hairpin RNA interference strategy - in order to mimic the cellular behavior in the absence of huLAP1. It is thought that LAP1 plays a role in the maintenance of the NE architecture by binding to lamins and chromosomes, but this is not well described.

Additionally, LAP1 is an interacting partner of the torsinA protein, the mutated protein in DYT1 dystonia, and can recruit torsinA to the NE. Thus, huLAP1 may also be involved in the physiological/pathological torsinA pathway. Therefore, it is believed that LAP1 can have a high relevance in biomedical field and more studies would be surely required to determine its specific function.

The specific goals of this dissertation are the following:

- To generate LAP1 shRNA constructs using the pSIREN-retroQ vector;
- To establish the SH-SY5Y cells transfection conditions for both LAP1 shRNA constructs;
- To determine the effects of huLAP1 knockdown using biochemical assays;
- To evaluate the effects of huLAP1 knockdown in cellular integrity by microscopy analysis.

The methodology carried out in this work was mostly based on “Knockout™ RNAi Systems” protocol of *Clontech* (Catalogue No. 631528).

MATERIALS AND METHODS

RNA INTERFERENCE - shRNA STRATEGY

5. shRNA SEQUENCE DESIGN

The effectiveness of shRNA methodology in the knockdown approach depends on choosing the proper target sequence within the gene of interest (*TOR1AIP1*) and the suitable design of oligonucleotides to generate the shRNA.

5.1. Selection of target sequences

Two regions of 19 nucleotides of the *TOR1AIP1* sequence (NM_001267578.1) were chosen according to some criteria. The sequences within 5' and 3' untranslated regions and nearby regions of the start codon (within 75 bases) could not be selected, since they may have regulatory protein binding sites which may interfere with the binding of the interfering RISC. The target sequences that contain a consecutive run of 3 or more T residues were also avoided, because it can cause premature termination of the transcript.

Additionally, the GC content of the 19 nucleotides should also be calculated, being around 40% and 60%. The selection of the candidate sequences was made according to criteria mentioned above, through the *Clontech designer tool* (**Figure 15**), available on <http://bioinfo.clontech.com/rnaidesigner/sirnaSequenceDesignInit.do>.

RNAi Target Sequence Selector

Accession Number (example: NM_000546)

Sequence (min length 75 nt)

```
AGGGAAGGGGCCGGCTCGCC
CCTCAAAATGGCGGACAGCGATGCGCCTGCGTACAGAACTCCTCCGTC
GCGCCAGGGCCGGCGGAAG
TGAGGTTCTCGGACGAGCCGCCAGAAGTGTACGCGACTTCGAGCCCTG
GTGGCCAAAGAAAGTCCCC
GTTGGGAAAACGAACCCGGCTAGAAGAGTTCGGTCCGATTCTGCGAAAG
AGGAAGTGAGAGAAAGCGG
TACTACCTTCGGTCTAGGCAGCGGAGGCAGCCGACCCAGGAAACCGA
GGAAATGAAGACGCGAAGGA
CTACCCGCCTTCAGCAGCAGCACTCAGAGCAGCCTCCGCTACAGCCGTCT
CCTGTTATGACCAGGAGAGG
```

Number to return

Sort by

Hairpin max Tm

Optimal GC(%)

Potential RNAi target sequences

Figure 15 - Clontech RNAi target sequence selector. The *TOR1AIP1* sequence was introduced to obtain potential target sequences (<http://bioinfo.clontech.com/rnaidesigner/sirnaSequenceDesignInit.do>).

As a result, 20 candidate target sequences were obtained and blast searches were performed through <http://blast.ncbi.nlm.nih.gov/Blast.cgi>. Such tool yielded the comparison between the candidate sequences and genome database to identify specific target sequences within the gene of interest with no significant homology to additional genes. Therefore, two distinct shRNA target sequences were properly selected.

5.2. Oligonucleotides design

A synthesis of two complementary oligonucleotides was required, a top strand and a complementary bottom strand, for each shRNA target sequence. For this purpose, inserting the selected target sequence into the online designer tool of *Clontech*, available on <http://bioinfo.clontech.com/rnaidesigner/oligoDesigner.do>, the oligonucleotides were properly designed (**Figure 16**).

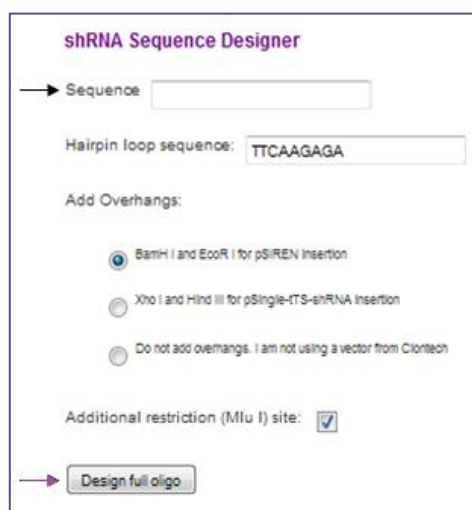


Figure 16 - Designing of oligonucleotides through the shRNA sequence designer (*Clontech*). The selected target sequence is inserted (black arrow) in shRNA sequence designer tool and then the complementary oligonucleotide pair is properly designed (purple arrow).

The designed sequences were highly purified, ensuring a higher percentage of full-length nucleotides, which allowed the cloning of the complete and functional insert.

The sequences of the oligonucleotides included:

- Restriction sites that enable directional cloning of the oligonucleotides into the vector: the *Bam*H I restriction site overhang on the 5' top strand and the *Eco*R I restriction site overhang on the 5' bottom strand;

- A target sense sequence with 19 nucleotides;
- A 7-9 nucleotide hairpin loop sequence, normally the 5'-TTCAAGAGA- 3' sequence;
- A target antisense sequence with 19 nucleotides;
- A RNA Pol III terminator sequence, which consists of a 5 or 6 thymidine residues;
- A unique restriction site (*Mlu* I), downstream of the terminator sequence, for restriction digest analysis to verify the presence of the shRNA oligonucleotides into the RNAi-Ready pSIREN-RetroQ Vector after the ligation;
- One base for the restriction site at the 3' end (when digested with *Eco*R I).

These oligonucleotides were commercially synthesized by *Nzytech*.

6. CLONING INTO RNAi-READY pSIREN-RETROQ VECTOR

The Knockout RNAi System from *Clontech* includes the RNAi-Ready pSIREN-RetroQ vector (*see appendix*) that uses the cell's own Pol III to transcribe a designed shRNA, using the human U6 promoter. Retroviral infection allowed the introduction of shRNA into the cell with high efficiency and moderate shRNA expression. Two different oligonucleotides were selected and further cloned, in order to interfere with two different regions of the huLAP1B, further mentioned. Thus, each respective top and bottom strands of the oligonucleotide were annealed and then ligated into the vector. The same procedure was followed for a negative control missense oligonucleotide.

6.1. shRNA oligonucleotides annealing

Each oligonucleotide (*Nzytech*) was resuspended in TE buffer to a concentration of 100 μ M. Next, the oligonucleotides were mixed at 1:1 ratio (10 μ L + 10 μ L), which resulted in 50 μ M of each double-stranded oligonucleotide (assuming 100% of annealing). Then, the mixture was added to the thermal cycler (*Mastercycler personal, Eppendorf*):

- Heat at 95°C for 30 seconds (to disrupt the hairpin and promote the intermolecular annealing);
- Heat at 72°C for 2 minutes;
- Heat at 37°C for 2 minutes;
- Heat at 25°C for 2 minutes

The mix was stored at -20°C until the ligation was performed.

6.2. Ligation of oligonucleotides into pSIREN vector

The pSIREN-RetroQ vector was previously digested with *EcoR* I and *Bam*H I restriction endonucleases (*New England Biolabs* - *NEB*). The annealed oligonucleotides were diluted with TE buffer to a concentration of $0,5\ \mu\text{M}$. Therefore we ensured that they were in appropriate amount to perform ligation with good efficiency. Subsequently, a ligation reaction for each of two oligonucleotides was assembled.

For each ligation ($20\ \mu\text{L}$), the following reagents (*Clontech*) were mixed in a microtube:

- $13,75\ \mu\text{L}$ of nuclease-free H_2O ;
- $2\ \mu\text{L}$ of 10X T4 DNA Ligase Buffer;
- $1,25\ \mu\text{L}$ of linearized pSIREN vector ($20\ \text{ng}/\mu\text{L}$);
- $2\ \mu\text{L}$ of diluted, annealed oligonucleotide ($0,5\ \mu\text{M}$);
- $1\ \mu\text{L}$ of 10X shRNA Ligation Enzyme Mix ($10\ \text{mg}/\text{mL}$).

It was also made a ligation using a negative control shRNA annealed oligonucleotide (*Nzytech*), simultaneously. The reaction mixture was incubated during 3 hours at room temperature to perform the ligation (**Figure 17**) and then stored at -20°C until the transformation has been performed.

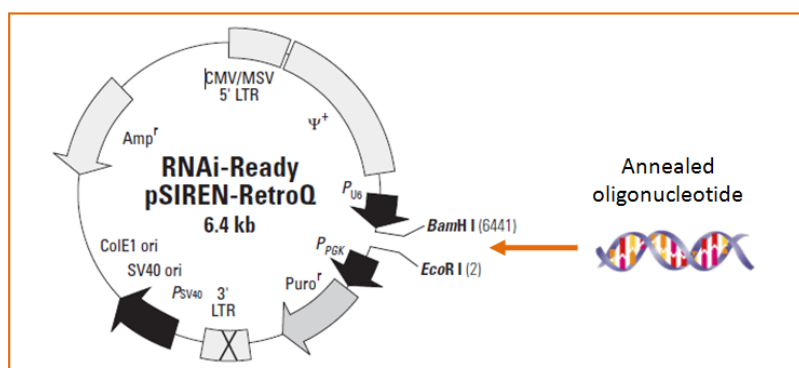


Figure 17 - Schematic representation of the ligation of the oligonucleotide to pSIREN-retroQ vector. RNAi-Ready pSIREN-RetroQ is provided as a linearized vector designed to express a short hairpin RNA (shRNA) and is digested with *Bam*H I and *Eco*R I.

6.3. Bacterial transformation and DNA isolation

After the ligations, bacteria cells were transformed with the pSIREN-retroQ constructs in order to obtain high yields of plasmid DNA for further isolation.

6.3.1. Transformation of *E.coli* XL1-Blue

Subsequently, 50 μ L of *E.coli* XL1-Blue competent cells were thawed on ice and 5 μ L of each DNA ligation were added to cells. Then, the microtube was incubated on ice during 20 minutes, followed by a thermal shock at 42°C in water bath for 70 seconds. Next, the microtubes were placed on ice again for 2 minutes and, subsequently, 450 μ L of SOC medium (*see appendix*) was added to each tube. The microtubes were incubated at 37°C for 60 minutes with shaking at 170 rpm. After that, the culture was centrifuged at 14000 rpm during 1 minute and the supernatant was discarded. The pellet of cells was resuspended in the remaining liquid and spread on the LB/ampicilin plates, which were incubated at 37°C for 16 hours, until the arising of colonies. Control transformations were also performed simultaneously. These included a negative control transformation of vector without DNA.

6.3.2. Extraction of plasmid DNA - alkaline lysis method

A single colony was inoculated into a test-tube with 3 mL of LB medium/ampicilin and then incubated at 37°C overnight with shaking at 170 rpm. Subsequently, 1.5mL of the culture was poured to a microtube, followed by a centrifugation at 14000 rpm during 90 seconds (all centrifugations were performed at 4°C). The supernatant was discarded and the pellet was resuspended in 100 μ L of solution I (*see appendix*) and mixed by vortexing. Then, it was added 200 μ L of solution II (*see appendix*) and mixed through five gentle inversions, placing it on ice immediately. Lastly, 150 μ L of solution III (*see appendix*) was mixed by ten careful inversions. The mixture was then incubated 5 minutes on ice and, next, a centrifugation was performed during 10 minutes (14000 rpm). The clear supernatant was transferred to a new microtube and 2.5 volumes of ethanol 100% were added in order to precipitate the DNA. After incubation at -20°C during 1 hour, samples were centrifuged for 20 min at 14000 rpm and 4°C. The supernatants were discarded and the pellets rinsed with 750 μ L of 70% ethanol, and then samples were incubated for 5 minutes at -20°C before new centrifugation for 5 minutes at 14000 rpm and 4°C. After discarding the supernatant, the pellet dried at 37°C for 1 hour

and then was resuspended with 50 μL of water with RNase (20 $\mu\text{g}/\text{mL}$). The DNA was conserved at -20°C until the accomplishment of a restriction analysis.

6.3.3. DNA restriction and electrophoretic analysis

A restriction analysis of plasmid DNA was performed to figure out if the pretended DNA oligonucleotides were efficiently cloned.

For DNA restriction, the reaction was made according to manufacturer's instructions, with the following reagents (NEB):

- Buffer 10X (NEB buffer 3);
- BSA 100X;
- 1 μL of *Mlu* I restriction enzyme (10 U/ μL);
- 1 μL of *Sal* I restriction enzyme (20 U/ μL).

The mix solution was completed with distilled water to achieve the volume of 20 μL . Once the mix reaction was ready, 10 μL of the mix reaction was added per 2 μL of DNA into a microtube. Finally, the samples were incubated at 37°C during 2 hours for enzymatic digestion, before further analysis by electrophoresis. The required amount of agarose (0,8% gel) was weighed and dissolved with 1X TAE buffer. The agarose was heated until dissolved and homogenized. The electrophoresis apparatus (*Bio-Rad*) was prepared and the comb was correctly placed. The agarose solution was allowed to cool to 60°C and then the ethidium bromide (0,5 $\mu\text{g}/\text{mL}$) was added and gently mixed. The gel was poured into the gel tray until polymerization. The appropriate amount of 6X Loading Buffer (LB) was added to the DNA samples. Distilled water was added to make up the volume, when appropriate. The gel was placed into the electrophoresis tank, covered with 1X TAE (*see appendix*) and the comb was removed carefully. Then, DNA marker (DNA 1 Kb Plus Ladder, *Invitrogen*) was loaded into the gel as well as the DNA samples. The gel run approximately 50 minutes at 100 Volts. The gel was visualized and analysed in an ultraviolet light transilluminator (*Alphamager[®] HP System, Alpha Innotech*) and photographs were taken.

6.4. DNA sequencing

The DNA samples were purified and amplified by PCR for further sequencing to confirm the presence and sequence of the oligonucleotides.

6.4.1. DNA purification with column QIAquick

Five volumes of PB buffer (*Qiagen*) were added to each DNA sample and mixed by vortexing. The mixture was transferred to a QIAquick column (*Qiagen*) and then a centrifugation was made at 14000 rpm during 1 minute. The supernatant was discarded followed by addition of 750 μ L of PE buffer (*Qiagen*) to the column. After that, another centrifugation of 1 minute was performed (14000 rpm) and the filtrate was discarded. The column was inserted into a new tube and 50 μ L of Milli-Q water was added into the center of the column. A last centrifugation of 1 minute (14000 rpm) was made to elute the DNA that was further stored at -20°C.

6.4.2. PCR sequencing

A PCR reaction was assembled for each ligation mixture, by combining the following reagents in a PCR tube:

- 1,5 μ L of 10X U6 Forward Sequencing Primer (*Clontech - see appendix*);
- 4 μ L of Sequencing Mix (composed of dye terminators, deoxynucleoside triphosphates, *ampliTaq* DNA polymerase, FS, *rTth* pyrophosphatase, magnesium chloride and buffer) (*Applied Biosystems*);
- 4 μ L of purified DNA.

The mix solution was made up with distilled water to achieve the volume of 20 μ L.

The samples were well mixed and placed into the thermal cycler, using the following program:

- Heat at 96°C for 1 minute;

25 cycles of:

- 96°C for 30 seconds;
- 42°C for 15 seconds;

- 60°C for 4 minutes.

The samples were purified after PCR by ethanol and sodium acetate precipitation.

6.4.3. Precipitation of amplified DNA

After the PCR, the samples were transferred to microtubes and 2,5 volumes of ethanol 100% were added, followed by addition of 1/10 of 3M sodium acetate (pH = 5.2) to each sample. They precipitated on ice during 30 minutes. After that, a centrifugation at 13000 rpm of 20 minutes (4°C) was performed. The supernatant was discarded and 250 µL of ethanol 70% was also added. It was stored 5 minutes at -20°C and then another centrifugation was made at 13000 rpm of 5 minutes (4°C). The supernatant was discarded and the pellet dried at 37°C during 1 hour, approximately. The DNA samples were sequenced using an automated DNA sequencer (*ABI PRISM 310, Applied Biosystems*).

6.5. DNA isolation and purification

The *E. coli* bacteria were transformed, as described previously, with the recombinant DNA and subsequently isolated and purified through “Maxiprep DNA Purification System” (*Promega*) to obtain higher amounts of DNA.

6.5.1. Maxiprep DNA purification system

Once the *E.coli* transformation, a pre-culture of a single colony was performed as previously and then 1 mL of each culture was transferred to 1L of LB medium with ampicillin (50 µg/µL). The culture was incubated overnight at 37°C with shaking at 170 rpm. Later, each culture was divided into four 250 mL tubes and centrifuged at 4,000 g for 15 minutes. The supernatants were discarded and the pellets resuspended in 30 mL of Ressuspension Solution (*see appendix*). Then, 30 mL of Lysis Solution (*see appendix*) was added and mixed by gently inversions until the solution becomes clear and viscous. Then, 30 mL of Neutralization Solution (*see appendix*) were also added and carefully inverted. Next, a centrifugation was performed at 15000 g during 15 minutes (slow deceleration). Each supernatant was transferred to a new 250 mL tube. Then, 0.5 volume of isopropanol was added, followed by a centrifugation of 15000 g for 15 minutes (slow deceleration). The supernatant was discarded and the DNA pellet was resuspended in 4 mL of Milli-Q water. After that, 15 mL of Wizard

Maxipreps DNA Purification Resin (*Promega*) were added to DNA solution. Next, the mix resin/DNA was transferred to a PureYield™ Maxi Binding Column (*Promega*) and vacuum was applied. The column was washed with 25 mL of Column Wash Solution (*see appendix*) and vacuum was again applied. This step was repeated twice. Then, 10 mL of ethanol 80% was added to the column and vacuum was again turned on. The column was assembled into a 50 mL tube and a centrifuged at 1300 g during 5 minutes. The supernatant was discarded and the column was placed into the vacuum system to dry. The column was then placed into a new 50 mL tube and 3 mL of 65°C pre-heated nuclease-free water was added. After 1 minute, the DNA was eluted through two centrifugations at 1300 g during 5 minutes each.

6.5.2. DNA precipitation and concentration measurement

After DNA isolation by Maxiprep system, the samples were transferred to microtubes and 2,5 volumes of ethanol 100% were added, followed by addition of 1/10 of 3M sodium acetate (pH = 5.2) for each sample and let to precipitate at -20° overnight. Later, a centrifugation at 13000 rpm of 20 minutes (4°C) was performed. The supernatant was discarded and 700 µL of ethanol 70% was also added. It was stored 5 minutes on ice and then another centrifugation was made. The supernatant was discarded and the pellet dried at 37°C during 1 hour, approximately. The pellet was resuspended in 50 µL of Milli-Q water. The DNA concentration and the purity ratio (260/280 nm) were measured on a *NanoDrop Spectrophotometer ND-1000 (Thermo Scientific)*. The DNA samples were conserved at -20°C.

7. CELL CULTURE

SH-SY5Y human neuroblastoma cells are derived from the cell line SK-N-SH (ATCC, Barcelona, Spain; CLR-2266), from a bone marrow biopsy of neuroblastoma patients. The cells were grown in Minimal Essential Medium (MEM):F12 (1:1), supplemented with 10% Fetal Bovine Serum (FBS) with 2 mM L-glutamine, 100 U/mL penicillin and 100 mg/mL streptomycin (Antibiotic/antimycotic (AAs, *Gibco*) - complete SH-SY5Y cell medium. Cultures were maintained at 37°C and 5% CO₂ and were subcultured whenever they achieved 90-95% of confluence.

7.1. Resazurin cell viability assay

The resazurin viability assay is a fluorescence assay that detects metabolic activity in cells. The blue nonfluorescent resazurin reagent is reduced to highly fluorescent resorufin (pink colour) by dehydrogenase enzymes in metabolically active cells. This conversion only occurs in viable cells and, thus, the amount of resorufin produced is proportional to the number of viable cells in the sample. The resorufin formed in the assay can be quantified by measuring the relative fluorescence units.

It was added 10% of resazurin/SDS% solution to SH-SY5Y cell medium (1 mL) and the plate was shaken. The plates were incubated at 37°C during 4 hours. Then, the cell medium was removed and the absorbance was measured through 570 and 600 nm, using the *Infinite M200* (Tecan).

7.2. Transient transfection with shRNA constructs

7.2.1. Transient transfection using Lipofectamine 2000™

According to the manufacturer's protocol (*Invitrogen*), Lipofectamine 2000™ transfection reagent is a cationic liposome which forms a complex with negatively charged DNA molecules to overcome the electrostatic repulsion of the cell membrane. The complexes are thought to deliver nucleic acids through endosomes after endocytosis of the complex, although the exact mechanism for gene transfection mediated by cationic liposomes is still unclear (**Figure 18**).

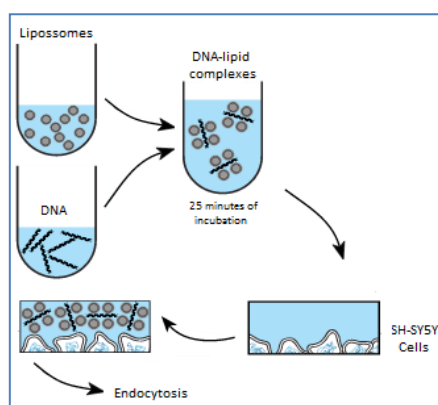


Figure 18 - Mechanism of action of Lipofectamine 2000™ transfection reagent. Lipofectamine is a cationic liposome based reagent that functions by complexing with nucleic acids, allowing them to overcome the electrostatic repulsion of the cell membrane and to be endocytosed. Adapted from *Invitrogen*.

SH-SY5Y human neuroblastoma cells were grown in 6-well plates at a density of $2,0 \times 10^6$ of cells per plate, using complete SH-SY5Y cell medium until 90% of confluence. The DNA (2 μg and 5 μg) and Lipofectamine 2000™ (*Invitrogen*) were each diluted in SH-SY5Y serum- and AAs-free medium and incubated for 5 minutes at room temperature (1 μg of DNA to 2 μg of Lipofectamine). Then, the DNA solution was added to the diluted Lipofectamine tubes, drop by drop, followed by gentle mixing with the micropipette. In order to form the DNA-lipid complexes, the tube was allowed to rest for 20 minutes at room temperature. Afterwards, the solution was carefully added, drop by drop, into the 6-well plates containing AAs-free medium. Cells were incubated at 37°C and 5% CO₂. The cell medium was replaced 6 hours after transfection and cells further incubated at 37°C and 5% CO₂ for 24 hours and 48 hours. At these time points, cells were harvested by adding boiling 1% SDS. The cell lysates were then boiled (10 min), sonicated (10 seconds) and stored at -20°C for further using.

7.2.2. Transient transfection of SH-SY5Y using TurboFect™

According to the manufacturer's protocol (*Thermo Scientific*), the TurboFect™ Transfection Reagent is a sterile solution of a proprietary cationic polymer in water, which interacts with DNA. Such polymer forms positively-charged, stable and highly diffusible complexes that are endocytosed. The "proton-sponge" effect of TurboFect™ buffers endosomal pH by provoking massive proton accumulation and passive chloride influx. Rapid osmotic swelling causes endosomal rupture, allowing translocation of DNA to the nucleus (**Figure 19**). These complexes protect DNA from degradation and facilitate efficient plasmid delivery into cells.

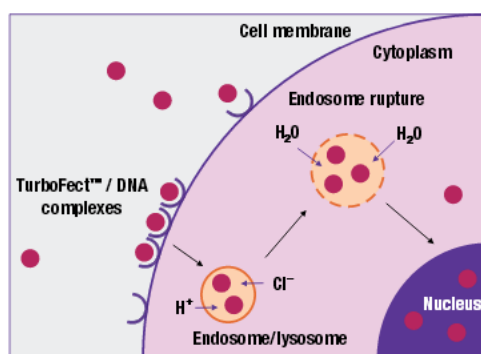


Figure 19 - Mechanism of action of TurboFect transfection reagent. TurboFect is an efficient, easy-to-use, non-immunogenic transfection reagent to deliver DNA plasmids and expression vectors into eukaryotic cells (*Thermo Scientific*).

SH-SY5Y cells were grown in 6-well plates at a density of $2,0 \times 10^6$ of cells per plate, using complete medium until 90% of confluence. Each amount of DNA (2 μg or 5 μg) was diluted in serum- and AAs-free medium. The TurboFect™ Transfection Reagent (*Thermo Scientific*) was vortexed and then added to the diluted DNA in a 1:1 proportion. The mixture were mixed by vortexing and rested for 20 minutes at room temperature for complexes formation, while the culture medium was replaced for AAs-free medium. Afterwards, the solution was carefully added, drop by drop, into the 6-well plates containing the cell medium. The cells were incubated at 37°C and 5% CO₂. The cell medium was replaced 6 hours after transfection and cells further incubated at 37°C and 5% CO₂ for 24 hours and 48 hours. At this time points cells were harvested by adding boiling 1% SDS or fixed using 4% paraformaldehyde for immunocytochemical analysis.

8. BCA PROTEIN CONCENTRATION ASSAY

The total concentration of proteins was measured through the BCA protein assay, in which the proteins reduce the Cu²⁺ to Cu⁺, obtaining an alkaline purple-coloured solution (biuret reaction), detected by BCA reagent (Bicinchoninic Acid) of Pierce® BCA Protein Assay Kit (*Thermo Scientific*). The protein standards composition is described on **Table 1**.

Table 1 - Standard preparations used in BCA protein assay. BSA, Bovine Serum Albumine; SDS, Sodium Dodecyl Sulfate; WR, Working Reagent.

Standards	BSA (μL)	1% SDS (μL)	Protein Mass (μg)	WR (μL)
P ₀	-	25	0	200
P ₁	1	24	2	200
P ₂	2	23	4	200
P ₃	5	20	10	200
P ₄	10	15	20	200
P ₅	20	5	40	200

The protein samples were diluted in 1% SDS (2,5 μL of protein in 22,5 μL of 1% SDS). The Working Reagent (WR) was prepared by combining BCA reagent A with BCA reagent B (50:1 proportion). Then, 200 μL of WR was added to each well, followed by incubation at 37°C for 30 minutes. The microplate cooled at room temperature and then the absorbance was

measured at 562 nm, using the *Infinite M200 (Tecan)* and *I-control™* software. A standard curve was obtained by plotting BSA standard absorbances vs BSA concentrations and, therefore, it was used to calculate the total protein concentration of each sample. Duplicates of samples and standards were always prepared.

9. SDS-POLYACRILAMIDE GEL ELECTROPHORESIS (SDS-PAGE)

After the determination of the total protein concentration, the proteins were separated using SDS-PAGE. The SDS - Polyacrylamide gel electrophoresis consists in a technique which allows the electrophoresis of proteins on a polyacrylamide gel in order to separate them, according to their molecular weight. A 10% polyacrilamide running gel and a 3,5% stacking gel (*see appendix*) were prepared to visualize the huLAP1B and huLAP1C proteins, with 68 kDa and 55 kDa, respectively. Once the gels polymerized, the samples were prepared, by the addition of ¼ volume of loading buffer (LB) and boiled for 10 minutes. The used protein marker was the “Precision Plus Protein™ Dual Color Standards” (*Bio-Rad*). The gel ran at 90mA for approximately 4 hours. Subsequently, the proteins were transferred to a nitrocellulose membrane (*GE Healthcare Life Sciences*) at 200 mA, during approximately 18 hours.

10. IMMUNOBLOTTING

Ponceau S staining of proteins bands has been applied to assess equal gel loading. This loading control practice has been described as a fast, inexpensive and nontoxic method, and binding is fully reversible in a few minutes. The nitrocellulose membranes were incubated in Ponceau S solution for 7 minutes, followed by a brief rinse in distilled water. The membranes were then scanned in a GS-800 calibrated imaging densitometer (*Bio-Rad*). After that, membranes were washed in 1X TBST for 2–3 minutes with gentle agitation and 1X in distilled water until the staining was completely eliminated.

10.1. Membranes incubation

First, the membranes were hydrated in 1X TBS for 5 minutes and then soaked in 5% low fat milk/1X TBST, with shaking, for blocking the unspecific binding sites (normally for 1 hour, depending on the primary antibody). Once blocked, the membrane was incubated with

primary antibody diluted in 3% BSA/1X TBST or 3% low fat milk/1X TBST, depending on the antibody. The specifications for the used primary antibodies are described on the following

Table 2.

Table 2 - Primary antibodies used in the immunoblotting procedure. *LAP1, Lamina-Associated Polypeptide 1; ON, overnight; PARP, Poly (ADP-Ribose) Polymerase.*

Primary antibody	Expected labeling	Dilution	Dilution solution	Time of incubation	Provider
Rabbit anti-LAP1	LAP1 (55kDa, 68kDa)	1:20000	3% BSA/1X TBST	4 hours with shaking and left ON	<i>Kindly provided by Dr. William T. Dauer</i>
Mouse anti-acetylated α-tubulin	α -acetylated tubulin (\approx 50 kDa)	1:1000	3% low fat milk/1X TBST	2 hours with shaking	<i>Sigma</i>
Rabbit anti-cleaved PARP (214/215) cleavage site specific polyclonal antibody	Cleaved PARP (85 kDa)	1:1000	3% BSA/1X TBST	3 hours with shaking	<i>Millipore</i>
Rabbit anti-Lamin B1 (H-90)	Lamin B1 (67k Da)	1:1000	3% BSA/1X TBST	4 hours with shaking and left ON	<i>Santa Cruz Biotechnology</i>

Subsequently, the membranes were washed three times for 10 minutes in 1X TBST. After that, they were incubated with secondary antibody, according with primary antibody's specificity (**Table 3**). The membrane was washed three times for 10 minutes with 1X TBST.

Table 3 - Secondary antibodies used in the immunoblotting procedure. *ECL, Enhanced Chemiluminescence; LAP1, Lamina-Associated Polypeptides 1; PARP, Poly (ADP-Ribose) Polymerase.*

Secondary antibody	Dilution	Dilution solution	Time of incubation	Company
ECL™ Anti-Rabbit IgG , Horseradish Peroxidase Linked Whole Antibody (from donkey)	1:5000	3% Low fat milk/1X TBST	2 hours with shaking	<i>GE Healthcare Life Sciences</i>
ECL™ Anti-Mouse IgG , Horseradish Peroxidase Linked Whole Antibody (from donkey)	1:5000	3% Low fat milk/1X TBST	2 hours with shaking	<i>GE Healthcare Life Sciences</i>

10.2. Immunodetection

The membrane was incubated for 1 minute with ECL™ (Enhanced Chemiluminescence), combining a solution A and a solution B in a 100:1 proportion (*GE*

Healthcare Life Sciences) or, if appropriate, incubating with *Luminata™ Crescendo HRP Substrate (Millipore)* for 5 minutes in a dark room. The ECL™ and *Luminata™ Crescendo* are chemoluminescent non-radiative methods for detection of specific antigens, conjugated directly or indirectly with horseradish peroxidase-labelled antibodies. After the X-Ray films (*Kodak*) had been exposed, they were developed and fixed with appropriate solutions. Afterwards, the X-ray films were scanned in *GS-800 Calibrated Densitometer (Bio-Rad)* and quantified through the *1-D Analysis Quantity-One software (Bio-Rad)*.

11. IMMUNOCYTOCHEMISTRY

The SH-SY5Y human neuroblastoma cells were grown in glass coverslips, which were previously coated with poly-L-ornithine, until a 90% confluency has been reached. Afterwards, they were transfected with Lipofectamine 2000™ as previously described. 24 hours later, the cell medium (free-AAAs with serum) was removed and 1 mL of paraformaldehyde fixative solution was added to each well for 20 minutes. Next, three washes with 1mL of 1X PBS were performed, followed by permeabilization with 0,2 % triton X-100 diluted in 1X PBS during 10 minutes. After that, four washes were performed with 1X PBS and the blocking solution (3% BSA/1X PBS) was added for 1 hour. The blocking solution was removed and, then, the primary antibody was added (**Table 4**). It was washed again for three times with 1X PBS, followed by incubation with the secondary antibody (**Table 5**). To finish, three washes with 1X PBS were performed and the coverslips were mounted on microscope glass slides with one drop of mounting medium containing DAPI for nucleic acid staining (*Vectashield, Vector Laboratories*). Photographs were acquired using an inverted *Olympus IX81* epifluorescence microscope.

Table 4 - Detailed information about primary antibodies used in immunocytochemistry procedure LAP1, Lamina-Associated Polypeptides 1.

Primary antibody	Dilution	Time of incubation	Company
Rabbit anti-LAP1	1:4000	1 hour and 30 minutes	<i>Kindly provided by Dr. William T. Dauer</i>
Mouse anti-acetylated α -tubulin	1:250	1 hour and 30 minutes	<i>Sigma</i>
Rabbit anti-Lamin B1 (H-90)	1:50	2 hours	<i>Santa Cruz Biotechnology</i>

Table 5 - Detailed information about secondary antibodies used in immunocytochemistry procedure. IgG, Immunoglobulin G.

Secondary antibody	Dilution	Time of incubation	Company
Alexa Fluor® Goat anti-rabbit 594 IgG (H+L)	1:300	1 hour and 30 minutes	<i>Invitrogen</i>
Alexa Fluor® Goat anti-mouse 488 IgG (H+L)	1:300	1 hour and 30 minutes	<i>Invitrogen</i>

12. CONFOCAL MICROSCOPY

SH-SY5Y cells morphology and cytoskeleton integrity were evaluated through confocal microscopy after human LAP1 knockdown. 450 cells were counted per condition: cells transfected with the shRNA control, construct 1, construct 2 or construct 1 and 2 together. Specifically, the nuclei and the corresponding nuclear envelopes labeled with DAPI and anti-LAP1 antibody, respectively were counted.

RESULTS

13. GENERATION OF HUMAN LAP1 shRNA CONSTRUCTS

The generation of short hairpin RNA (shRNA) constructs for a knockdown approach involves three steps: the choice of the proper target sequence within the gene of interest (**Figure 20A**), the oligonucleotide design (**Figure 20B**) and further cloning into an expression vector (**Figure 20C**). Our gene of interest is the *TOR1AIP1* (NM_001267578.1), which encodes the human LAP1B protein (NP_001254507.1).

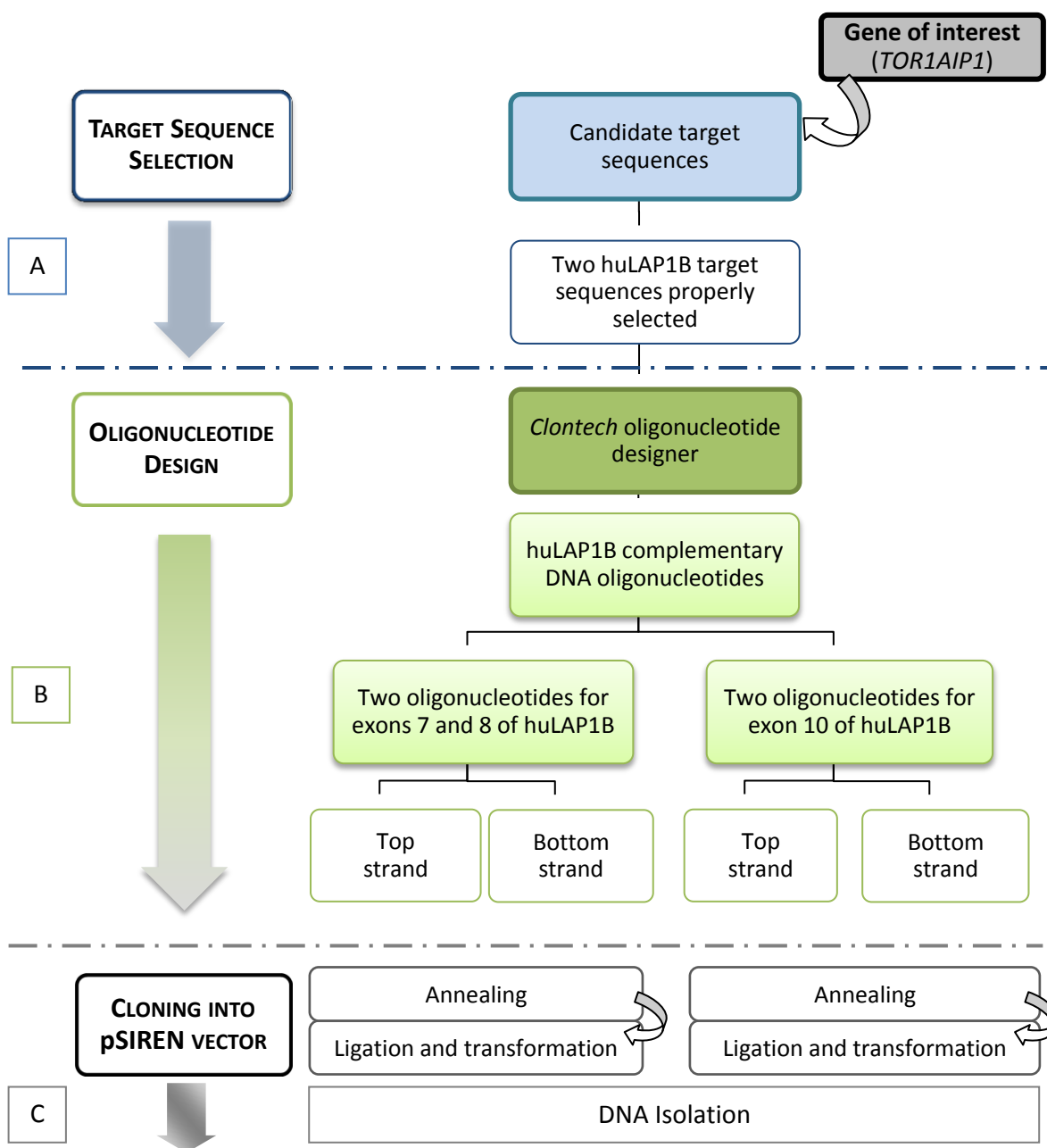


Figure 20 - Schematic illustration of the generation of human LAP1B shRNA constructs. *huLAP1*, human Lamina-Associated Polypeptides1; *shRNA*, short hairpin RNA; *TOR1AIP1*, Torsin1A-interacting protein 1.

13.1. Selection of target sequences

After the analysis of 20 potential RNAi target sequences for *TOR1AIP1* (Figure 21), two target sequences of 19 nucleotides were properly selected, according to the criteria previously described in *Materials and Methods*. Briefly, the selection was performed using the bioinformatic tool (*Clontech* designer) and the specificity of shRNAs for huLAP1B was tested using the Blast tool (<http://blast.ncbi.nlm.nih.gov/Blast.cgi>). The Blast results clearly indicated that each selected LAP1B target sequence has 100% homology with our gene of interest and no significant homology with additional genes.

Potential RNAi target sequences

The following 19-base sequences are potential siRNAs specific to the entered sequence of the length 4054 bp. Click on the sequence to design an shRNA species.

	Sequence	Position	GC(%)	HpTm(C)	dTm(C)	Blast Search
1	GACTTAGGACAGGCAAGTT	85	47	0.0	1.7	Blast search
2	GGTCATAAAGCCATCTTC	414	47	0.0	1.7	Blast search
3	TCGCGATCGACTAAAGCTA	431	47	0.0	1.7	Blast search
4	CGACTAAAGCTACGTCAAC	438	47	0.0	1.7	Blast search
5	GAGGAAATGAAGACGCGAA	818	47	0.0	1.7	Blast search
6	AGGAAATGAAGACGCGAAG	819	47	0.0	1.7	Blast search
7	CTGTCAGGAGCATAACAAGA	987	47	0.0	1.7	Blast search
8	CCACCAGATCATCTAGTCA	1209	47	0.0	1.7	Blast search
9	GTGCTAAGCTCAGGATATC	1295	47	0.0	1.7	Blast search
10	GGACCAGGATGCAAATGA	1356	47	0.0	1.7	Blast search
11	TGGCTACTTCCTCTGATAG	1478	47	0.0	1.7	Blast search
12	GGTCAAGATGAGAAGCTGT	1604	47	0.0	1.7	Blast search
13	GTCTCAGCCTGCTATCTTA	1675	47	0.0	3.5	Blast search
14	GGGACAGATAAAGCTACTC	1799	47	0.0	1.7	Blast search
15	GAGGTAGACCAAGAAGTGA	1841	47	0.0	1.7	Blast search
16	GACCAAGAACTGAGCAATG	1847	47	0.0	1.7	Blast search
17	GAGGAAGAGACACTTGGAA	2006	47	0.0	1.7	Blast search
18	GGAAGAGACACTTGGAAACA	2008	47	0.0	1.7	Blast search
19	GGAACAAGTCTAGGCCTAA	2021	47	0.0	3.5	Blast search
20	GACCCAGACAAACTGAATG	2120	47	0.0	1.7	Blast search

Figure 21 - Potential RNAi target sequences for *TOR1AIP1* gene. The two selected target sequences were the number 9 and 18 (highlighted). The positions of targets in mRNA sequence of *TOR1AIP1* (4054 bp) were 1295 and 2008 bp, respectively. The guanine cytosine content was suitable (47%). Available on <http://bioinfo.clontech.com/rnaidesigner/sirnaSequenceDesignInit.do>. RNAi, RNA interference.

The first shRNA target sequence (sequence 9) is directed to a region located between exon 7 and exon 8 of *TOR1AIP1* sequence (1296-1315 bp). The second target sequence (sequence 18) is within the exon 10 of *TOR1AIP1*, located at position 2009-2027 bp (Figure 22).

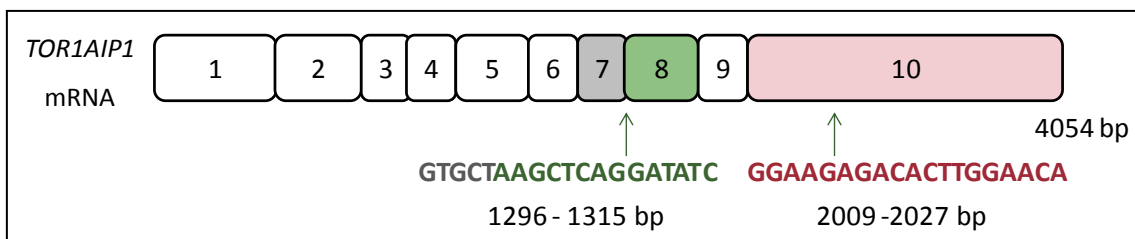


Figure 22 - Localization of selected target sequences for *TOR1AIP1* gene. The first target sequence includes 5 nucleotides of the exon 7 (grey) and 14 nucleotides of the exon 8 (green). The second target sequence includes 19 nucleotides of the exon 10 (red). Therefore these two oligonucleotides are directed against the exon 7/8 and exon 10, respectively.

13.2. Oligonucleotides design

For each shRNA selected target sequence, the synthesis of two complementary oligonucleotides was required: a top strand (including the target sequence) and a complementary bottom strand. For this purpose, the oligonucleotides were properly designed (**Figure 23**) using a bioinformatic tool (*Clontech* designer). We called “oligonucleotide 1” to target sequence directed for exons 7 and 8 of *TOR1AIP1*. The oligonucleotide that includes the target sequence for exon 10 was named “oligonucleotide 2”.

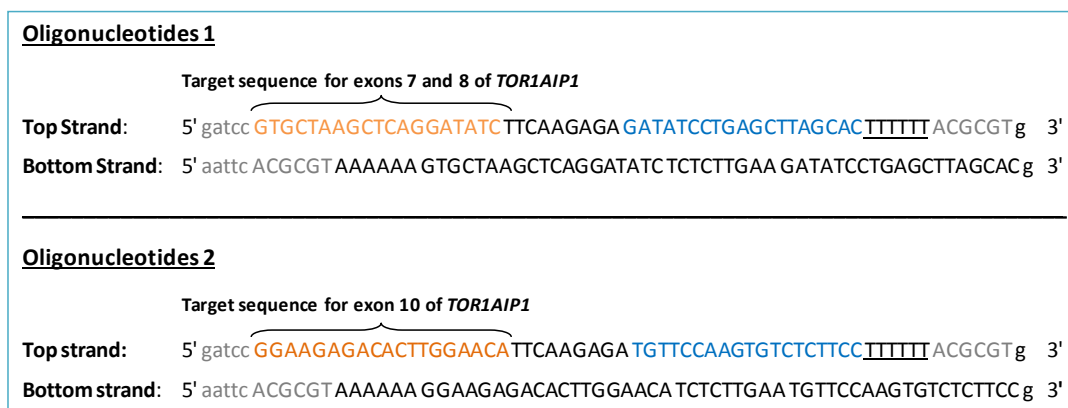


Figure 23 - Designed oligonucleotides (1 and 2) for *TOR1AIP1* gene. Top and bottom strands are represented 5' to 3'. The unique restriction site (*Mlu* I) allows the confirmation of insertion of the clones after ligation (ACGCGT). 5' *Bam*HI and 3' *Eco*RI overhangs are necessary for further directional cloning into the vector. Target sense sequence (orange); TTCAAGAGA (hairpin loop); antisense sequence (blue); terminator sequence (underlined); restriction sites (grey). Available on <http://bioinfo.clontech.com/rnaidesigner/oligoDesigner.do>.

Once designed and commercial synthesized, the oligonucleotide 1 and oligonucleotide 2 were annealed and then ligated into the vector pSIREN-retroQ. Next, *E. coli* XL1-blue was transformed with the shRNA constructs for further DNA isolation. Finally, the cloning of constructs was confirmed through restriction analysis and sequencing (Figure 24).

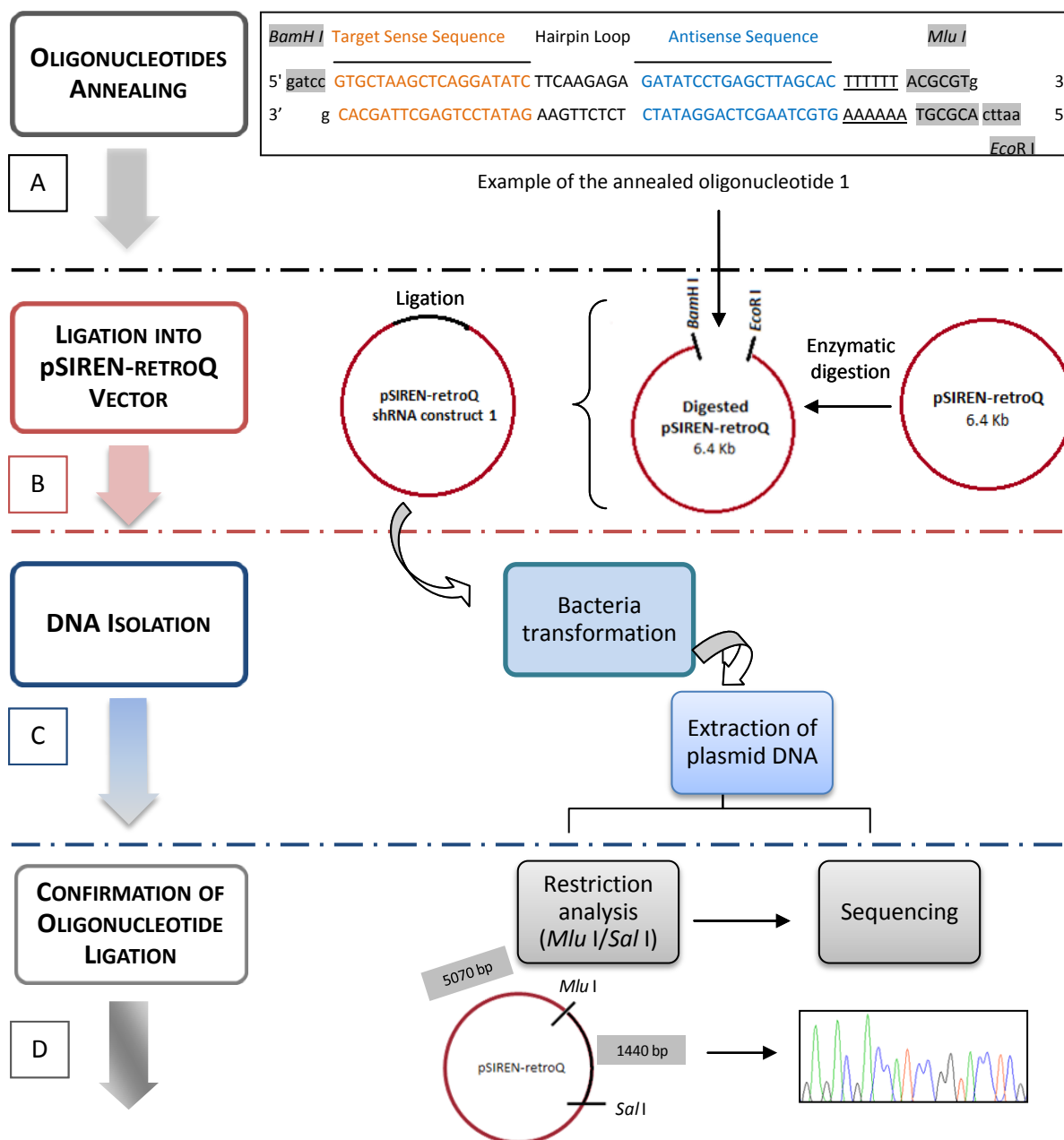


Figure 24 - Schematic illustration of shRNA cloning into the pSIREN-retroQ vector. As an example, this figure represents the oligonucleotide 1 that allows the generation of shRNA against exon 7/8 (construct 1). The restriction endonucleases *BamH* I and *EcoR* I were used to open the vector, while *Mlu* I and *Sal* I allowed the confirming restriction analysis.

13.2.1. shRNA oligonucleotides annealing

The top and bottom strands of each oligonucleotide (oligonucleotide 1 and oligonucleotide 2) were annealed, as represented in **Figure 25**.

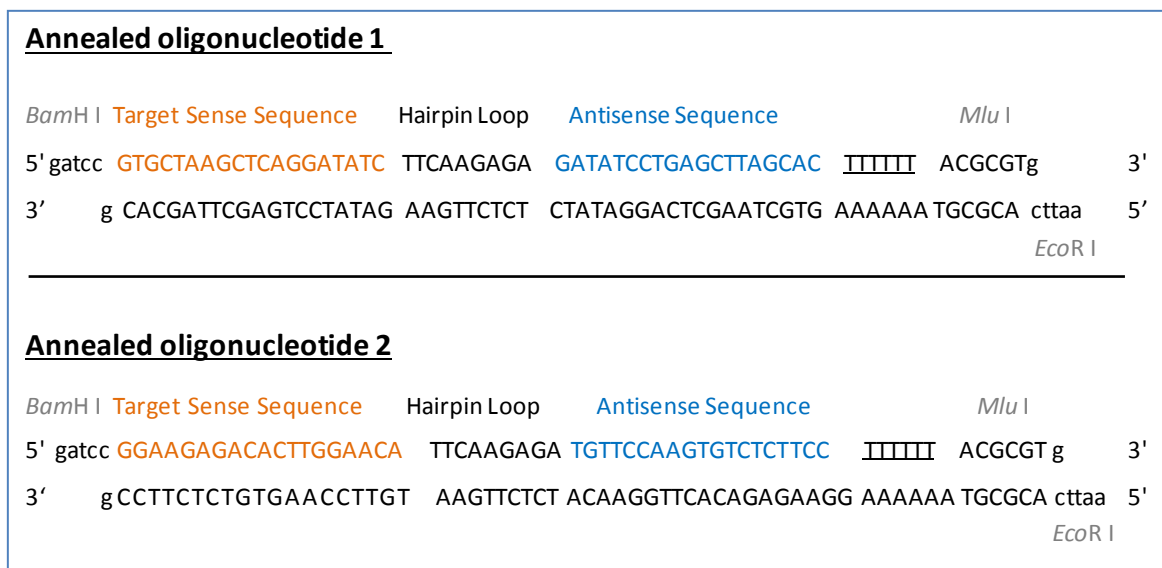


Figure 25 - Annealed oligonucleotides (1 and 2). Top strand are shown 5' to 3' and bottom strand 3' to 5'. Target sense sequence (orange); TTCAAGAGA (hairpin loop); antisense sequence (blue); terminator sequence (underlined); restriction sites (grey).

Additionally, the annealing of the negative control (missense oligonucleotide obtained commercially) was also performed. The sense sequence of the latter does not align with any human transcript (**Figure 26**).

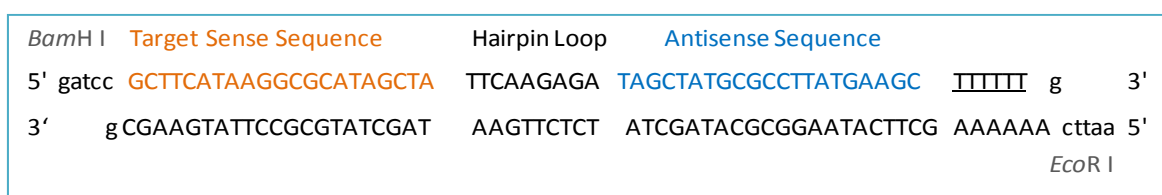


Figure 26 - Annealed negative control (missense oligonucleotide obtained commercially). The target sequence of the negative control does not align with any human transcript. Target sense sequence (orange); TTCAAGAGA (hairpin loop); antisense sequence (blue); terminator sequence (underlined); restriction sites (grey).

After the annealing step, the oligonucleotides were cloned into the pSIREN-retroQ vector and the resulting constructs were further selected and isolated. From now on, we

will entitle pSIREN-retroQ constructs as huLAP1B construct 1 and huLAP1B construct 2, corresponding to the oligonucleotide 1 and oligonucleotide 2, respectively.

13.2.2. Restriction analysis

The restriction digestion of the positive clones was performed to confirm the presence of positive results that correspond to the correct insertion of both oligonucleotides into the pSIREN-retroQ. The results are presented in **Figure 27** and revealed the presence of two fragments: one of approximately 1440 bp that corresponds to the weight of oligonucleotide 1 or 2 (65 bp) plus part of the vector (1375 bp) and a second fragment of 5070 bp that corresponds to the rest of the vector. Therefore, the presence of both oligonucleotides was confirmed since two fragments with the expected size were obtained. The two observed fragments (**Figure 27A** and **B**) demonstrated that *Mlu* I enzyme cleaved the unique restriction site within each oligonucleotide and *Sal* I cleaved within the pSIREN-retroQ vector, as expected. The positive results with restriction digestion were further confirmed by automated DNA sequencing.

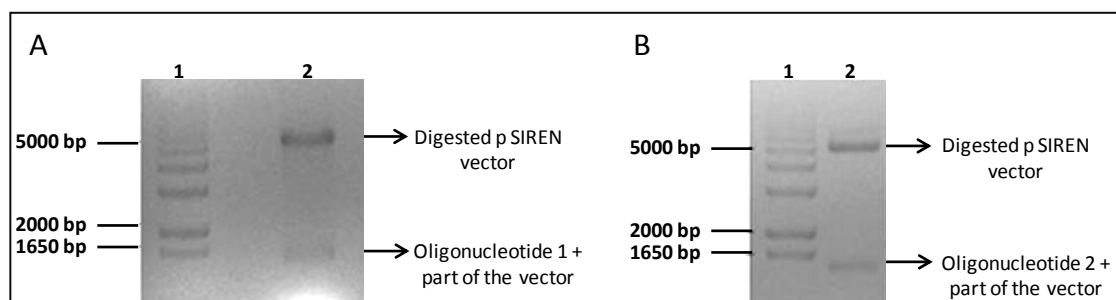


Figure 27 - Restriction analysis of both human LAP1B constructs. **A)** Lane 1, 1 Kb⁺ DNA ladder (*Invitrogen*); Lane 2, Positive clones (digested pSIREN-retroQ vector; oligonucleotide 1 + part of the vector) digested with *Mlu* I and *Sal* I restriction endonucleases. **B)** Lane 1, 1 Kb⁺ DNA ladder; Lane 2, Positive clones (digested pSIREN-retroQ vector; oligonucleotide 2 + part of the vector) with *Mlu* I and *Sal* I restriction enzymes.

13.2.3. DNA sequencing

The confirmation of both constructs was achieved through DNA sequencing, using an appropriate primer (*see appendix* - vector information). Some ambiguities were seen and the sequences were further confirmed by visual analysis. The results for both constructs are presented in **Figure 28A** (huLAP1 construct 1) and **Figure 28B** (huLAP1 construct 2).

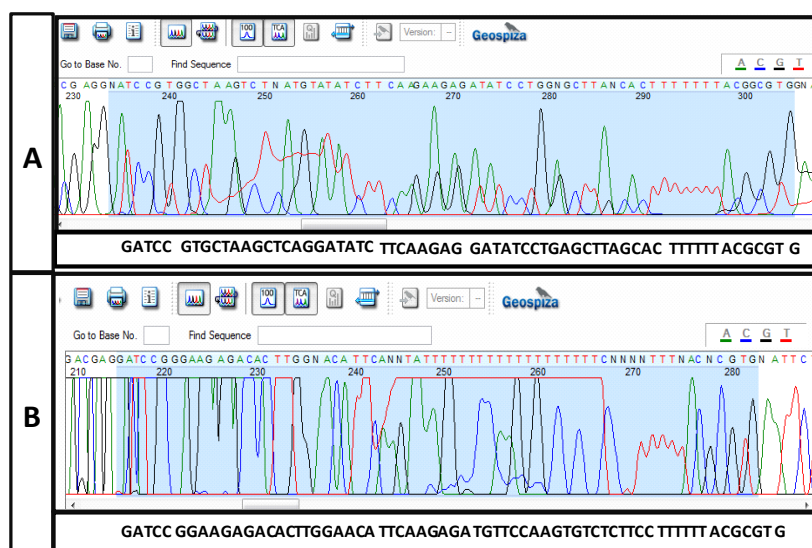


Figure 28 - Sequencing analysis of the pSIREN-retroQ constructs for human LAP1B. A) Sequencing analysis of the pSIREN-retroQ construct 1. **B)** Sequencing analysis of the pSIREN-retroQ construct 2. The oligonucleotide sequence was confirmed (blue) through the *FinchTV software* (Geospiza, Inc.).

14. ESTABLISHMENT OF SH-SY5Y CELLS TRANSFECTION CONDITIONS FOR huLAP1 shRNA CONSTRUCTS

The human neuroblastoma SH-SY5Y cells were transfected with each human LAP1 shRNA construct (huLAP1 construct 1 and huLAP1 construct 2) separately and also with both constructs, simultaneously (**Figure 29**). Their effect on huLAP1 knockdown was monitored by SDS-PAGE, followed by immunoblotting using a specific antibody against LAP1 as already described in *Materials and Methods*. The effect was evaluated for the well characterized huLAP1B isoform and also for the one we believe that is the human LAP1C, which is likely to be the most abundant isoform of LAP1 in cultured cells.



Figure 29 - Schematic representation of the procedure used for determination of the efficiency of interfering shRNA constructs. The transfection conditions were optimized and SH-SY5Y cells were transfected with both huLAP1 shRNA constructs.

Essentially, we tested two different transfection reagents (Lipofectamine and TurboFect), two different DNA concentrations (2 μg and 5 μg) and also two different periods

of transfection incubation (24 hours and 48 hours). The transfection conditions were optimized to establish the best RNA interference efficiency.

14.1. Optimization of cell transfection conditions

Two different amounts of each shRNA construct (2 μ g and 5 μ g) as well as two distinct transfection methodologies (using Lipofectamine 2000TM and TurboFectTM) were used. The protein levels of the huLAP1 were quantified 24 hours (**Figure 30**) and 48 hours (**Figure 31**) upon transfection. Concerning to knockdown efficiency, it was evaluated the effect of the shRNA constructs on the expression of the two human LAP1 isoforms (huLAP1B and huLAP1C). Moreover, expression of LAP1 isoforms was always compared between cells transfected with the shRNA control and cells transfected with the LAP1 specific shRNAs. The levels of huLAP1B and huLAP1C were quantified by densitometry and plotted upon their correction to the loading control (Ponceau S).

14.1.1. 24 hours post-transfection

Using the Lipofectamine methodology for 24 hours (**Figure 30A and C**) the knockdown results were more evident for huLAP1B than huLAP1C. In overall, for huLAP1C all tested conditions produced a quite similar interference percentage around 20-40% (**Figure 30C**). However, for huLAP1B isoform, the knockdown efficiency was higher using 5 μ g of each tested construct and the achieved interference using the construct 1, construct 2 and both together was approximately 40%, 40% and 60%, respectively (**Figure 30A**). However, when the cells were transfected for 24 hours using the TurboFect reagent, with the same amounts of each construct, the results were more evident for huLAP1C isoform. We could observe interferences around 70%, 60% and 80% (**Figure 30D**) for 5 μ g of Construct 1, Construct 2 and Construct 1 and 2, respectively. For human LAP1B isoform, the interferences are quite lower and were around 35%, 25% and 50% for each construct (**Figure 30B**). Upon 24 hours of transfection, the maximum knockdown efficiency was observed in TurboFect transfection with both construct 1 and 2 together, where was achieved 80% of interference for huLAP1C. Indeed, it was also achieved an acceptable knockdown, around 40%, with the Lipofectamine reagent with the same time of transfection.

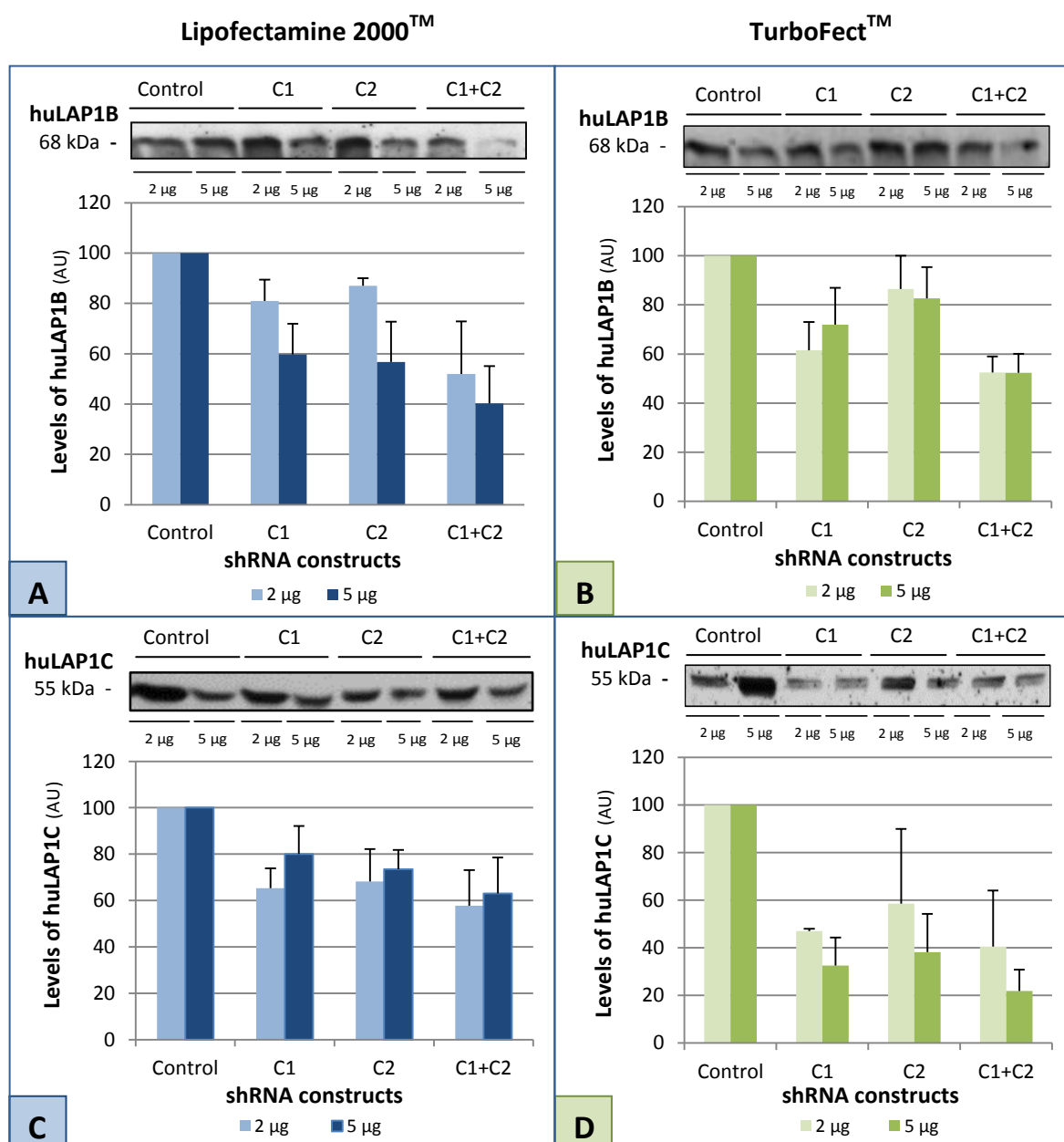


Figure 30 - Knockdown levels of human LAP1B/C 24 hours upon shRNA transfection. The transfection with Lipofectamine (left column) and TurboFect (right column) was tested using 2 µg and 5 µg of shRNA constructs. The knockdown was evaluated for both LAP1 isoforms: huLAP1B (A, B) and huLAP1C (C, D). AU, arbitrary units; C1, shRNA construct 1; C2, shRNA construct 2; C1+C2, construct 1 and 2; huLAP1, human LAP1.

14.1.2. 48 hours post-transfection

Surprisingly, upon 48 hours of transfection the effects of knockdown were not so clear than those observed with 24 hours of transfection using the same two methodologies and DNA concentrations. The SH-SY5Y cells transfected with Lipofectamine for 48 hours produced

a knockdown not so significant, even with the two concentrations tested. Therefore, the obtained interference for huLAP1B isoform using 5 μg of the construct 1, construct 2 and both constructs together were around 40%, 25% and 60%, respectively (**Figure 31A**). For the huLAP1C isoform, the percentages were approximately 40%, 10% and 50% (**Figure 31C**).

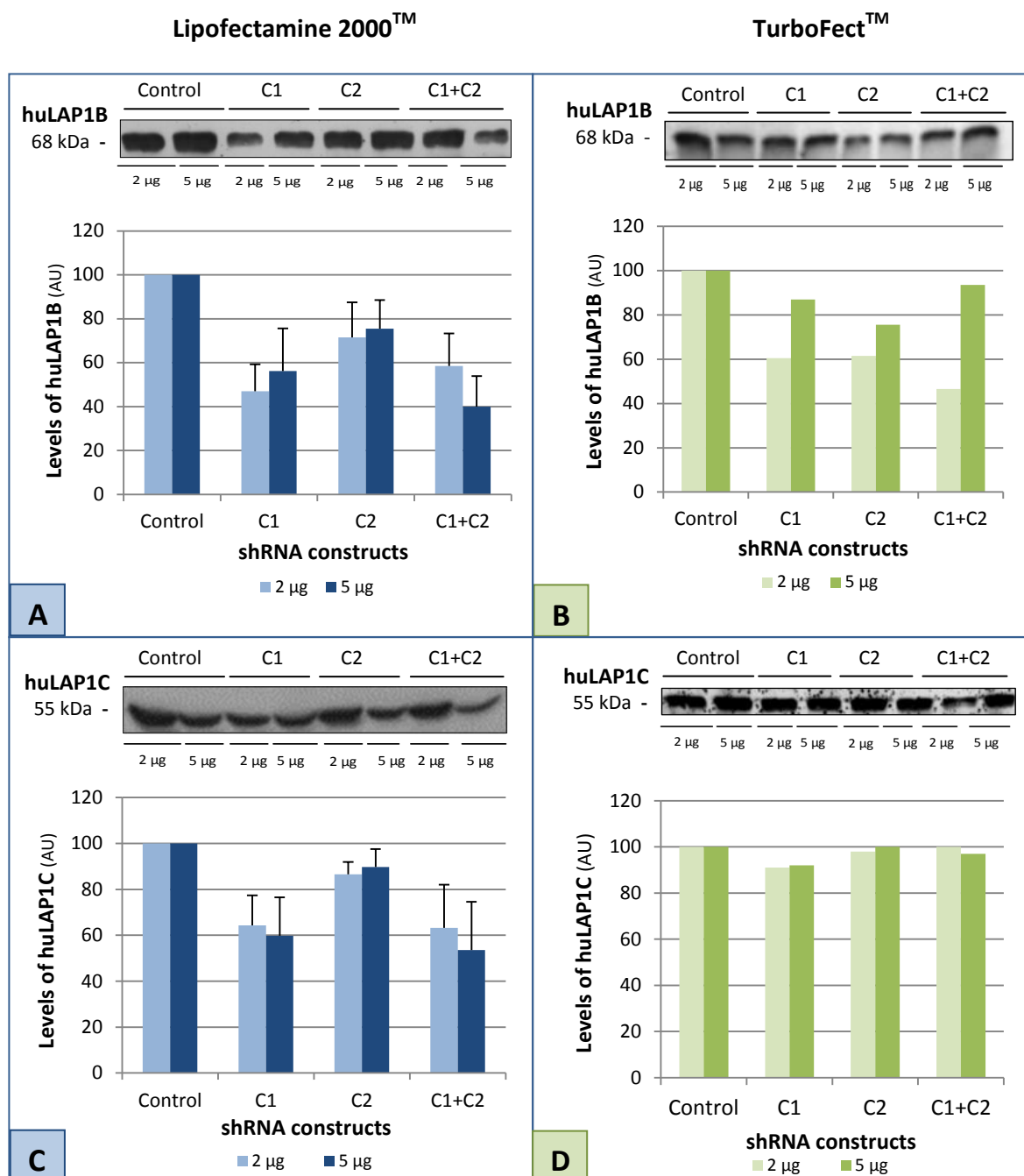


Figure 31 - Knockdown levels of human LAP1B/C 48 hours upon shRNA transfection. The transfection with Lipofectamine (left column) and TurboFect (right column) was tested, both with 2 μg and 5 μg of shRNAs. The knockdown was evaluated for huLAP1B (**A**, **B**) and huLAP1C (**C**, **D**). AU, arbitrary units; C1, shRNA construct 1; C2, shRNA construct 2.

Using the TurboFect reagent during same period of time, unexpected results were observed, using 5 µg of constructs, since a very low interference was achieved. However, the interference for huLAP1B isoform using 2 µg was 40%, 40% and 50% (**Figure 31B**) for construct 1, construct 2 and both constructs together, respectively. For the huLAP1C isoform, the observed knockdown was approximately 10%, 5% and 0% (**Figure 31D**), respectively.

All together, these results point that the optimized transfection conditions for a higher knockdown efficiency are the ones achieved interference using the TurboFect™ transfection reagent, whereby 5 µg of shRNA each construct were transfected. The time of transfection that proved to be more effective for knocking-down LAP1 was 24 hours. The percentages of interference for all tested conditions are visualized in the next **Table 6**, where the best conditions are highlighted in red.

Table 6 - Knockdown efficiency of human LAP1B/C using several transfection conditions. Two different transfection reagents were used (Lipofectamine and TurboFect) as well as two different time points post-transfection (24 hours and 48 hours). Two DNA concentrations were also tested (2 µg and 5 µg) with both constructs. *C1, construct 1, C2, construct 2; C1+C2, construct 1 + 2. Optimized conditions are seen in red.*

Lipofectamine™			TurboFect™		
24 Hours					
Isoforms	µg of DNA	Knockdown efficiency (%) (C1; C2; C1+C2)	Isoforms	µg of DNA	Knockdown efficiency (%) (C1; C2; C1+C2)
huLAP1B	2 µg	40, 40, 60	huLAP1B	2 µg	40, 20, 50
	5 µg	40, 40, 60		5 µg	35, 25, 50
huLAP1C	2 µg	30, 30, 40	huLAP1C	2 µg	60, 40, 60
	5 µg	20, 30, 40		5 µg	70, 60, 80
Lipofectamine™			TurboFect™		
48 Hours					
Isoforms	µg of DNA	Knockdown efficiency (%) (C1; C2; C1+C2)	Isoforms	µg of DNA	Knockdown efficiency (%) (C1; C2; C1+C2)
huLAP1B	2 µg	55, 30, 40	huLAP1B	2 µg	40, 40, 50
	5 µg	40, 25, 60		5 µg	15, 25, 10
huLAP1C	2 µg	40, 15, 40	huLAP1C	2 µg	10, 5, 0
	5 µg	40, 10, 50		5 µg	10, 0, 5

15. TO DETERMINE THE EFFECTS OF huLAP1 KNOCKDOWN USING BIOCHEMICAL ASSAYS

Once determined the best conditions for interfering with LAP1, that correspond to transfection with 5 μg of each construct using the TurboFect™ reagent for 24 hours, we performed additional experiments, in order to determine the effects of knocking-down LAP1B for the cell integrity, particularly NE integrity and microtubules dynamics. For that we have chosen to evaluate the intracellular levels of several proteins, including LAP1 (LAP1B and C) to confirm the efficiency of knocking-down, laminB1 to confirm NE integrity, α -tubulin acetylated to evaluate the microtubule dynamics and also cleaved poly(ADP-ribose) polymerase (PARP) for the overall analysis of cellular integrity. Analyzing the intracellular levels of both LAP1B and LAP1C revealed that we interfere with both isoforms as we expected and for huLAP1B isoform, the interferences were around 30%, 20% and 50% for each construct. We observe interferences around 70%, 60% and 80% for 5 μg of the shRNA constructs (construct 1, construct 2 and construct 1+2) when huLAP1C was knocked-down (Figure 32).

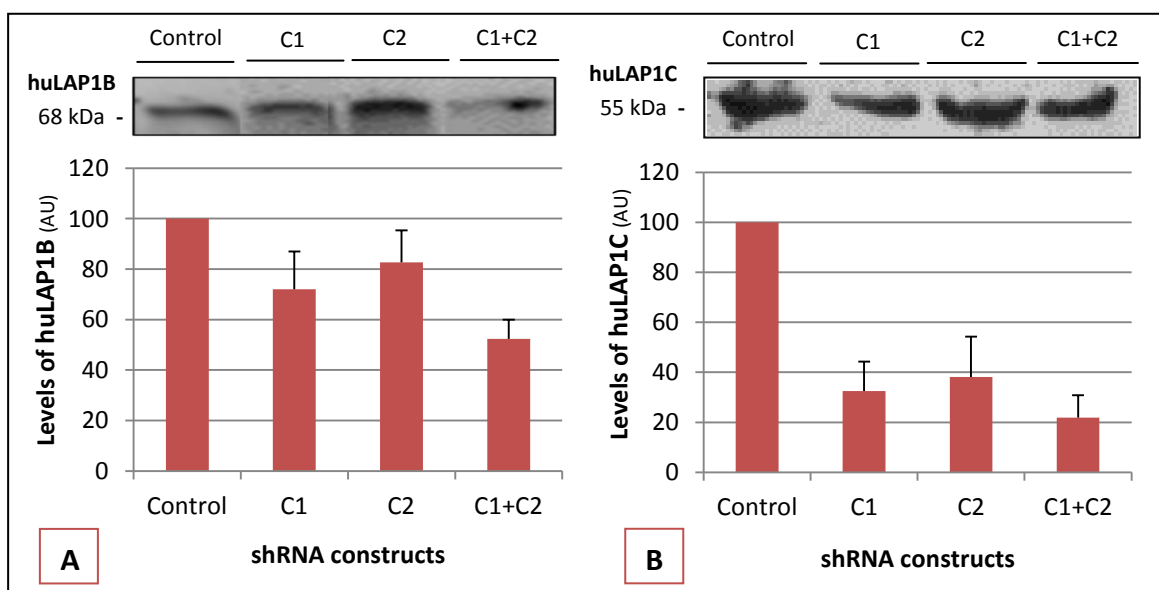


Figure 32 – Intracellular levels of human LAP1B/C after 24 hours of shRNA transfection with TurboFect™. A) Levels of human LAP1B; B) Levels of human LAP1C. AU, arbitrary units; C1, shRNA construct 1; C2, shRNA construct 2.

Once confirmed that knockdown of huLAP1B was achieved, the intracellular levels of the other three proteins were evaluated by immunoblotting. The intracellular levels of

laminB1, which is a crucial protein of the nuclear lamina was evaluated (**Figure 33**). A decrease of laminB1 intracellular levels was observed, achieving 70% after transfection of construct 2. Also with construct 1 and 2 together a significant decrease of laminB1 was observed (approximately 60%).

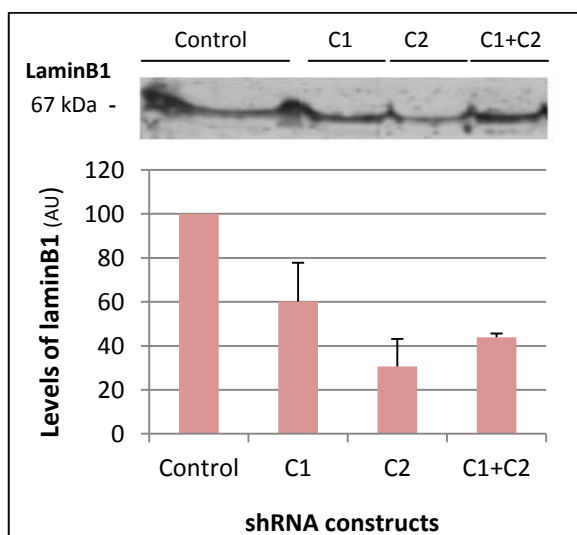


Figure 33 - LaminB1 intracellular levels after huLAP1 knockdown in SH-SY5Y cells. Cells were transfected with shRNA control, construct 1, 2 or both for 24h using TurboFect. The amount of lamin B1 decreased when huLAP1 is knocked-down. LaminB1 is part of the nuclear lamina, interacting with huLAP1. AU, arbitrary units; C1, shRNA construct 1; C2, shRNA construct 2; C1+C2, shRNA construct 1 and 2.

In overall a dramatic change in laminB1 expression is observed with all constructs being more pronounced with construct 2. In order to evaluate the microtubules dynamics, which is an indirect measure of cytoskeleton integrity, the acetylated α -tubulin was quantified after huLAP1 knock-down. There is a considerable decrease in acetylated α -tubulin reaching 50% when the two constructs, C1 and C2, were transfected together (**Figure 34**).

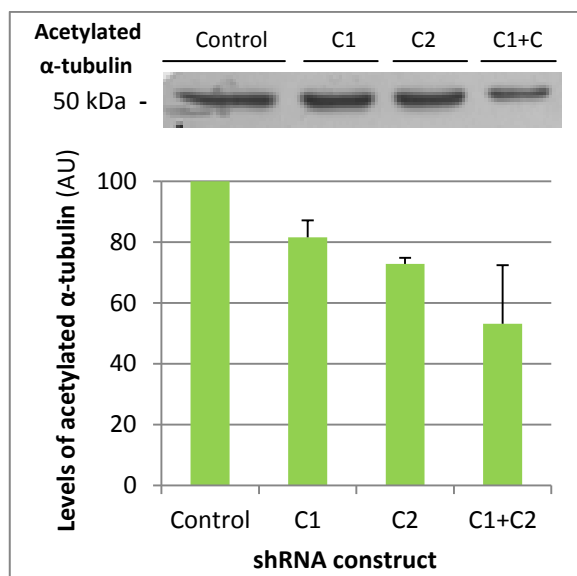


Figure 34 - Acetylated α -tubulin intracellular levels after huLAP1 knockdown in SH-SY5Y cells. Cells were transfected with shRNA control, construct 1, 2 or both for 24h using TurboFect. The amount of acetylated α -tubulin decreased with the knockdown of huLAP1. Acetylated α -tubulin composes the cellular cytoskeleton, especially the microtubules of mitotic spindle. AU, arbitrary units; C1, shRNA construct 1; C2, shRNA construct 2; C1+C2, shRNA construct 1 and 2.

PARP is a DNA-binding enzyme that is cleaved by caspase-3 and -7 during apoptosis. Thus, the cleavage of PARP into two fragments of 85 kDa and 25 kDa has been considered indicative of caspase activation and has been used as a marker for apoptosis (72,73). The antibody that we used to detect cleaved PARP (*Millipore*) recognizes the 85 kDa fragment. The results of cleaved PARP have shown that there is a slight tendency to have increased levels particularly with C2 construct (**Figure 35**). However, no significant alterations were observed so far.

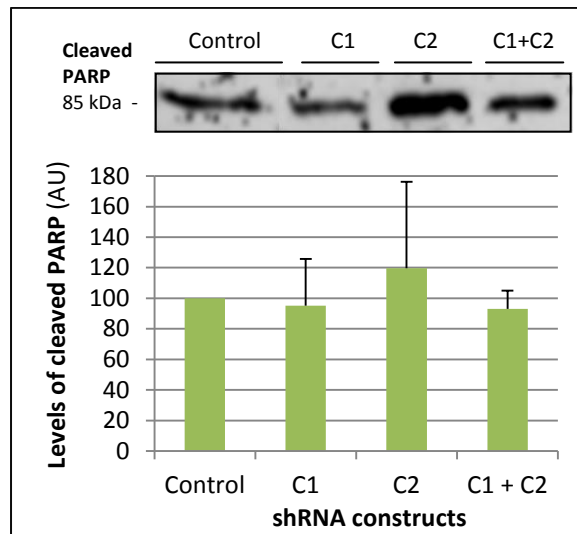


Figure 35 – Cleaved PARP levels after huLAP1 knockdown in SH-SY5Y cells. Cells were transfected with shRNA control, construct 1, 2 or both for 24h using TurboFect. Transfection of construct 2 caused a slight tendency to have increased levels of cleaved PARP. AU, arbitrary units; C1, shRNA construct 1; C2, shRNA construct 2.

Additionally, the resazurin cell viability assay was performed to check the presence of metabolically inactive and active cells. No significant results were observed among shRNA constructs, with all cells exhibiting metabolic activity.

16. TO EVALUATE THE EFFECTS OF huLAP1B/C KNOCKDOWN IN CELLULAR INTEGRITY BY MICROSCOPY

SH-SY5Y cells morphology and cytoskeleton integrity was also evaluated through fluorescence and confocal microscopy after huLAP1 knockdown. Thus, 450 cells were counted per condition: cells transfected with the shRNA control, construct 1, construct 2 or construct 1 and 2 together. Specifically, the nuclei and the corresponding nuclear envelopes labeled with DAPI and anti-LAP1 antibody, respectively, were counted. Immunodetection of huLAP1 in the NE was seen to decrease around 50% using both constructs together, while approximately 40% of huLAP1 silencing was seen using construct 1 or construct 2 (**Figure 36**).

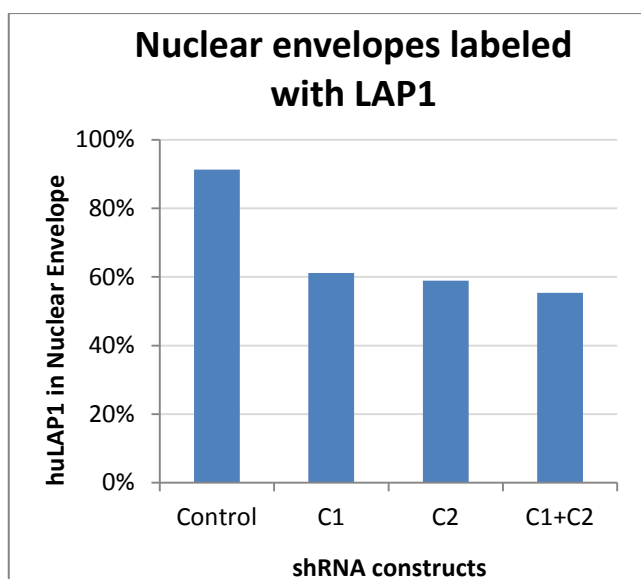


Figure 36 - Number of visible nuclear envelopes labeled with LAP1 in SH-SY5Y cells after LAP1 knockdown. After the immunochemistry, 450 nuclei were counted through the DAPI staining and then the nuclear envelopes labeled with LAP1 were also counted through visual analysis on epifluorescence microscope. AU, arbitrary units; C1, shRNA construct 1; C2, shRNA construct 2; C1+C2, shRNA construct 1 and 2; huLAP1, human LAP1.

Analyses of the intracellular levels of both LAP1 isoforms in this latter knockdown, revealed that huLAP1B expression decreases 0%, 10% and 35% using construct 1, construct 2 and construct 1+2, respectively. We observed interferences for LAP1C around 38%, 43% and 39% after transfection of construct 1, construct 2 and construct 1+2, respectively (**Figure 37**).

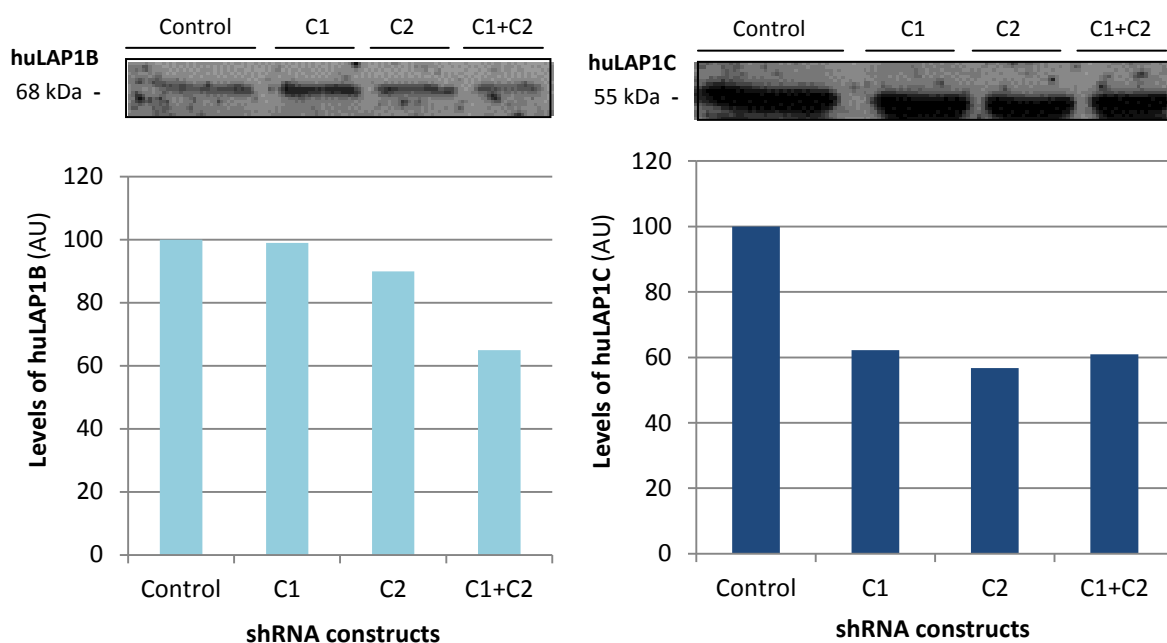


Figure 37 - Intracellular levels of human LAP1B/C after knockdown. A) Levels of human LAP1B; **B)** Levels of human LAP1C. AU, arbitrary units; C1, shRNA construct 1; C2, shRNA construct 2.

Then, we analyzed SH-SY5Y cells upon LAP1 knockdown by confocal microscopy.

Additionally, in these same LAP1 knocked-down cells, the morphology of nuclei was also analyzed. We evaluated the amount of acetylated α -tubulin as well as its distribution in cells, when LAP1 protein is depleted.

In control cells (**Figure 38A**), we have seen that LAP1 is present in the perinuclear region, while the morphology of the nucleus and the distribution of acetylated α -tubulin was normal. In transfected cells with the shRNA construct 1 (**Figure 38B**), we have seen that LAP1 was efficiently knocked-down in approximately 50% of cells where it is just visible a punctated pattern in membrane and also within the nucleus. In this case, the nucleus has an abnormal reniform morphology with a normal distribution of chromatin. Abnormally, the acetylated α -tubulin is more concentrated in cell shrinkage sites. Concerning transfected cells with construct 2 (**Figure 38C**), the nuclear morphology observed is normal in some cells while is reniform in others (not shown). The abnormal distribution of chromatin is also present here while a decrease of acetylated α -tubulin staining is also evident. Finally, in both cell transfected constructs (**Figure 38D**), the nuclear morphology observed is normal in some cells while is reniform in others. Once more, we observed an abnormal chromatin distribution

while a more pronounced decrease of acetylated α -tubulin staining compared to cells transfected with construct 2.

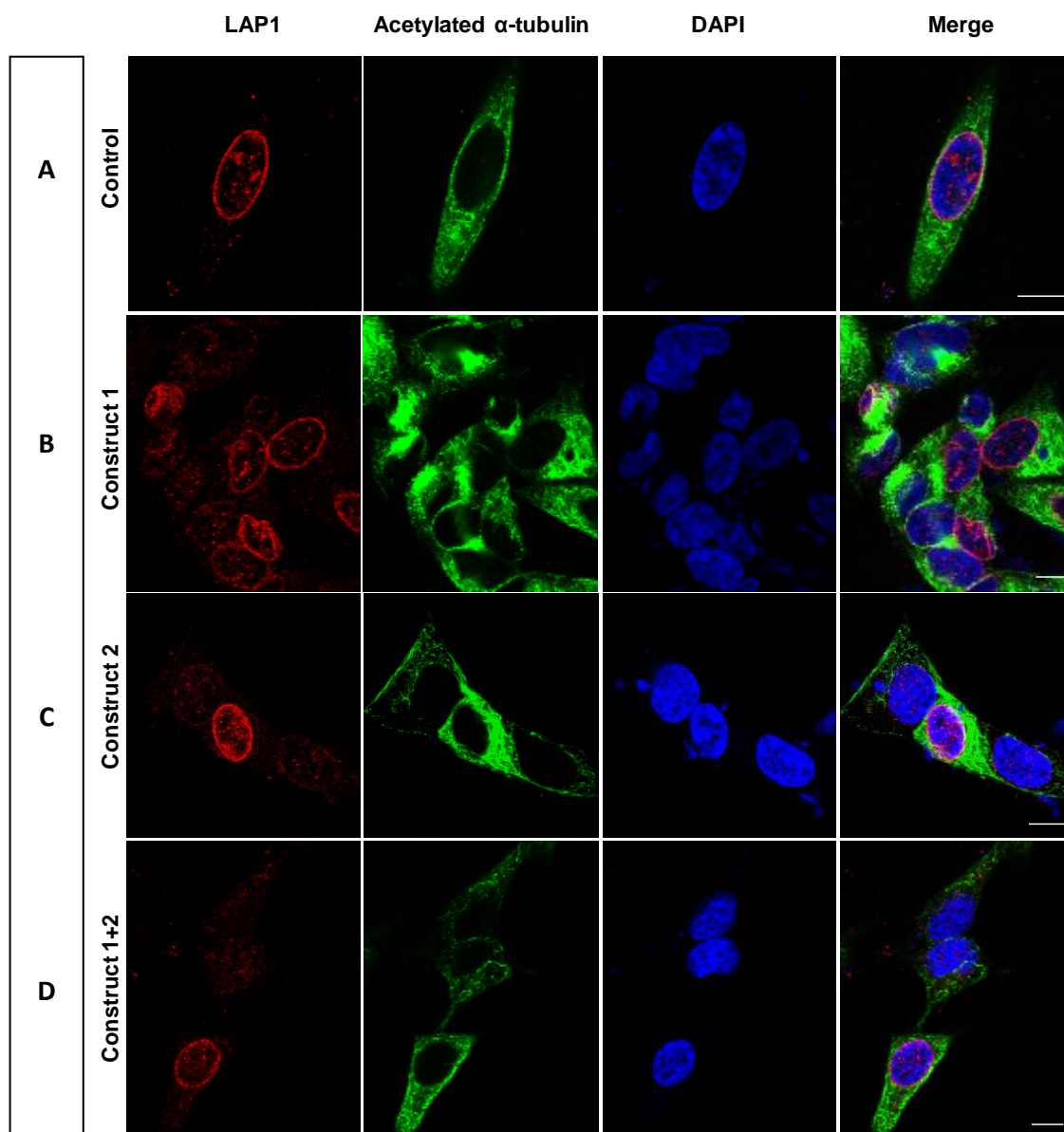


Figure 38 - Effects of LAP1 knockdown in cellular nuclei and acetylated α -tubulin distribution. LAP1 was detected using a rabbit anti-LAP1 conjugated to secondary antibody Alexa Fluor[®] Goat anti-rabbit 594 IgG (red). Acetylated α -tubulin was detected using mouse anti-acetylated α -tubulin conjugated to secondary antibody Alexa Fluor[®] Goat anti-mouse 488 IgG (green). Nucleic acids were stained with DAPI (blue). Co-localization of LAP1, acetylated α -tubulin and DAPI can be observed in the merge figure. **A)** Control; **B)** shRNA construct 1; **C)** shRNA construct 2; **D)** shRNA construct 1+2. *Bar, 10 μ m.*

DISCUSSION

The RNA interference (RNAi) strategy is a specific and selective methodology, through which the expression of a targeted gene is knocked-down to mimic what happens at a cellular level, if a specific gene is weakly expressed. Therefore, this technique represents a powerful approach for unraveling the putative gene function in mammalian cells (46–48). Among the several variants of regulatory RNAs, there are the short hairpin RNAs (shRNAs), which are processed through expression of shRNA vectors, for example the pSIREN-retroQ. They demonstrated to mediate a long-lasting gene silencing of constructs, only using few copies of shRNA, since it can be continuously produced by the host cell (46,58). It is believed that less than five copies of shRNA integrated in host genome are enough to achieve an effective gene knockdown. Such conclusion is a great advantage because it may result in less off-target effects. The less off-target effects can also be explained by the endogenous processing and nuclear regulation, after the transcription of DNA oligonucleotides into shRNAs (48,69). The ability of this method to reduce the expression of a specific gene allows the understanding of its physiological function, generating loss-of-function phenotypes (47,50).

LAP1 proteins are type two integral membrane proteins of to the inner nuclear membrane. Thus, they are potential biochemical markers for INM integrity and are very useful models for biogenesis studies of the nuclear membranes (1,6,25). LAP1 function remains poorly understood and few information is available. Regarding LAP1 isoforms, there is information for *Rattus norvegicus* where 3 isoforms (LAP1A, B and C) were previously identified (5). However, only one human LAP1 isoform (LAP1B) was fully sequenced. Using human cell lines, we detect mainly two isoforms: LAP1B and a lower molecular weight isoform that we hypothesize to be huLAP1C, as previously mentioned (25). Concerning their physiological functions, it has been hypothesized that LAP1 may have a role as lamina attachment site and assembly to the inner nuclear membrane (4–6). Additional putative functions have been proposed to be related with arrangement and structure of lamin filaments and reassembly of the NE at the end of mitosis (7). For this purpose, the previously described shRNA methodology was applied to mimic the SH-SY5Y cell behavior when we reduced the expression of huLAP1, through an induced knockdown. Therefore, the shRNA strategy was quite essential for the analysis of LAP1 role in human neuronal-like cells (2,23).

In order to establish the best knockdown efficiency, the transfection of shRNA constructs was evaluated in several conditions. Essentially, we tested two different

transfection reagents (Lipofectamine and TurboFect), two different DNA concentrations (2 µg and 5 µg) and also two different post-transfection periods (24 hours and 48 hours). As negative control, a missense oligonucleotide was also transfected in the same conditions of huLAP1B constructs, for comparison. Using the Lipofectamine methodology for 24 hours, the knockdown results were somewhat more pronounced for huLAP1B (maximum of 60% of interference) than huLAP1C (maximum of 40% of interference), as we expected since the selection of target sequences was made from the huLAP1B transcript, the only sequenced human LAP1 isoform. Since we also observe interference of huLAP1C, whose sequence is not described, our main hypothesis was that the chosen target sequences for huLAP1B have high homology with huLAP1C. However, the knockdown results using TurboFect transfection reagent in the same conditions (24 hours upon transfection), were more evident for huLAP1C (maximum of 80% of interference) than for huLAP1B (maximum of 50% of interference), contrary to our expectations. So, we can assume that the selected LAP1 target sequences for knockdown, in fact, seem to be present in both isoforms.

From all these experiments, we concluded that the chosen LAP1 targeted sequences, in fact, interfere with both huLAP1 isoforms. Additionally, we were able to determine that the TurboFect methodology produced the best interference results for both isoforms. In fact, using the TurboFect reagent for 24 hours it was achieved the best knocking-efficiency (maximum of 80% interference). Such difference can be explained in part by the mechanism of action of the different transfection reagents. In the case of TurboFect, the formed TurboFect/DNA complexes protect DNA from degradation and the mechanism of translocation to nucleus is established. The nuclear translocation happens after the endocytosis of the complexes, whose endosomes are further disrupted due to quick osmotic swelling (*Invitrogen*). On the other hand, the mechanism of Lipofectamine transfection reagent is not so clearly understood, and it is known that some concentrations of Lipofectamine can be toxic for DNA, affecting the growth, apoptosis and cell cycle (74).

Using Lipofectamine or TurboFect for 24 hours, the knockdown efficiency was higher with 5 µg of each tested construct, since the higher amount of DNA oligonucleotides results in more copies of *in vivo* transcribed shRNAs. Thus, 5 µg of transfected DNA was optimized to achieve the interference using the construct 1, construct 2 and both constructs together (40%, 40% and 60%). Both constructs together were always the most efficient to induce a

better knockdown, since each of them is loaded into one RISC/Ago2 complex. Therefore, in this case, two complexes with the shRNA constructs are directed to the two selected target sequences of *TOR1AIP1* transcript, producing a more efficient degradation of the sequence, as we expected.

Surprisingly, upon 48 hours of transfection, the effects of knockdown were not so clear than those observed with 24 hours of transfection using the same two methodologies. Using the TurboFect reagent during 48 hours, unexpected results were observed, since for the huLAP1C isoform, no significant knockdown was observed. The latter observation could be explained by a possible prejudicial effect of TurboFect, upon 48 hours of transient transfection with the shRNA constructs.

In conclusion, the optimized post-transfection time was 24 hours, with the TurboFect transfection reagent. The optimized concentration of DNA was 5 µg and transfection of both constructs together had revealed the best knockdown efficiency.

Once determined the best conditions for human LAP1 knocking-down, we evaluated biochemically the intracellular levels of three proteins when huLAP1 is depleted: laminB1, which is particularly important for NE integrity; acetylated α-tubulin, a marker for microtubules stability; and cleaved PARP for overall cellular integrity evaluation. For that, we evaluate the intracellular levels of cleaved PARP, acetylated α-tubulin and laminB1 using specific antibodies against which of the proteins.

Concerning to laminB1 intracellular levels, a significant decrease was observed, upon SH-SY5Y cell transfection with all huLAP1 shRNA constructs. Since a tight association of LAP1 with chromatin proteins and lamina is described, NE fragmentation may occur simultaneously with the disruption of these protein-protein interactions. Thus, it is likely that lack of LAP1 and subsequent disruption of the binding with chromatin proteins lead to nuclear membrane disintegration, followed by entire NE disruption. Therefore, B-type lamins also disassembled, since they are suspended in the INM. On the other hand, reduction of intracellular laminB1 levels may be due to the disassembly of the attachment sites of laminB1 to NE through LAP1. Thus, without LAP1 protein, the laminB1 may disconnect of the INM, leading to an abnormal morphology and instability of the NE. In conclusion, since LAP1 is depleted, we can assume that the laminB1 decrease may be explained by the disruption of laminB1 attachment sites to NE or, otherwise, by a resulting disintegration of the NE upon LAP1 absence (75). Additionally,

it was already observed that laminB-deficient cells undergo apoptosis, regardless of nuclear assembly of lamins A/C, suggesting NE targeting of B-lamins is essential for cell survival (76).

Acetylation of α -tubulin plays an important role for stabilizing microtubule structures, which are responsive for movement of chromosomes during mitosis and for maintenance of cellular morphology. Thus, it allows an indirect measure of cytoskeleton integrity. In order to evaluate the microtubule dynamics, the acetylated α -tubulin was quantified upon huLAP1 knockdown. There is a considerable decrease in acetylated α -tubulin levels after LAP1 knockdown. Such decreasing may be explained by a possible disruption of the linker of nucleoskeleton and cytoskeleton (LINC) complexes. As previously described, LINC complex is composed of SUN proteins which are associated with nuclear lamina and nesprins (from ONM). Once reduced the intracellular lamina levels and assuming the disintegration of lamins, the lamina-associated SUN proteins may disintegrate from LINC complex. Therefore, the connection between nucleoskeleton and cytoskeleton may be disrupted, which can explain the decreased levels of acetylated α -tubulin. Another possible explanation for reduced levels of acetylated α -tubulin, is the impairment of spindle microtubule formation during mitosis. Thus, it may result in weak mitotic asters, which may fail to align chromosomes. Such assumption may culminate in cell death because mitosis can not progress. This hypothesis is also supported by a recent report which suggests that LAP1 is associated with microtubule spindle assembly (29,34). In conclusion, the microtubule dynamics is impaired and, subsequently, the cytoskeleton integrity becomes compromised with decreased levels of LAP1.

For an overall analysis of cellular integrity we evaluated the levels of a cleaved fragment of PARP (85 kDa), which may be considered a marker for apoptosis (72,73). We decided to evaluate the apoptosis because the characteristic chromatin condensation is secondary to a series of nuclear events, such as proteolytic degradation of specific nuclear proteins that include lamins (76). The results of cleaved PARP have shown that there is a slight tendency to have increased levels of this protein. However, the ratio with total PARP protein should have been evaluated for a more accurate result.

SH-SY5Y cells morphology and cytoskeleton integrity were also evaluated through fluorescence and confocal microscopy, upon huLAP1 knockdown. Through immunoblotting, we have seen that intracellular levels of both huLAP1B and huLAP1C isoforms were knocked-

down. For huLAP1B, we observed interferences around 0%, 10% and 35% (construct 1, construct 2 and construct 1+2, respectively) and, for huLAP1C, we observed interferences around 38%, 43% and 39% (construct 1, construct 2 and construct 1+2, respectively). These interference percentages are coincident with the cellular nuclear envelope counts, through fluorescence microscopy.

Then, we analyzed the same knocked-down cells by confocal microscopy. In control cells, we have seen that LAP1 is present in the perinuclear region, while the nuclear morphology and the distribution of acetylated α -tubulin were normal. In transfected cells with construct 1, the nucleus presents an abnormal morphology and a distinct concentration of acetylated α -tubulin around the nucleus, which may be a sign of cell shrinkage or even by compensatory stabilization of NE architecture. In this case, huLAP1B was not efficiently knocked-down, so these alterations should arise from huLAP1C deficiency. In transfected cells with construct 2, there is also evidence of reniform nuclei and abnormal distribution of chromatin within the nucleus. We may hypothesize that huLAP1B seems to be partially involved with chromatin distribution, since in this condition an additional interference with huLAP1B was obtained (10%), compared to the last case for construct 1. This chromatin condensation can be explained as a consequence of laminB1 disintegration, which may result in the beginning of the apoptotic process.

Subsequently, decreased levels of acetylated α -tubulin were observed. In transfected cells with both constructs, this condition seems to represent an intermediary phenotype, since the nuclei are reniform and chromatin is also abnormally distributed. It can be explained by the similar percentage of interference of both isoforms (39% for LAP1C and 35% for LAP1B). The acetylated α -tubulin levels are reduced probably because of lack of NE integrity. The abnormal distribution of chromatin within the nucleus is also observed and probably happens because of the LAP1 disrupted interaction with laminB1.

LAP1 associates with mitotic chromosomes (4) and, therefore, with decreased levels of LAP1, it may lead to an abnormal distribution within nuclei (construct 2 and construct 1+2). In conclusion, huLAP1B seems to play a role in chromatin organization. On the other hand, decreased levels of acetylated α -tubulin which indicate microtubule instability, may lead to fail in chromosome alignment and, subsequently, lead to cell death. Additionally, huLAP1B

isoform seems to be involved in decreased levels of tubulin, which may be the result of an initial apoptotic process.

However, more work will be needed to fully evaluate the role of LAP1 on these processes. The shRNA strategy would be an important tool to accomplish these objectives.

CONCLUDING REMARKS

The conclusions of this work are the following:

- The human LAP1 was efficiently knocked-down using TurboFect, 5 µg of DNA and 24h post-transfection;
- Both constructs together produced the best knockdown efficiency.

- **When LAP1 is knocked-down:**
 - NE integrity is affected (levels of laminB1 decrease);
 - Microtubule stability is compromised (acetylated α -tubulin decrease);
 - Cellular integrity might be affected (slight increase of cleaved PARP).

FUTURE PERSPECTIVES

The future perspectives of this work are the following:

- Evaluate apoptosis in knocked-down huLAP1 cells by other approaches
- Analyze the integrity of the NE through immunofluorescence with laminB1 antibody in knocked-down huLAP1 cells

- Understand the role of LAP1 in mitosis:
 - Find out novel LAP1 binding partners in mitotic structures
 - Formation and/or stability of the mitotic spindle
 - Reassembly of the nuclear envelope

References

1. Schirmer EC, Foisner R. Proteins that associate with lamins: many faces, many functions. *Experimental Cell Research*. 2007;313(10):2167–79.
2. Hutchison CJ, Alvarez-Reyes M, Vaughan OA. Lamins in disease: why do ubiquitously expressed nuclear envelope proteins give rise to tissue-specific disease phenotypes? *J Cell Sci*. 2000/12/12 ed. 2001;114(1):9–19.
3. Mendez-Lopez I, Worman HJ. Inner nuclear membrane proteins: impact on human disease. *Chromosoma*. 2012/02/07 ed. 2012;121(2):153–67.
4. Foisner R, Gerace L, Cell. Integral membrane proteins of the nuclear envelope interact with lamins and chromosomes, and binding is modulated by mitotic phosphorylation. *Cell*. 1993;73(0092-8674):1267–79.
5. Senior A, Gerace L. Integral membrane proteins specific to the inner nuclear membrane and associated with the nuclear lamina. *J Cell Biol*. 1988/12/01 ed. 1988;107(6 Pt 1):2029–36.
6. Martin L, Crimando C, Gerace L, Chem JB. cDNA cloning and characterization of lamina-associated polypeptide 1C (LAP1C), an integral protein of the inner nuclear membrane. *J Biological Chemistry*. 1995;270(N.15, April 14):8822–8.
7. Yang L, Guan T, Gerace L. Integral membrane proteins of the nuclear envelope are dispersed throughout the endoplasmic reticulum during mitosis. *J Cell Biol*. 1997/06/16 ed. 1997;137(6):1199–210.
8. Goldman RD, Gruenbaum Y, Moir RD, Shumaker DK, Spann TP. Nuclear lamins: building blocks of nuclear architecture. *Genes Dev*. 2002/03/06 ed. 2002;16(5):533–47.
9. Gruenbaum Y, Wilson KL, Harel A, Goldberg M, Cohen M. Nuclear Lamins - Structural proteins with fundamental functions. *Journal of Structural Biology*. 2000;129(2-3):313–23.
10. Lisa P, Burke B, Biol JC. Internuclear exchange of an inner nuclear membrane protein (p55) in heterokaryons: in vivo evidence for the interaction of p55 with the nuclear lamina. *J Cell Biol*. 1990;111(6 Pt 1):2225–34.
11. Schirmer EC, Gerace L. Organellar proteomics: the prizes and pitfalls of opening the nuclear envelope. *Genome Biol*. 2002/05/02 ed. 2002;3(4):1–4.
12. Life Technologies [Internet]. 2013. Available from: <http://www.invitrogen.com/site/us/en/home/Products-and-Services/Applications/Cell-Analysis/Cellular-Imaging/Fluorescence-Microscopy->

and-Immunofluorescence-IF/Organelle-Stains-for-Fluorescence-Imaging-Selection-Guide.htm

13. Vlcek S, Foisner R. A-type lamin networks in light of laminopathic diseases. *Biochim Biophys Acta*. 2006/08/29 ed. 2007;1773(5):661–74.
14. Dauer WT, Worman HJ. The Nuclear Envelope as a Signaling Node in Development and Disease. *Developmental Cell*. 2009;17(5):626–38.
15. Jungwirth M, Kumar D, Jeong D, Goodchild RE, Biol BMCC. The nuclear envelope localization of DYT1 dystonia torsinA-DeltaE requires the SUN1 LINC complex component. *BMC Cell Biol*. 2011;12:1471–2121.
16. Mendez-Lopez I. [Laminopathies. Nuclear lamina diseases]. *Med Clin (Barc)*. 2011/06/03 ed. 2012;138(5):208–14.
17. Holmer L, Worman HJ. Inner nuclear membrane proteins: functions and targeting. *Cellular and Molecular Life Sciences*. 2001;58:1741–7.
18. Laguri C, Gilquin B, Wolff N, Romi-Lebrun R, Courchay K, Callebaut I, et al. Structural characterization of the LEM motif common to three human inner nuclear membrane proteins. *Structure*. 2001 Jun;9(6):503–11.
19. Cohen T V, Klarmann KD, Sakchaisri K, Cooper JP, Kuhns D, Anver M, et al. The lamin B receptor under transcriptional control of C/EBPepsilon is required for morphological but not functional maturation of neutrophils. *Human molecular genetics*. 2008 Oct 1;17(19):2921–33.
20. Ozawa R, Hayashi YK, Ogawa M, Kurokawa R, Matsumoto H, Noguchi S, et al. Emerin-lacking mice show minimal motor and cardiac dysfunctions with nuclear-associated vacuoles. *The American journal of pathology*. 2006 Mar;168(3):907–17.
21. Maison C, Pырpasopoulou A, Theodoropoulos PA, Georgatos SD, Embo J. The inner nuclear membrane protein LAP1 forms a native complex with B-type lamins and partitions with spindle-associated mitotic vesicles. *EMBO Journal*. 1997;16(No. 16):4839–50.
22. Ott CM, Lingappa VR. Integral membrane protein biosynthesis: why topology is hard to predict. *J Cell Sci*. 2002/04/26 ed. 2002;115(Pt 10):2003–9.
23. Goodchild R, Dauer WT, Biol JC. The AAA+ protein torsinA interacts with a conserved domain present in LAP1 and a novel ER protein. *J Cell Biol*. 2005;168(No. 6, March 14):855–62.
24. Jungwirth M, Dear ML, Brown P, Holbrook K, Goodchild R. Relative tissue expression of homologous torsinB correlates with the neuronal specific importance

- of DYT1 dystonia-associated torsinA. *Hum Mol Genet.* 2009/12/18 ed. 2010;19(5):888–900.
25. Kondo Y, Kondoh J, Hayashi D, Ban T, Takagi M, Kamei Y, et al. Molecular cloning of one isotype of human lamina-associated polypeptide 1s and a topological analysis using its deletion mutants. *Biochemical and Biophysical Research Communications.* 2002;294(0006-291X):770–8.
 26. Vander Heyden AB, Naismith T V, Snapp EL, Hodzic D, Hanson PI. LULL1 retargets TorsinA to the nuclear envelope revealing an activity that is impaired by the DYT1 dystonia mutation. *Mol Biol Cell.* 2009/04/03 ed. 2009;20(11):2661–72.
 27. Santos M. Validation of LAP1B as a novel protein phosphatase 1 regulator. *Biology Department.* [Aveiro]: University of Aveiro; 2009. p. 120.
 28. Zhu L, Millen L, Mendoza JL, Thomas PJ. A unique redox-sensing sensor II motif in TorsinA plays a critical role in nucleotide and partner binding. *J Biol Chem.* 2010/09/24 ed. 2010;285(48):37271–80.
 29. Kim CE, Perez A, Perkins G, Ellisman MH, Dauer WT. A molecular mechanism underlying the neural-specific defect in torsinA mutant mice. *Proc Natl Acad Sci U S A.* 2010/05/12 ed. 2010;107(21):9861–6.
 30. Esteves SLC, Korrodi-Gregório L, Cotrim CZ, van Kleeff PJM, Domingues SC, da Cruz e Silva O a B, et al. Protein phosphatase 1 γ isoforms linked interactions in the brain. *Journal of molecular neuroscience : MN.* 2013 May;50(1):179–97.
 31. Esteves SLC, Domingues SC, da Cruz e Silva OAB, Fardilha M, da Cruz e Silva EF. Protein phosphatase 1 α interacting proteins in the human brain. *Omics : a journal of integrative biology.* 16(1-2):3–17.
 32. Blethrow JD, Glavy JS, Morgan DO, Shokat KM. Covalent capture of kinase-specific phosphopeptides reveals Cdk1-cyclin B substrates. *Proceedings of the National Academy of Sciences of the United States of America.* 2008 Feb 5;105(5):1442–7.
 33. Zhao C, Brown RSH, Chase AR, Eisele MR, Schlieker C. Regulation of Torsin ATPases by LAP1 and LULL1. *Proceedings of the National Academy of Sciences of the United States of America.* 2013 May 23;110(17):1545–54.
 34. Neumann B, Walter T, Hériché J-K, Bulkescher J, Erfle H, Conrad C, et al. Phenotypic profiling of the human genome by time-lapse microscopy reveals cell division genes. *Nature.* 2010 Apr 1;464(7289):721–7.
 35. Naismith T V, Dalal S, Hanson PI. Interaction of TorsinA with Its Major Binding Partners Is Impaired by the Dystonia-associated Delta GAG Deletion. *Journal of Biological Chemistry.* 2009;284(41):27866–74.

36. Kustedjo K, Deechongkit S, Kelly JW, Cravatt BF. Recombinant expression, purification, and comparative characterization of torsinA and its torsion dystonia-associated variant Delta E-torsinA. *Biochemistry*. 2003 Dec 30;42(51):15333–41.
37. Goodchild RE, Dauer WT. Mislocalization to the nuclear envelope: an effect of the dystonia-causing torsinA mutation. *Proceedings of the National Academy of Sciences of the United States of America*. 2004 Jan 20;101(3):847–52.
38. Atai NA, Ryan SD, Kothary R, Breakefield XO, Nery FC. Untethering the nuclear envelope and cytoskeleton: biologically distinct dystonias arising from a common cellular dysfunction. *Int J Cell Biol*. 2012/05/23 ed. 2012;1–18.
39. Van de Vosse DW, Wan Y, Wozniak RW, Aitchison JD. Role of the nuclear envelope in genome organization and gene expression. *Wiley Interdiscip Rev Syst Biol Med*. 2011/02/10 ed. 2011;3(2):147–66.
40. Fahn S. Classification of movement disorders. *Mov Disord*. 2011/06/01 ed. 2011;26(6):947–57.
41. Tanabe LM, Kim CE, Alagem N, Dauer WT. Primary dystonia: molecules and mechanisms. *Nat Rev Neurol*. 2009/10/15 ed. 2009;5(11):598–609.
42. Leung JC, Klein C, Friedman J, Vieregge P, Jacobs H, Doheny D, et al. Novel mutation in the TOR1A (DYT1) gene in atypical early onset dystonia and polymorphisms in dystonia and early onset parkinsonism. *Neurogenetics*. 2001/08/29 ed. 2001;3(3):133–43.
43. Phukan J, Albanese A, Gasser T, Warner T. Primary dystonia and dystonia-plus syndromes: clinical characteristics, diagnosis, and pathogenesis. *Lancet Neurol*. 2011/10/28 ed. 2011;10(12):1074–85.
44. Ozelius LJ, Lubarr N, Bressman SB. Milestones in dystonia. *Mov Disord*. 2011/06/01 ed. 2011;26(6):1106–26.
45. Dystonia Medical Research Foundation [Internet]. Chicago; 2010. Available from: http://www.dystonia-foundation.org/pages/highlights_from_the_5th_international_dystonia_symposium/652.php
46. Paddison PJ, Caudy AA, Bernstein E, Hannon GJ, Conklin DS. Short hairpin RNAs (shRNAs) induce sequence-specific silencing in mammalian cells. *Genes Dev*. 2002/04/18 ed. 2002;16(8):948–58.
47. Scherr M, Eder M. Gene silencing by small regulatory RNAs in mammalian cells. *Cell Cycle*. 2007;6(4):444–9.

48. Rao DD, Vorhies JS, Senzer N, Nemunaitis J. siRNA vs. shRNA: similarities and differences. *Adv Drug Deliv Rev.* 2009/04/25 ed. 2009;61(9):746–59.
49. Napoli C, Jorgensen R. Introduction of a Chimeric Chalcone Synthase Gene into Petunia Results in Reversible Co-Suppression of Homologous Genes in trans. *Plant Cell.* April 1990. 1990;2(4):279–89.
50. Zhou F, Malik FA, Yang HJ, Li XH, Roy B, Miao YG. Application of short hairpin RNAs (shRNAs) to study gene function in mammalian systems. *African Journal of Biotechnology.* 2010;9(54):9086–91.
51. Barbosa AS, Lin CJ. Silenciamento de Genes Com RNA Interferência: Um Novo Instrumento para Investigação da Fisiologia e Fisiopatologia do Córtex Adrenal. *Arq Bras Endocrinol Metabol.* 2005/03/12 ed. 2004;48(5):612–9.
52. Fire A, Montgomery MK, Kostas SA, Driver SE, Mello CC XS. Potent and specific genetic interference by double-stranded RNA in *Caenorhabditis elegans*. *Nature.* 1998;391:806–11.
53. Hammond SM, Caudy AA, Hannon GJ. Post-transcriptional gene silencing by double-stranded RNA. *Nat Rev Genet.* 2001/03/17 ed. 2001;2(2):110–9.
54. Hutvagner G, Zamore PD. RNAi: nature abhors a double-strand. *Curr Opin Genet Dev.* 2002/03/15 ed. 2002;12(2):225–32.
55. Bernstein E, Caudy AA, Hammond SM, Hannon GJ. Role for a bidentate ribonuclease in the initiation step of RNA interference. *Nature.* 2001/02/24 ed. 2001;409(6818):363–6.
56. Nykanen A, Haley B, Zamore PD. ATP requirements and small interfering RNA structure in the RNA interference pathway. *Cell.* 2001/11/10 ed. 2001;107(3):309–21.
57. De Fougères A, Vornlocher HP, Maraganore J, Lieberman J. Interfering with disease: a progress report on siRNA-based therapeutics. *Nat Rev Drug Discov.* 2007/06/02 ed. 2007;6(6):443–53.
58. Yu JY, DeRuiter SL, Turner DL. RNA interference by expression of short-interfering RNAs and hairpin RNAs in mammalian cells. *Proc Natl Acad Sci U S A.* 2002;99(9):6047–52.
59. Elbashir SM, Lendeckel W, Tuschl T. RNA interference is mediated by 21- and 22-nucleotide RNAs. *Genes Dev.* 2001;15(2):188–200.

60. Taxman DJ, Livingstone LR, Zhang J, Conti BJ, Iocca HA, Williams KL, et al. Criteria for effective design, construction, and gene knockdown by shRNA vectors. *BMC Biotechnol.* 2006/01/26 ed. 2006;6:7.
61. Paul CP, Good PD, Winer I, Engelke DR. Effective expression of small interfering RNA in human cells. *Nat Biotechnol.* 2002/05/01 ed. 2002;20(5):505–8.
62. Sui G, Soohoo C, Affar el B, Gay F, Shi Y, Forrester WC. A DNA vector-based RNAi technology to suppress gene expression in mammalian cells. *Proc Natl Acad Sci U S A.* 2002/04/18 ed. 2002;99(8):5515–20.
63. Life Technologies [Internet]. Available from: http://www.invitrogen.com/etc/medialib/en/images/ics_organized/applications/nucleic_acid_purification/data_image/560_wide.Par.11963.Image.560.614.1..gif
64. Kunkel T. GR. P. Transcription of a human U6 small nuclear RNA gene in vivo withstands deletion of intragenic sequences but not of an upstream TATATA box. *Nucl. Acids Res.* 1989;17:7371–9.
65. Brummelkamp TR, Bernards R, Agami R. A system for stable expression of short interfering RNAs in mammalian cells. *Science.* 2002;296(5567):550–3.
66. Zeng Y, Yi R, Cullen BR. Recognition and cleavage of primary microRNA precursors by the nuclear processing enzyme Drosha. *EMBO J.* 2004/11/27 ed. 2005;24(1):138–48.
67. Urbich C, Kuehbacher A, Dimmeler S. Role of microRNAs in vascular diseases, inflammation, and angiogenesis. *Cardiovasc Res.* 2008/06/14 ed. 2008;79(4):581–8.
68. S.M. Hammond A.A. Caudy, R. Kobayashi, G.J. Hannon SB. Argonaute2, a link between genetic and biochemical analyses of RNAi. *Science.* 2001;293:1146–50.
69. Rao DD, Senzer N, Cleary MA, Nemunaitis J. Comparative assessment of siRNA and shRNA off target effects: what is slowing clinical development. *Cancer Gene Therapy.* 2009;16(11):807–9.
70. Bridge AJ, Pebernard S, Ducraux A, Nicoulaz AL, Iggo R. Induction of an interferon response by RNAi vectors in mammalian cells. *Nat Genet.* 2003/06/11 ed. 2003;34(3):263–4.
71. Sledz CA, Holko M, de Veer MJ, Silverman RH, Williams BR. Activation of the interferon system by short-interfering RNAs. *Nat Cell Biol.* 2003/08/28 ed. 2003;5(9):834–9.

72. Bressenot A, Marchal S, Bezdetnaya L, Garrier J, Guillemin F, Plénat F. Assessment of apoptosis by immunohistochemistry to active caspase-3, active caspase-7, or cleaved PARP in monolayer cells and spheroid and subcutaneous xenografts of human carcinoma. *The journal of histochemistry and cytochemistry*. 2009 Apr;57(4):289–300.
73. Koh DW, Dawson TM, Dawson VL. Mediation of cell death by poly(ADP-ribose) polymerase-1. *Pharmacological research: the official journal of the Italian Pharmacological Society*. 2005 Jul;52(1):5–14.
74. Zhong Y-Q, Wei J, Fu Y-R, Shao J, Liang Y-W, Lin Y-H, et al. [Toxicity of cationic liposome Lipofectamine 2000 in human pancreatic cancer Capan-2 cells]. *Nan fang yi ke da xue xue bao = Journal of Southern Medical University*. 2008 Nov;28(11):1981–4.
75. Buendia B, Courvalin J-C. Domain-Specific Disassembly and Reassembly of Nuclear Membranes during Mitosis 1 nuclear membranes may proceed in a domain-specific. *Biol, J Cell*. 1997;144(230):133–44.
76. Steen RL, Collas P. Mistargeting of B-type lamins at the end of mitosis: implications on cell survival and regulation of lamins A/C expression. *The Journal of cell biology*. 2001 Apr 30;153(3):621–6.

APPENDIX

30% ACRYLAMIDE/0,8% BISACRYLAMIDE

- Weigh 29,2 g of acrylamide
- Weigh 0,8 g of bisacrylamide

Dissolve the solutes in distilled water. Make up the volume to 100 mL of deionised water and then filter through a 0,2 µm filter and store at 4°C.

ALKALINE LYSIS SOLUTIONS

a) Solution I

- 50 mM glucose
- 25 mM Tris-HCl; pH 8.0
- 10 mM EDTA

b) Solution II

- 0,2 N NaOH
- 1% SDS

c) Solution III

- 3 M potassium acetate
- 2 M glacial acetic acid

AMPICILIN

- Weigh 2,5 g of ampicilin sodium salt (50 µg/µL)

Dissolve the ampicilin in 50 mL of sterile water and filter it through a syringe. Aliquot into sterile microtubes.

10% APS

- Weigh 1 g of ammonium persulfate

Dissolve the solute in 10 mL of deionised water.

LURIA-BERTANI MEDIUM (LB MEDIUM)

- Weigh 25 g of LB

Dissolve the LB in distilled water and autoclave it for 25 minutes. Next, make up the volume of 1 L with distilled water.

LOADING GEL BUFFER (4X)

- Add 2,5 mL of 1M Tris solution (pH 6.8) (250 mM)
- Weigh 0,8 g of SDS (8%)
- Add 4 mL of glycerol (40%)
- Add 2 mL of β -Mercaptoethanol (2%)
- Weigh 1 mg of bromophenol blue (0,01%)

Adjust the volume to 10 mL of deionised water. Store at room temperature in darkness.

LGB (LOWER GEL BUFFER)

- Weigh 181,65 g of Tris
- Weigh 4 g of SDS

Dissolve the solutes in distilled water. Adjust the pH to 8.9 and make up the volume to 1L of deionised water.

MAXIPREP SOLUTIONS

d) Cell Ressuspension Solution

- Add 30 mL of Tris-HCl (1M) (Cf = 50mM)
- Add 6 mL of EDTA (0,5M) (Cf = 10mM)
- Add 3 mL of RNase A (10 mg/mL) (Cf = 100 μ g/mL)

Dissolve it and adjust the volume with 264 mL of deionised water.

e) Cell Lysis Solution

- Weigh 2,4 g of NaOH (0,2M)

- Weigh 3 g of SDS (1%)

Dissolve the solutes in distilled water. Adjust the volume to 300 mL of distilled water.

f) Neutralization Solution

- Weigh 77,73 g of potassium acetate, pH = 4.8 (1,32M)

Dissolve it in distilled water and adjust the volume to 600 mL with deionised water.

g) Column Wash Solution

- Weigh 4,633 g of potassium acetate (0,2M)
- Add 4,9 mL of Tris-HCl (1M) (Cf = 80 mM)
- Add 47,2 μ L of EDTA (0,5M), (Cf = 40 μ M)

Dissolve the solutes and adjust the volume with 340 mL of distilled water.

4% PARAFORMALDEHYDE

- Weigh 4 g of paraformaldehyde

Dissolve the paraformaldehyde in 25 mL of distilled water by heating at 58°C. Add 1-2 drops of 1M NaOH to clarify the solution. Filter the solution (0,2 μ m filter) and then add 50 mL of 2X PBS. Adjust the volume to 100 mL with deionised water.

1X PBS

Dissolve one pack of BupH Modified Dulbecco's Phosphate Buffered Saline Pack (*Pierce*) in 500 mL of deionised water. Final composition:

- 8 mM of sodium phosphate
- 2 mM of potassium phosphate
- 40 mM of NaCl
- 10 mM of KCl

Sterilize by filtering through a 0,2 μ m filter and store at 4°C.

PLATES OF LB MEDIUM/AMPICILIN

Plates of LB medium containing ampicilin antibiotic (50 µg/µL) were made. The LB medium and agar were weighed and mixed with distilled water. Then, it was autoclaved during 20 minutes and, after the cooling to 55°C, the ampicilin was added. The LB/agar containing the antibiotic was poured into plates (approximately 20 mL for each). The plates have cooled until solidified.

10X RUNNING BUFFER

- Weigh 30,3 g of Tris (250 mM)
- Weigh 144,2 g of glycine (2.5 M)
- Weigh 10 g of SDS (1%)

Dissolve the solutes in distilled water. Adjust the pH to 8.3 and the volume to 1L.

RESOLVING GEL SOLUTION (10%)

- Add 12,35 mL of H₂O
- Add 5 mL of 30% Acryl/0,8% Bisacyl solution
- Add 7,5 mL of LGB (4X)
- Add 150 µL of 10% APS
- Add 15 µL of TEMED

STACKING (UPPER) GEL SOLUTION (3,5%)

- Add 6,60 mL of H₂O
- Add 1,2 mL of 30% Acryl/0,8% Bisacyl solution
- Add 2,0 mL of LGB (4X)
- Add 200 µL of 10% APS
- Add 100 µL of 10% SDS
- Add 10 µL of TEMED

10% SDS

- Weigh 1 g of SDS

Dissolve the solute in 10 mL of deionised water.

SH-SY5Y COMPLETE MEDIUM

- Weigh 4,805 g of MEM
- Weigh 5,315 g of F12
- Weigh 0,055 g of sodium piruvate
- Weigh 1,5 g of sodium bicarbonate
- Add 10 mL of Antimycotic antibiotic

Dissolve the solute in distilled water and adjust pH to 7.2 - 7.4. Add 100 mL of FBS and 2,5 mL of L-glutamine. Make up the volume to 1L with deionised water and filter (0,2 μ m)

STRIPPING SOLUTION

- Weigh 3,76 g of Tris-HCl (pH 6.7) (62.5 mM)
- Weigh 10 g of SDS (2%)
- Add 3,5 mL of beta-mercaptoetanol (100 mM)

Dissolve the solutes in deionised water and adjust to pH 6.7. Add the mercaptoethanol and adjust volume to 500 mL.

SOB MEDIUM

- Weigh 25,5 g of SOB Broth

Dissolve the SOB Broth in distilled water. Add 10 mL of 250 mM KCl (1,86 g of KCl in 100 mL of deionised water) and then adjust the pH to 7.0 with 5N NaOH. Add 5 mL of a sterile solution of 2M $MgCl_2$ (19 g of $MgCl_2$ in 90 mL of distilled water). Complete the volume to 1 L with deionised water and autoclave the solution.

SOC MEDIUM

SOC medium is similar to SOB medium, except for the presence of 20 mM glucose. After the sterilization of SOB medium by autoclaving, it should cool to 60°C and add 20 mL of 1M glucose.

The 1M glucose solution is prepared by weighing 18 g of glucose in 90 mL of distilled water. Then, it is dissolved and the volume is adjusted to 1L with deionised water. The 1M glucose solution is sterilized by filtration.

50X TAE BUFFER

- Weigh 242 g of Tris base
- Add 57,1 mL of glacial acetic acid
- Add 100 mL of 0,5M EDTA (pH 8.0)

10X TBS

- Weigh 12,11 g of Tris (10 mM)
- Weigh 87,66 g of NaCl (150 mM)

Dissolve the solutes in distilled water. Adjust the pH to 8.0 with HCl and make up the volume to 1L of deionised water.

10X TBST

- Weigh 12,11 g of Tris (10mM)
- Weigh 87,66 g of NaCl (150 mM)

Dissolve the solutes in distilled water. Adjust the pH to 8.0 with HCl and make up the volume to 995 mL of deionised water. Add 5 mL of Tween 20 (0,05%).

1X TRANSFER BUFFER

- Weigh 3,03 g of Tris
- Weigh 14,41 mL of glycine

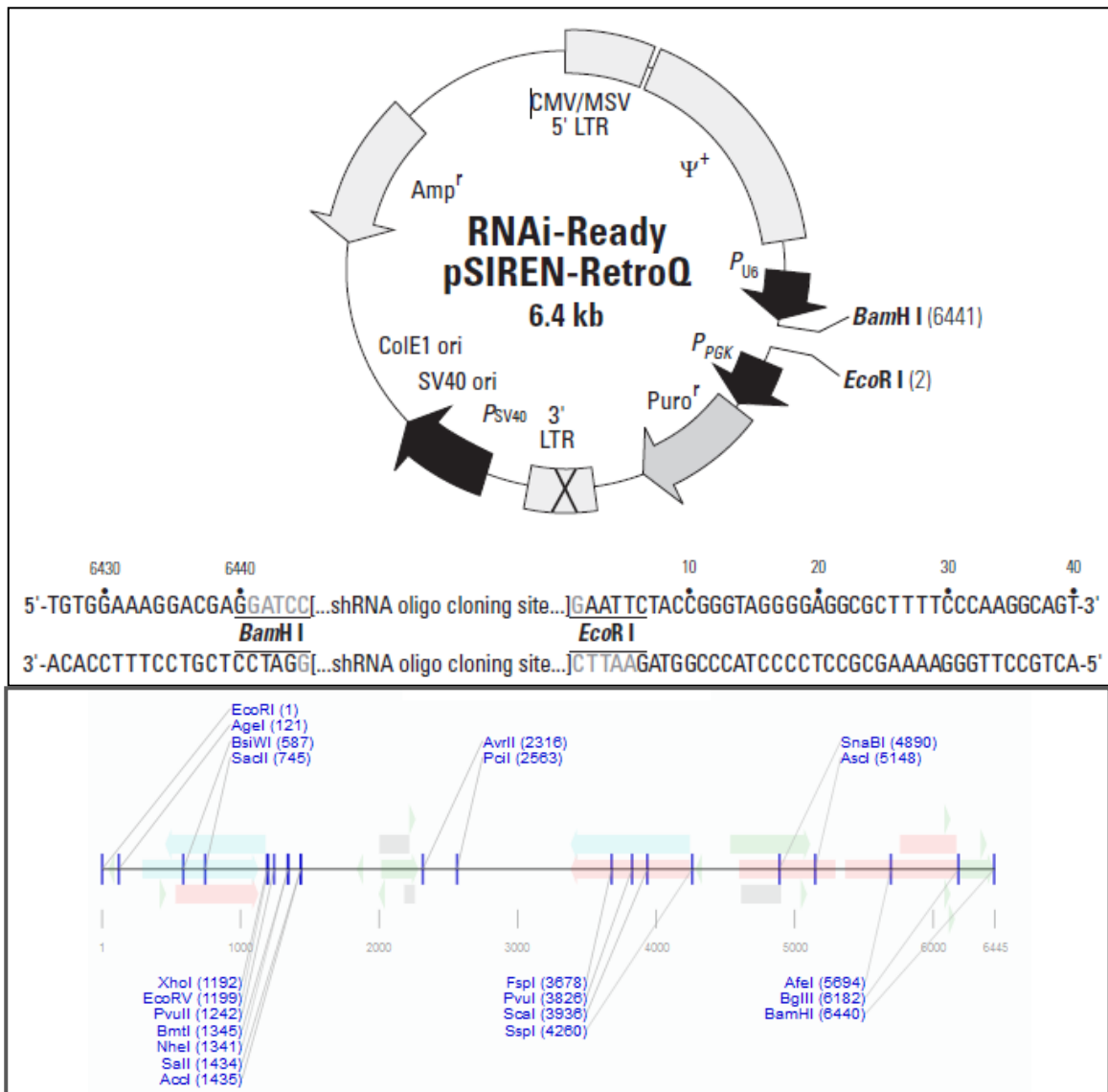
Dissolve the solutes in distilled water. Adjust the pH to 8.3 with HCl and make up the volume to 800 mL with distilled water. Add 200 mL of methanol (20%).

UGB (UPPER GEL BUFFER)

- Weigh 75,69 g of Tris

Dissolve the solutes in distilled water. Adjust the pH to 6.8 and make up the volume to 1L of deionised water.

VECTOR INFORMATION



Restriction Map and Cloning Site of the RNAi-Ready pSIREN-RetroQ Retroviral Vector (Clontech). Unique restriction sites are in bold. RNAi-Ready pSIREN-RetroQ is a self-inactivating retroviral expression vector designed to express a short hairpin RNA (shRNA) using the human U6 promoter (RNA Polymerase III-dependent). This vector is used for targeted gene silencing when a dsDNA oligonucleotide encoding an appropriate shRNA is ligated into the vector. The vector contains a puromycin resistance gene for the selection of stable transfectants. This retroviral vector is optimized to eliminate promoter interference through self-inactivation, which is provided by a deletion in the 3' LTR enhancer region. The hybrid 5' LTR consists of the cytomegalovirus (CMV) type I enhancer and the mouse sarcoma virus (MSV) promoter. pSIREN-RetroQ also contains a bacterial origin of replication and *E. coli* Ampicillin resistance gene for propagation and selection in bacteria. U6 Forward Sequencing Primer: 6188-6206 (5'-GGGCAGGAAGAGGGCCTAT - 3').